OCTOBER 1977

ORO 5178-78-1
UC 62

LIQUID METAL COOLED SOLAR CENTRAL RECEIVER FEASIBILITY STUDY AND HELIOSTAT FIELD ANALYSIS

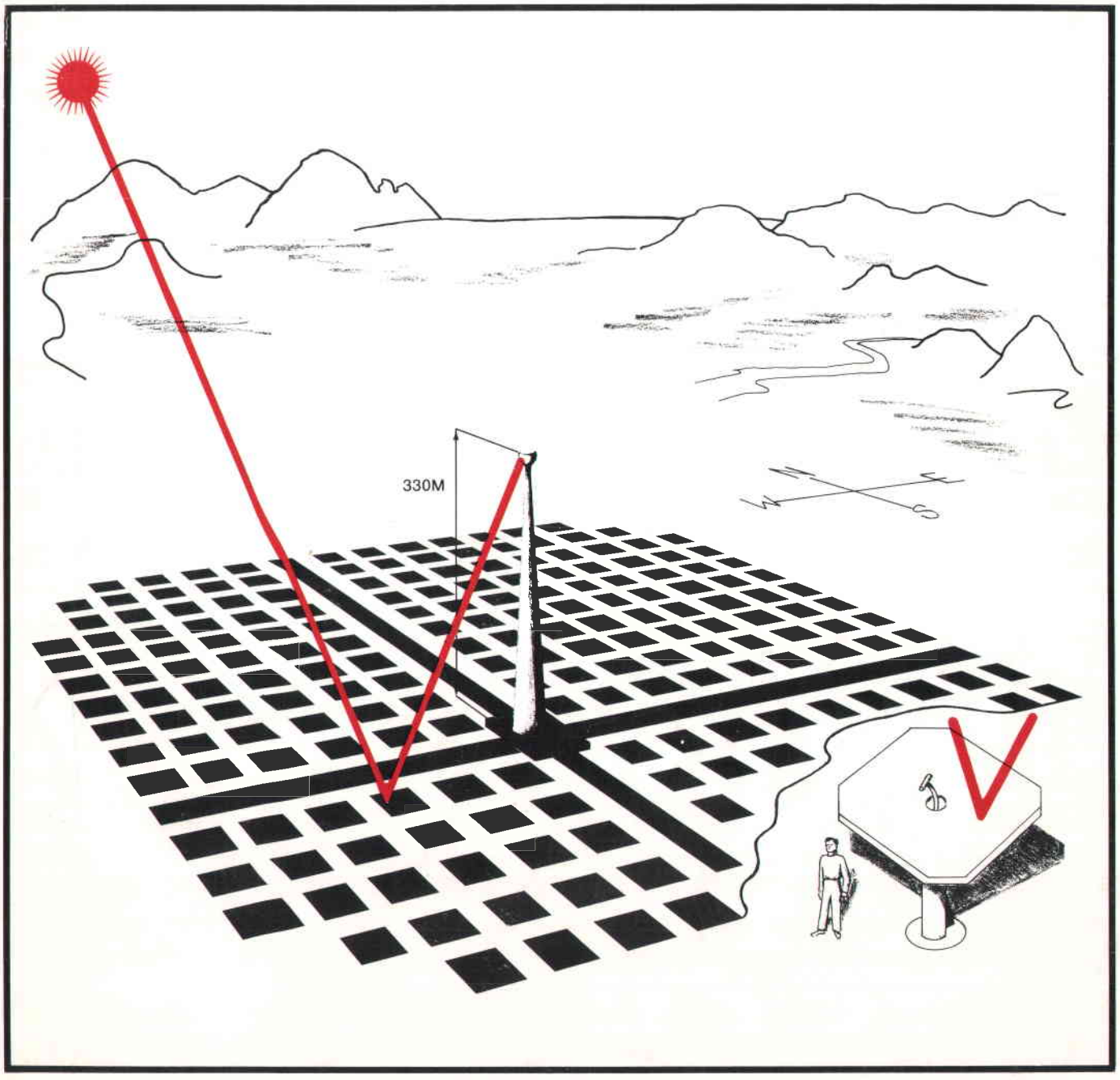

FINAL REPORT—Part I
Liquid Metal Cooled Solar Central Receiver
Prepared by the
Solar Energy Laboratory, University of Houston
Under ERDA Grant No. EG-76-G-05-5178

McDONNELL DOUGLAS CORPORATION

Rocketdyne Division
ROCKWELL INTERNATIONAL
Atomics International Division

NOTICE

Printed in the United States of America
Available from
National Technical Information Service
U. S. Department of Commerce
5285 Port Royal Road
Springfield, Virginia 22161
Price: Printed Copy $6.75; Microfiche $3.00

October 1977

BIBLIOGRAPHIC DATA SHEET	1. Report No. ORO 5178-78-1	2.	3. Recipient's Accession No.
4. Title and Subtitle Liquid Metal Cooled Solar Central Receiver Feasibility Study and Heliostat Field Analysis			5. Report Date 30 October 1977 6.
7. Author(s) L. Vant-Hull, G. C. Coleman, T. Springer & Co-Workers			8. Performing Organization Rept. No.
9. Performing Organization Name and Address Solar Energy Laboratory University of Houston Houston, Texas 77004			10. Project/Task/Work Unit No. 11. Contract/Grant No. EG-76-G-05-5178
12. Sponsoring Organization Name and Address Solar Energy Division Department of Energy Washington, D.C.			13. Type of Report & Period Covered Annual 6/15/76-6/15/77 14.

15. Supplementary Notes

16. Abstracts A conceptual design for a 100 MWe Solar Tower System employing liquid sodium as a heat transfer fluid and as a storage medium is generated. This design intentionally parallels the current commercial baseline design for a water/steam transfer fluid in order to enhance comparisons between the two approaches and to maximize the application of the limited funds in this study to the unique features of the liquid sodium system. Heat transfer at the receiver and the steam generator were considered in detail. Components for the liquid sodium loop currently under test on development were identified for a 10 MWe pilot plant and a 100 MWe demonstration plant. Economic comparisons with the MDAC water/steam receiver are favorable.

17. Key Words and Document Analysis. 17a. Descriptors
Solar Energy
Solar Energy Concentrator
Solar Furnaces
Solar Power Generation
Solar Reflectors
Power Generators
Liquid Metal
Liquid Sodium

17b. Identifiers/Open-Ended Terms
Central Receiver
Solar Tower--Power Tower
Optical Transmission
Design Optimization
Liquid Metal
Heat Transfer

17c. COSATI Field/Group

18. Availability Statement	19. Security Class (This Report)	21. No. of Pages
NTIS	UNCLASSIFIED	162
	20. Security Class (This Page) UNCLASSIFIED	22. Price 6.75

ORO 5178-78-1
UC 62

LIQUID METAL COOLED SOLAR CENTRAL RECEIVER FEASIBILITY STUDY AND HELIOSTAT FIELD ANALYSIS

STUDY TEAM AND MANAGERS
Lorin L. Vant-Hull
Solar Energy Laboratory
UNIVERSITY OF HOUSTON

Gerry Coleman
MCDONNELL DOUGLAS ASTRONAUTICS COMPANY

Tom Springer
ATOMICS INTERNATIONAL

Jerry Friefeld
ROCKETDYNE

FINAL REPORT
PART I
A LIQUID SODIUM COOLED
CENTRAL RECEIVER SYSTEM
CONCEPTUAL DESIGN

PREFACE

This report is submitted to the Department of Energy under contract EG-76-G-05-5178 as the Final Report on the Liquid Metal Cooled Central Receiver Feasibility Study portion of the work. The work reported in this volume was carried out between June 15, 1976 and June 15, 1977. Reports generated under this contract are as follows:

ORO 5178-77-1	Executive Summary of Semi Annual Review May 1977
ORO 5178-78-1	Final Report - Liquid Metal Cooled Solar Central Receiver Feasibility Study October 1977
ORO 5178-78-2	Final Report - Heliostat Field Analysis to be issued in January 1978

The work covered in this report was distributed by a subcontract to McDonnell Douglas Astronautics Company and a futher subcontract to Rockwell International, as follows:

University of Houston - Program coordination, collector field optimization and performance

McDonnell Douglas - Heliostat analysis, system definition and evaluation.

Atomics International - Receiver, thermal transport and storage analyses.

Rocketdyne - Receiver analysis

The Department of Energy Program Manager was George Kaplan; the Technical Monitor was Lee Radosevitch of Sandia Laboratories, Livermore, California.

ABSTRACT

Results of analysis and design efforts by the University of Houston's Solar Energy Laboratory, McDonnell Douglas Astronautics Company (MDAC), and the Atomics International and Rocketdyne divisions of Rockwell International between 15 June 1976 and 14 June 1977 on Department of Energy Grant No. EG-76-G-05-5178 are presented. This is the final report on the Liquid Metal Cooled Solar Central Receiver Feasibility Study and Heliostat Field Analysis.

This study investigated the technical and economic feasibility of liquid sodium as the primary working fluid in a Solar Central Receiver Power Plant in order to significantly improve plant efficiency by using the greatly improved heat transfer capability of the liquid metal.

The conceptual definition of 100 MWe commercial scale solar power plant is presented.

TABLE OF CONTENTS

LIST OF FIGURES

LIST OF FIGURES (continued)

LIST OF TABLES

LIST OF TABLES (continued)

1.0 INTRODUCTION

DOE'S program to design and build the first 10 MWe solar power plant is presently well under way and proceeding on schedule. The first generation solar plant has been designed around a superheated steam/water cycle in order to minimize technical, cost,and schedule risks. The potential for higher efficiency and lower cost has led to the consideration of second generation systems based on either a hot gas cycle or a liquid metal cycle. The hot gas cycle is presently under study by several EPRI contractors. This report presents the results of a conceptual design study of an advanced liquid sodium solar power plant by the University of Houston, McDonnell Douglas, and the Atomics International and Rocketdyne Divisions of Rockwell International.

The advantages in a liquid sodium cooled system over the more conventional water/steam system involve improved turbine cycle and receiver efficiencies which are reflected directly in a reduction of the collector field requirement. The higher turbine cycle efficiency results from the availability of high temperature sodium (which serves as both the receiver coolant and the storage fluid) at the turbine building which lends itself easily to a turbine reheat cycle. Also, because of the constant steam conditions available at all operating times, the daytime and nighttime gross electrical outputs are identical. This is in contrast to water/steam systems where nighttime efficiencies are typically 70-80% of the daytime levels due to reductions in steam temperatures and pressures which occur for energy routed through thermal storage.

Sodium used as the primary receiver coolant permits a high heat flux environment to exist on the receiver absorbing surfaces because of the superior heat transfer characteristics of sodium. This condition translates into a high concentration ratio design, which minimizes receiver surface area and thereby minimizes receiver heat losses. The low vapor pressure of sodium means that thin-walled tubing and pipes can be used more extensively, further reducing hardware costs.

From a heat transfer standpoint, the thin-walled tubes used on the receiver absorbing panels minimize the thermal resistance and the resulting temperature gradient across the tube wall. Since no coolant phase change occurs in the receiver, unlike the water/steam cooled receiver, the issue of flow stability within the receiver is a lesser concern because a unique relationship exists between fluid velocity and pressure drop through the tubes. This fact would permit the sodium receiver to operate at a lower minimum flow condition than the water/steam counterpart.

The primary objectives of this study were to define the conceptual design of a 100 MWe Sodium-Cooled Solar Central Receiver Power Plant and determine its technical and economic feasibility. Included within those objectives were the tasks of determining preliminary cost estimates of the system and identifying key areas requiring further technology efforts. The limited scope of the study allowed consideration of only a limited number of high level trade studies necessary to define the conceptual design approach. The majority of the effort on this contract involved the expansion of a point design at the subsystem level to define the most cost effective configuration.

In addition to the liquid sodium-oriented activities, the present study also investigated the effects of haze, latitude, and slope on the operation of the first generation central receiver water/steam system. The energy cost of materials and construction of the water/steam system was also evaluated and compared with the energy produced over the life of the system. A favorable relationship was determined. This type of evaluation is gaining increased recognition as our economy expends its fossil fuel reserves in producing replacement energy resources.

In accordance with the study guidelines, DOE design criteria and subsystem designs resulting from the ongoing water/steam solar central receiver program were used wherever possible. The advanced plant design was also to be compatible with an advanced 100 MWe demo plant operational by 1985.

Figure 1-1 is the study schedule showing the specific tasks of this study.

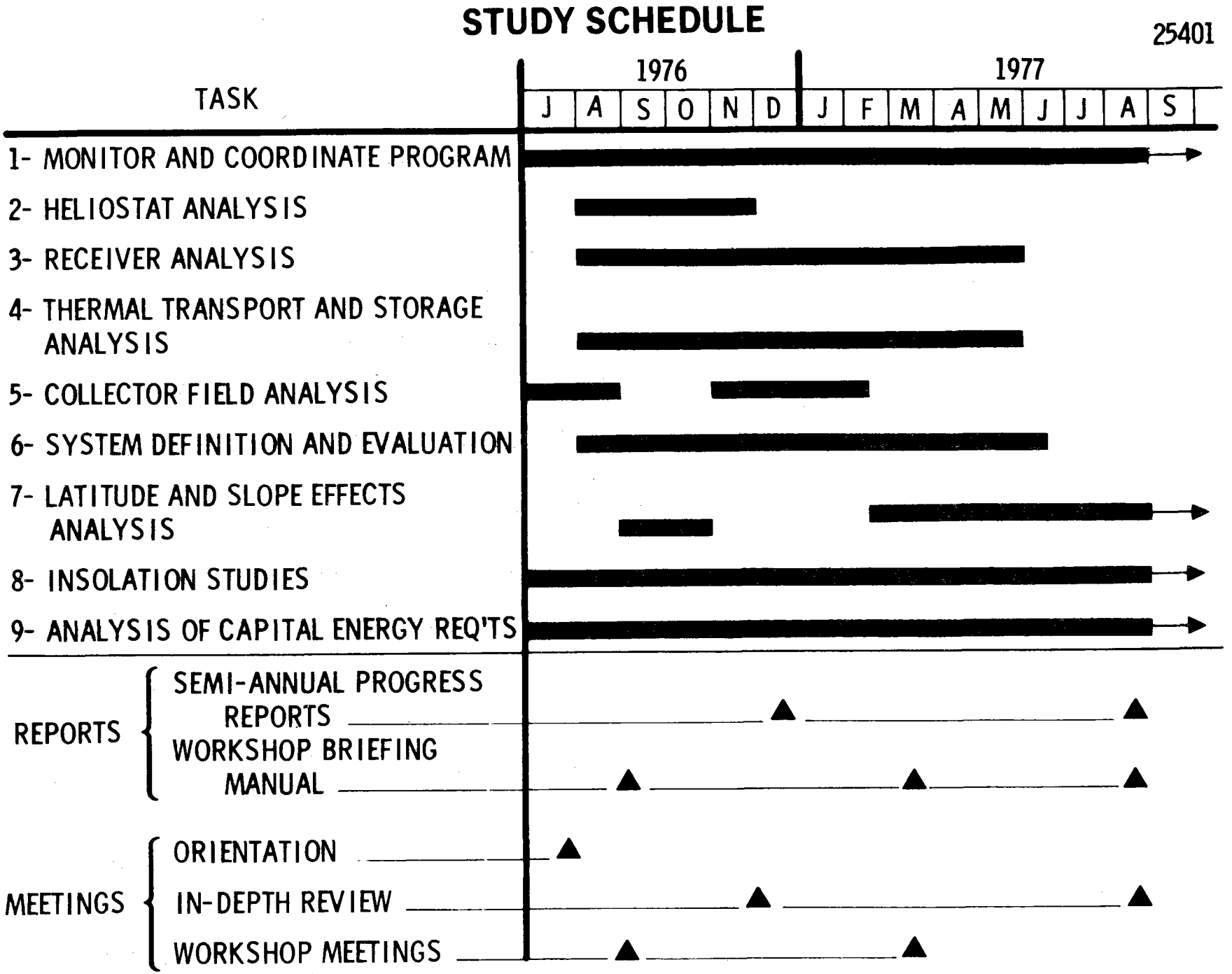

Figure 1-1 Study Schedule

2.0 SYSTEM DEFINITION

The principal system definition activities involved the development of a baseline liquid metal solar electric system description and the establishment of subsystem design requirements. In carrying out this activity, an effort was made to utilize, to the greatest extent possible, commercial system data which had been developed as part of a parallel program[1] for a water/steam system. This was done to permit the rather limited funds available on this study to be concentrated on the unique liquid metal aspects of the system while minimizing the duplication of other contract efforts. In addition, by maintaining similarities between the two systems, it was possible to make meaningful cost and performance comparisons.

In developing the system and subsystem level designs, certain selective extensions were made in current state-of-the-art liquid metal technology. This was done to permit greater design flexibility and minimize some of the design constraints which would be imposed if the design were required to use existing hardware. In general, a liquid metal technology base consistent with the 1985 time frame was assumed. This time frame was selected since it represents the earliest possible detailed design and construction period for the liquid metal solar electric system.

2.1 Requirements

A series of performance, design, and environmental requirements were established as a starting point for the study activity. These requirements, which are summarized in Table 2-1, parallel closely those which were developed for the commercial water/steam system. One notable exception, however, is the design point power level which occurs when operating exclusively from thermal storage. Unlike the water/steam system which suffers a degradation in power to $\sim$ 70 MWe when the energy is routed through thermal storage, the sodium

---

[1] ERDA Contract EY-76-C-03-1108, Central Receiver Solar Thermal Power System, Phase I.

system provides full 100 MWe output when operating from thermal storage since the sodium serves as both energy collection and thermal storage media. This characteristic is one of the attractive features of the liquid metal system.

The balance of the requirements is identical to those defined for the water/steam system. The thermal storage capacity is sized to produce the required power level for a period of up to six hours. The system is sized to be compatible with a 950 W/m^2 design point insolation level and is assumed to use wet cooling for heat rejection. The corresponding wet and dry bulb design point temperatures which influence both heat rejection and component heat loss are as indicated. The three wind speeds indicated are used respectively for receiver heat loss predictions, tower and heliostat deflection predictions during peak operating winds, and maximum survival design conditions. The indicated wind speeds are assumed to occur at a 10 m (32.8 ft) elevation with the speeds increasing as the 0.15 power with increase in elevation. The specified seismic environment is a Zone 3 condition, not near a great fault, with horizontal accelerations of 0.165 and 0.333 g for operational and survival environments. The availability level of 90 percent, exclusive of sunshine, represents an attainable goal for mature systems. The 30-year operational lifetime assumes a normal maintenance program.

2.2 System Analysis and Trade Studies

With the previously discussed requirements to serve as a starting point, it was possible to define a baseline system configuration and establish consistent design requirements for the subsystem design efforts. The approach used in establishing these requirements was to start with a well established turbine configuration and work backward in a power flow sense to establish the requirements for the thermal storage, receiver, and collector subsystems. Unlike the commercial water/steam system,which uses a non-reheat turbine cycle because of problems involved in reheating the steam, the liquid metal system can employ the more efficient reheat cycle because of the availability of high temperature energy on the ground.

Table 2-1

SYSTEM REQUIREMENTS

Design Point Power Levels	
• During Receiver Operation	100 MWe Net
• Operation Exclusively from Thermal Storage	100 MWe Net
Storage Capacity	6 Hours
Storage Fluid	Sodium
Design Insolation	950 W/m^2
Heat Rejection	Wet Cooling
Wet Bulb Temperature	23°C (74°F)
Dry Bulb Temperature	28°C (82.6°F)
Nominal Design Wind	3.5 m/Sec (8 mph)
Max Operating Wind (Including Gusts)	16 m/Sec (36 mph)
Max Survival Wind (Including Gusts)	40 m/Sec (90 mph)
Seismic Environment	Zone 3 (Not Near a Great Fault)
• Operating Earthquake	0.165 Horz G
• Survival Earthquake	0.333 Horz G
Availability (Exclusive of Sunshine)	90%
Lifetime	30 Years

The baseline reheat turbine configuration along with the corresponding steam conditions was defined as a result of a survey of existing and planned utility installations in the 100 MWe range. Plants planned and constructed in the early 1970's utilized steam conditions of 538°C (1000°F) and approximately 12.41 MPa (1800 psia) at the turbine inlet with a single 538°C (1000°F) reheat. Plants currently being planned for construction in the late 1970's indicate design pressures in the 12.76-13.45 MPa (1850-1950 psia) range with the turbine inlet and reheat temperatures being maintained at 538°C (1000°F). With this information as background, a turbine inlet condition of 538°C (1000°F), 13.79 MPa (2000 psia) and a 538°C (1000°F) reheat temperature was assumed which permits some additional growth in pressure, a continuation of the current trend. Due to turbine material constraints, the well established 538°C (1000°F) temperature limit for high pressure and reheat steam was maintained for the current conceptual design activity. A gross cycle efficiency of 39.5% was estimated for a reheat steam Rankine cycle operating at the indicated steam temperature and pressure conditions while exhausting at a 2-1/2 inch Hg condenser pressure.

With the steam conditions defined for the turbine cycle, it was possible to define the critical temperature and flow rate conditions for the balance of the water/steam and the sodium loops. After evaluating a series of piping alternatives, the baseline flow schematic and pertinent thermodynamic conditions were defined which are shown in Figure 2-1. The features of this configuration include a parallel superheater and reheater configuration (from a sodium flow standpoint) followed by the preheater/boiler stage. The parallel superheater and reheater were sized to have an identical outlet sodium temperature which is sufficient to satisfy the inlet requirements of the preheater/boiler stage. From the standpoint of the water/steam loop, the feedwater entering the preheater/boiler has been previously heated to 204°C (400°F) by the feedwater heaters which derive thermal energy from turbine extraction steam. The feedwater then passes through the preheater/boiler and superheater stages and is passed to the turbine inlet as superheated steam at the conditions indicated. The steam passing through the high pressure turbine section exhausts to the

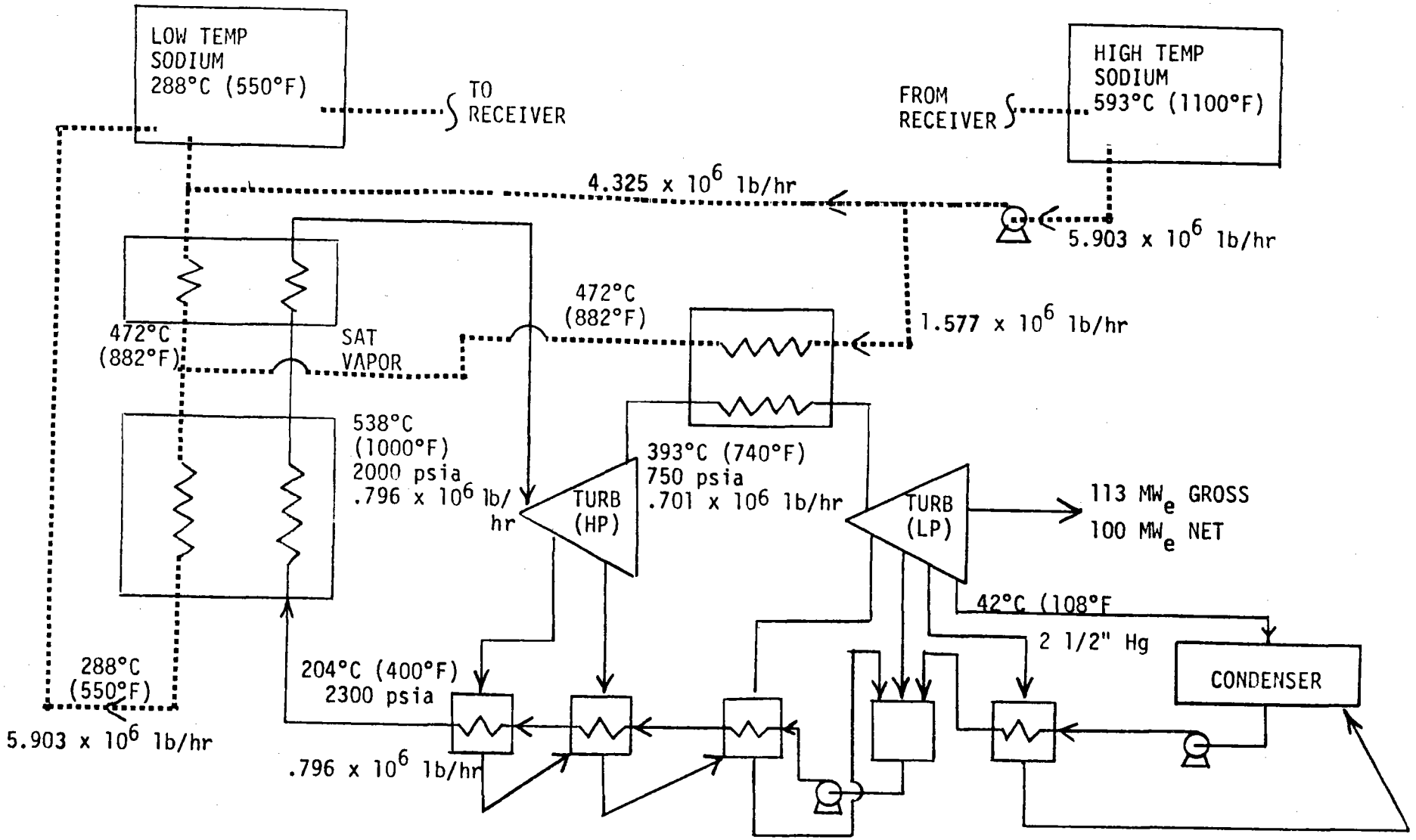

FIGURE 2-1 BASELINE STEAM GENERATION AND TURBINE SCHEMATIC

reheater at the indicated temperature and pressure. The reheater raises the steam temperature to the original 538°C (1000°F) level at which point it is introduced into the low pressure turbine section. The final exhaust steam is routed to the condenser where it is condensed and pumped through the feedwater heaters where it is heated and the cycle is repeated.

The sodium temperatures for the hot and cold reservoirs required to power the cycle were determined as a result of a series of studies which considered thermodynamic pinch point effects and tradeoffs between heat exchanger surface area and temperature differences across the heat exchanger while recognizing the desire to exercise the sodium over the greatest possible temperature range to maximize fluid inventory. In addition, constraints related to receiver tube materials and receiver heat losses also introduce an upper bound on the maximum practical sodium temperature. The resulting baseline heat transfer process for the preheater/boiler and superheater sections is shown in Figure 2-2 with the corresponding data for the reheater shown in Figure 2-3. In both of these figures the dashed lines represent the change in enthalpy for the sodium flow as it cools down while transferring energy to the water or steam (solid lines). The horizontal distance between the sodium and water/steam lines is a measure of the local temperature difference available for heat transfer.

The data for the preheater/boiler and superheater stages in Figure 2-2 show that the pinch point for heat transfer occurs at the beginning of the boiling process. This knee in the water/steam curve imposes a restriction on the minimum sodium temperature that can be achieved at the outlet of the unit since a sufficiently positive temperature potential must be maintained at the pinch point at all times. From a reheater design standpoint, Figure 2-3, a fairly large temperature potential is maintained between the sodium and steam due to the relatively poor heat transfer characteristics of low pressure steam. The result of the high temperature difference is a reduction in heat transfer surface area and a lowering of the steam side pressure drop over what would be necessary if lower sodium temperatures were used and larger heat exchangers. The slope of the lines in the two

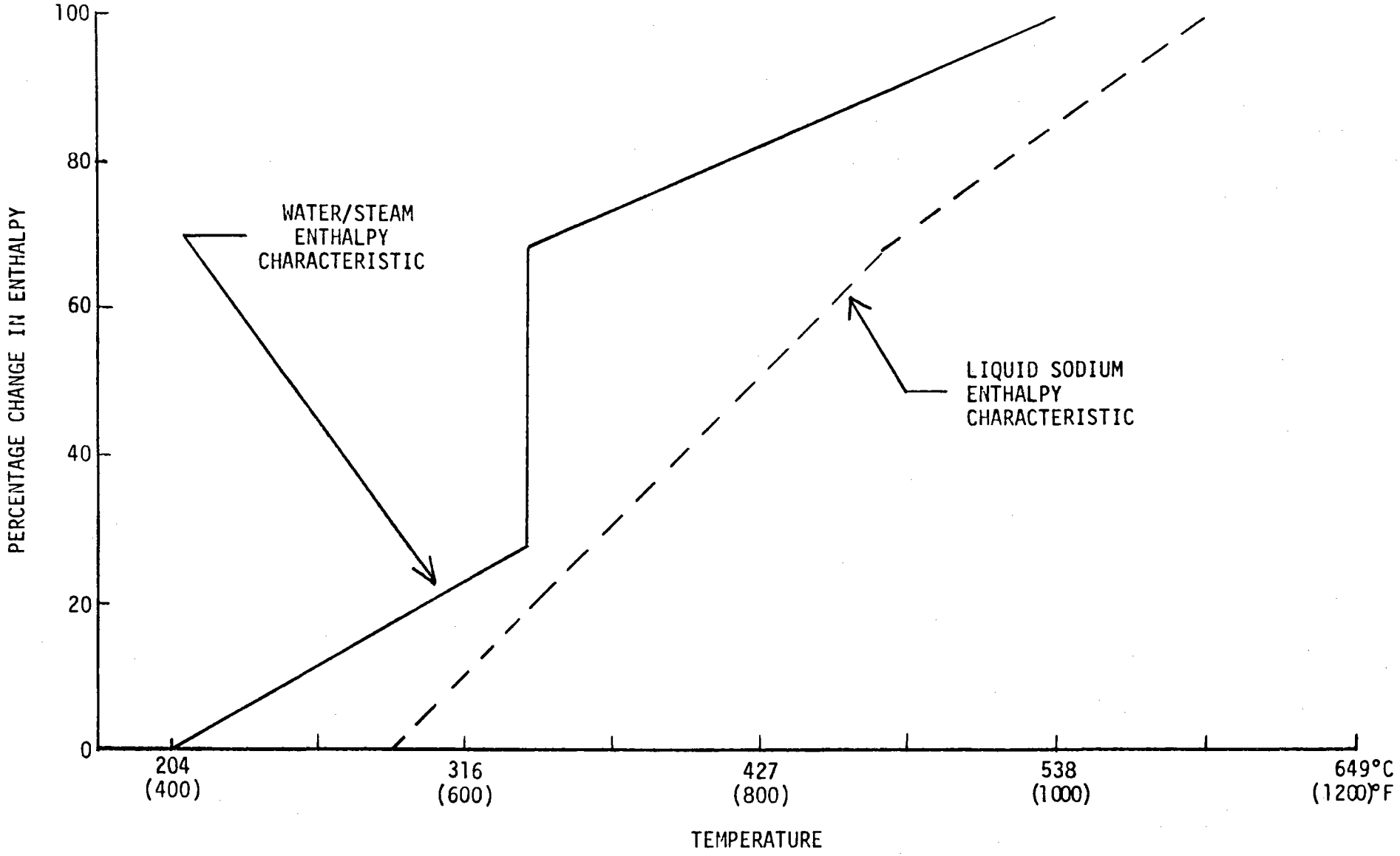

FIGURE 2-2 STEAM GENERATION PROCESS

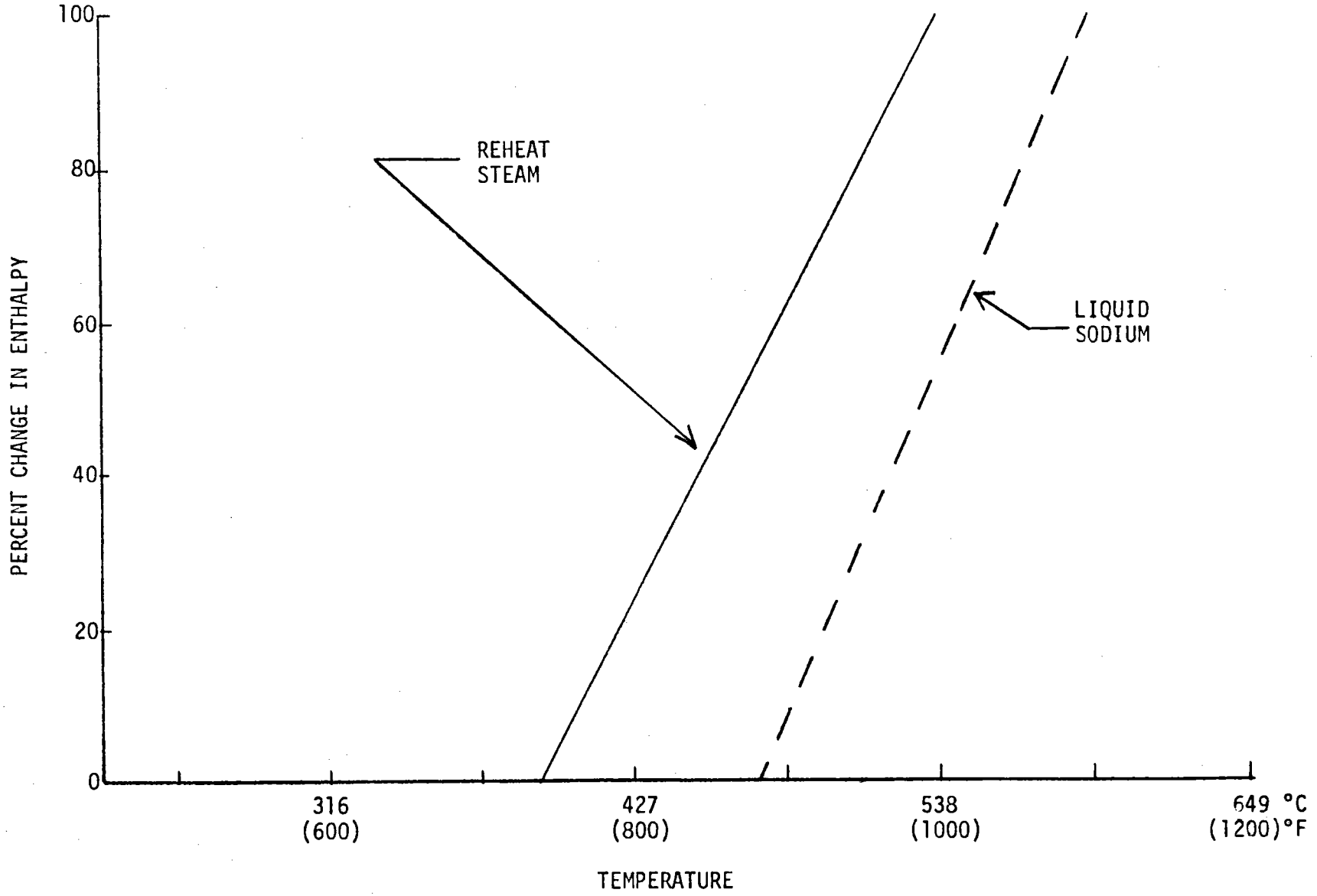

FIGURE 2-3 STEAM REHEAT PROCESS

plots corresponds to the $(\dot{M})$ (C_p) product of the flow. Since a higher sodium flow occurs in the preheater/boiler stage than the superheater stage, the slight change in sodium line slope as shown in Figure 2-2 results,
Based on the heat transfer process shown in Figures 2-2 and 2-3 along with supplemental cost and performance trade study data, sodium temperatures of 593°C (1100°F) and 288°C (550°F) were selected for the hot and cold reservoirs respectively. This would allow the sodium to be exercised over a 305°C (550°F) temperature range.

A measure of the performance for the overall system is shown on an itemized basis in Figure 2-4. In addition to factors related to the baseline turbine cycle, this figure includes effects related to the receiver and collector field which will be treated in greater detail in Sections 3 and 4 of this report. The stair-step format starts with the amount of power incident on the collector field when the heliostats are orientated normal to the sun (left bar) and progressively accounts for all losses resulting in 100 MW of net electrical power being produced by the generator. An itemized tabulation of the losses is shown on the right side of the figure. Also included in the figure is a power allocation to charge thermal storage. Since this power would be recovered at a later time, it should not be accounted as a system loss. The overall system efficiency between the power incident on the heliostats oriented normal to the sun and the net electrical power produced is 22.3% This includes all of the parasitic power loads required to power the system.

In an effort to reduce the overall cost of electricity produced by the system, a series of modifications to the baseline turbine cycle were considered. In general, these modifications were designed to permit the sodium to be exercised over a greater temperature range thereby reducing the storage inventory and tank capacity requirements. The offsetting penalties which occurred involved increasing system complexity and a general reduction in turbine cycle efficiency. These compensating effects are illustrated in the following example.

SYSTEM POWER FLOW (EQUINOX NOON)

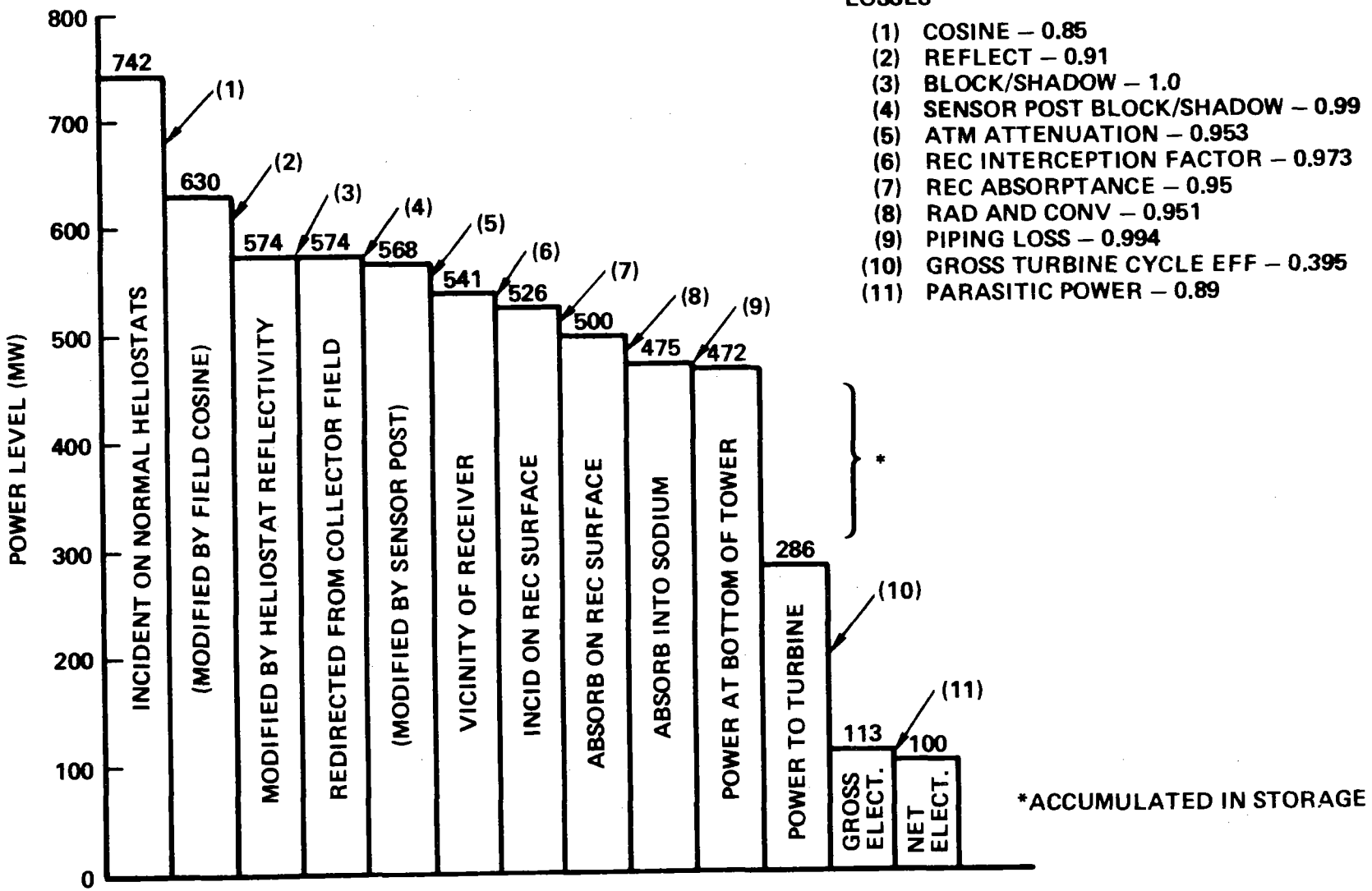

Figure 2-4 System Power Flow (Equinox Noon)

The impact of adding a toluene cycle which was designed to use the low temperature sodium reservoir as its energy source was investigated. A schematic diagram of the concept which was designed to operate in parallel with the baseline water/steam turbine is shown in Figure 2-5. In this configuration, 288°C (550°F) sodium which would otherwise be passed back to the receiver is passed through a toluene boiler where the temperature of moderate pressure toluene is raised to 260°C (500°F). The pressure of the toluene, which directly affects the toluene cycle efficiency, was limited by pinch point considerations in the toluene boiler. Throughout this study, the energy collection parts of the system, including the collector field, receiver, and tower were held constant, thus fixing the amount of thermal energy available to the turbine cycles over a given period.

The results of the study indicated that a reduction in sodium inventory and tank capacity of $\sim$ 30% would be realized with a corresponding reduction in sodium flow rates. The net effect of these factors is a reduction in capital cost of $\sim$ 5% even when the additional equipment associated with the toluene cycle was considered. From a thermodynamic standpoint, the total cycle efficiency decreases from 39.5% to $\sim$ 33% because of the lower conversion efficiency of the toluene cycle. This resulted in the cost of electricity actually increasing by $\sim$ 14% on an annual basis. As a result of this type of trade study, which considered the tradeoff between lower sodium inventory and lower cycle efficiency, the general conclusion which resulted showed the merits of maintaining high cycle efficiency, even if it required additional sodium inventory and storage tank capacity.

2.3 System Description

A summary schematic of the complete water/steam and sodium loops which includes the results of the subsystem design effort and serves as the baseline configuration is shown in Figure 2-6. In addition to the piping network information presented in Figure 2-1, this schematic illustrates the circulation loop between the storage tanks and the tower mounted receiver along with the receiver temperature conditions. As indicated, the inlet receiver flow is

PARALLEL ORGANIC RANKINE CYCLE

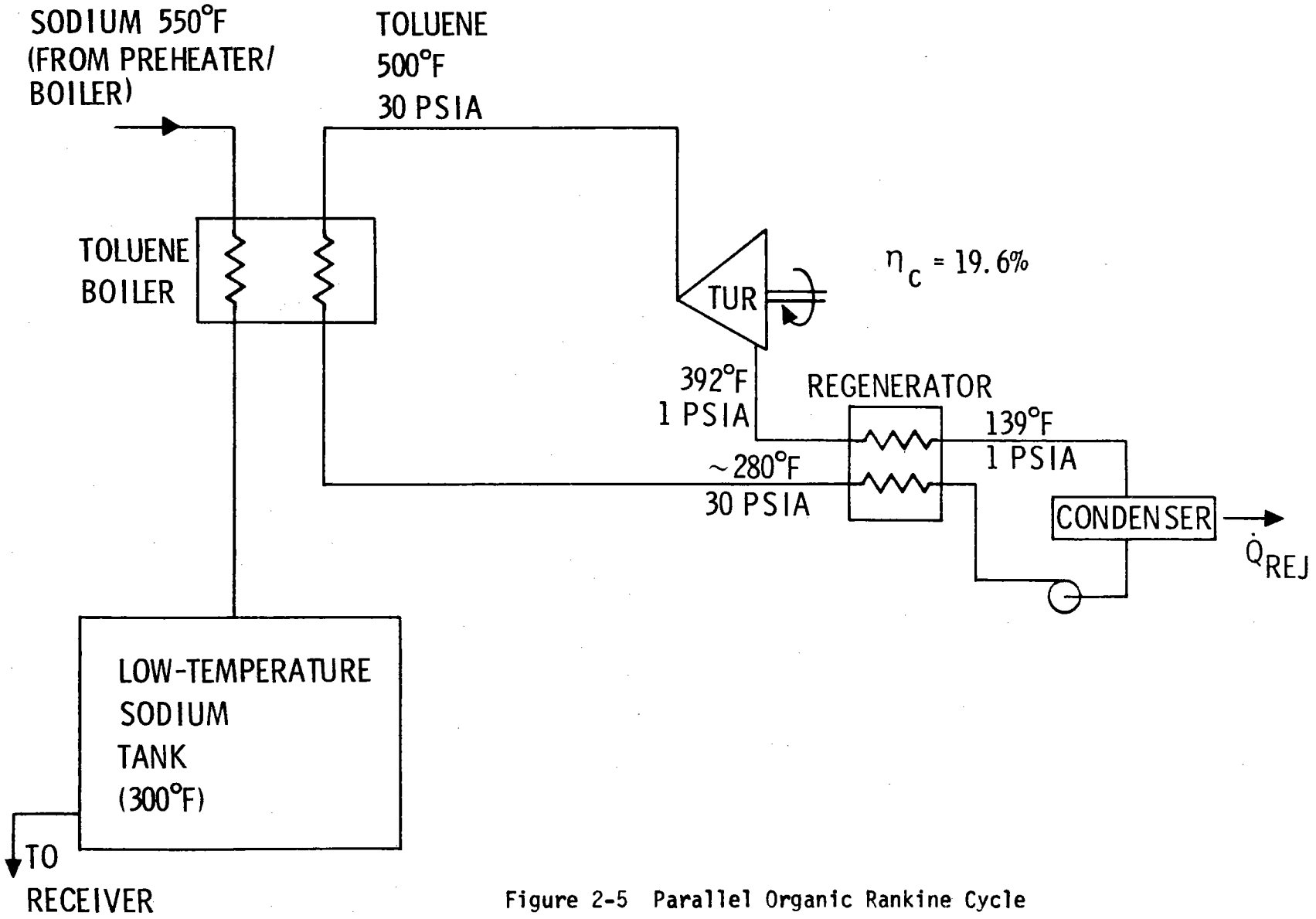

Figure 2-5 Parallel Organic Rankine Cycle

LIQUID SODIUM SYSTEM SCHEMATIC (REVISED BASELINE)

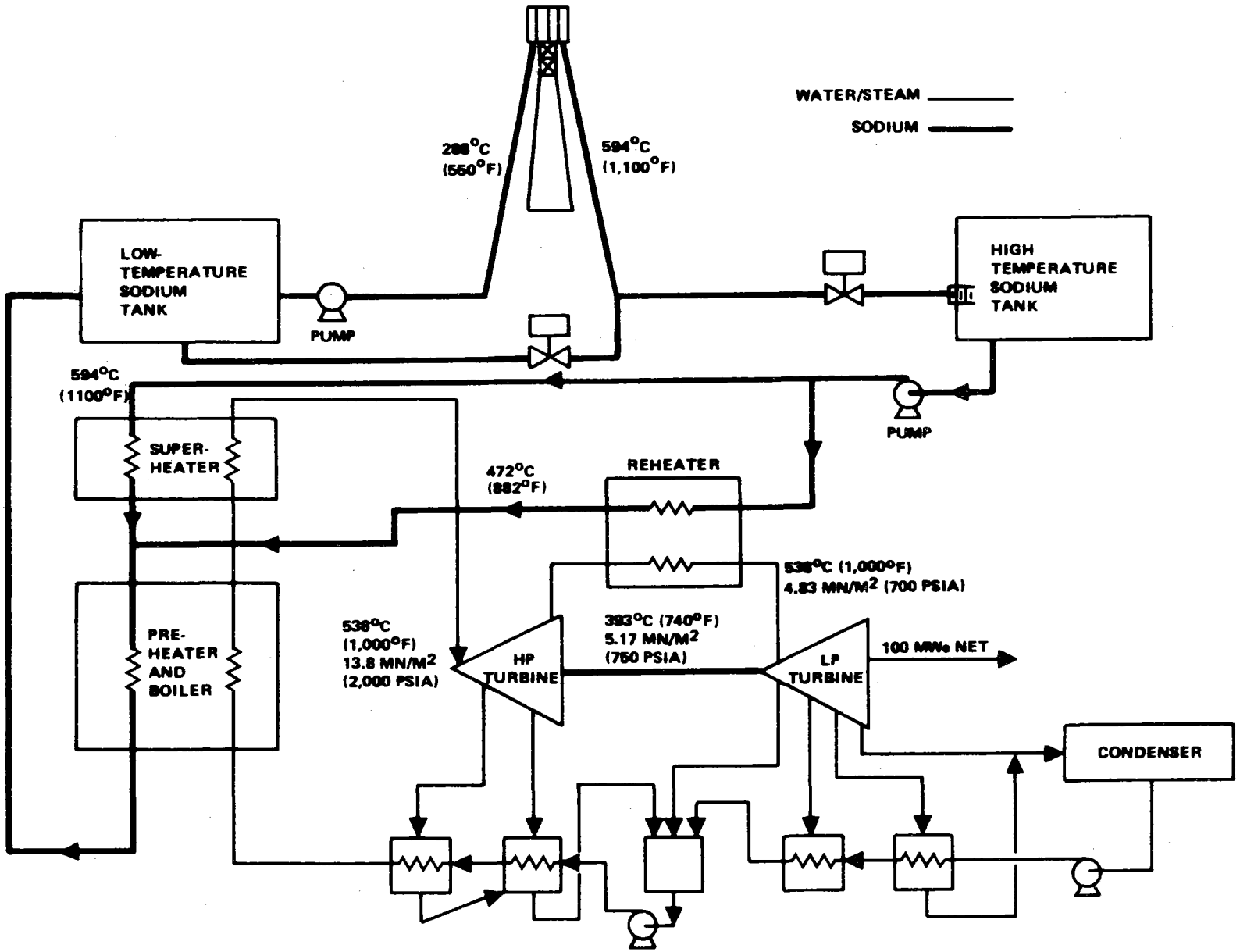

Figure 2-6. Liquid Sodium System Schematic (Revised Baseline)

drawn directly from the low pressure, low temperature sodium storage tank with a pump at the tank outlet providing the necessary head required for circulation. After absorbing the required heat energy in the receiver unit, the hot sodium travels through the downcomer, through a pressure reducing device and into the low pressure, high temperature storage tank. A pump at the outlet of the high temperature tank propels the sodium to the heat exchangers at the rate required to provide the nominal 100 MWe output.

A summary tabulation of the principal system level design and performance characteristics is shown in Table 2-2. This information represents data developed as a result of both system and subsystem design analyses carried out in response to the overall system requirements defined in Table 2-1 and the water/steam and sodium loop characteristics derived and discussed in Section 2.2. The subsystem design activities which led to many of these characteristics are described in the subsequent sections of this report.

Table 2-2

LIQUID SODIUM CENTRAL RECEIVER SUMMARY DATA

Net Electrical Power, MWe	100
Parasitic Power, MWe	
• Day	13
• Night	6
Insolation, W/m^2	950
Solar Power Absorbed, MWt	475
Plant Net Efficiency, %	22.3%
Collector Field Configuration	Single 360°, North Biased
Solar Multiple, Equinox Noon	1.66
Number of Heliostats	20,580 (Inverted)
Heliostat Shape and Size, m (ft)	Square, 6.5m x 6.5m (21.3 x 21.3 ft)
Number of Towers/Receivers	1
Receiver Mid-Point Elevation	258 m (846 ft)
Receiver Configuration	External Cylinder
Number of Receiver Panels	24
Receiver Height and Diameter, m (ft)	17 x 17 m (56 x 56 ft)
Receiver Maximum Heat Flux, MW/m^2	1.7
Sodium Temperatures, °C (°F)	288/593 (550/1100)
Receiver Sodium Flow Rate, Kg/Hr (lb/hr)	4.47×10^6 (9.83×10^6)
Thermal Storage Capacity, MWth	1610 (6 Hrs at 100 MWe)
Total Sodium Inventory, Kg (lbs)	15.3×10^6 (33.6×10^6 lbs)
Steam Generator and Reheater Type	Modular Steam Generator
Steam Conditions, MN/m^2, °C (psia, °F)	
Initial	13.8, 538°C (2000, 1000°F)
Reheated	4.8, 538°C (700, 1000°F)
Steam Flow Rate, Kg/Hr (lb/hr)	
Daytime	3.62×10^5 (7.962×10^5)
Nighttime	3.391×10^5 (7.460×10^5)
TSS Sodium Flow Rate, Kg/Hr (lb/hr)	2.69×10^6 (5.92×10^6)
Feedwater Temperature, °C (°F)	205 (400)
Turbine Back Pressure, MN/m^2 (in. Hg)	.009 (2.5)
Heat Rejection MW (Btu/Hr)	
Daytime	173 (590×10^6)
Nighttime	162 (553×10^6)

3.0 ELECTRICAL POWER GENERATION SUBSYSTEM

The Electrical Power Generation Subsystem (EPGS) includes all of the equipment necessary to convert the incoming thermal (steam) power into electrical power output which is compatible with the utility grid. In addition to the turbine and generator, this subsystem includes the feedwater heaters, condenser, cooling towers, water treatment equipment, and the electrical transformers and switch gear. With the exception of the turbine,which assumed some additional design growth in inlet pressure capability over current state-of-the-art turbines, the balance of the equipment identified above was assumed for this exercise to be conventional "off the shelf" items. This assumption was valid since conventional components are based on a well established technology. Deviation from this technology base would require additional development work.

3.1 Requirements

From a functional interface standpoint, the EPGS must interface with the steam generation and reheat equipment on its upstream side as shown in Figure 2-6 and be compatible with the utility grid on the output side. A summary of the principal operating requirements for the EPGS is shown in Table 3-1. It is seen that the net electrical output is identical for daytime and nighttime operating periods, although the gross output differs by $\sim$ 7 MWe. This difference is due to the difference in plant parasitic loads between daytime and nighttime operation. The turbine steam conditions, steam flow rates, heat rejection, and turbine exhaust pressure are identical to those discussed in Section 2. The generator output characteristics are typical of existing generators in the 100 MWe size range. The main transformer requirements are based on an assumed 115 KV utility grid voltage. The feedwater conditioning requirements are consistent with those established for single pass to superheat equipment.

Table 3-1

ELECTRICAL POWER GENERATION SUBSYSTEM OPERATING REQUIREMENTS

Gross Turbine-Generator Output	
• Daytime	113 MWe
• Nighttime	106 MWe
Net Turbine-Generator Output	
• Daytime	100 MWe
• Nighttime	100 MWe
Turbine Inlet Steam Conditions	
• High Pressure (Throttle) Steam	538°C (1000°F) 13.70 MPa (2000 psia)
• Low Pressure (Reheat) Steam	538°C (1000°F) 4.83 MPa (700 psia)
Maximum Turbine Inlet Flow Rate	.362 x 10^6 Kg/Hr (.796 x 10^6 lb/hr)
Heat Rejection	
° Method	Wet Towers
° Wet Bulb Temperature	23°C (73°F)
° Daytime	173 MWt (590 x 10^6 Btu/Hr)
° Nighttime	162 MWt (553 x 10^6 Btu/Hr)
Turbine Exhaust Pressure	8.46 kPa (2.5 in-Hg)
Generator Output	
° Generator Rating	135,000 KVA
° Power Factor	0.90
° Voltage	13,800 Volts
° Frequency	60 Cycle

Table 3-1

ELECTRICAL POWER GENERATION SUBSYSTEM OPERATING REQUIREMENTS

(Continued)

Main Transformer	
• Rating	130,000 KVA
• Voltage	13.8/115 KV
Feedwater Conditioning	
• Dissolved Solids	20-50 ppb
• pH	9.5

In addition, the turbine must be capable of withstanding daily startup and shutdown cycles over the 30-year plant operating life. This condition translates into a 10,000 cycle life which imposes operating restrictions on the rate of change of metal temperature in the turbine. In a similar sense, operating restrictions imposed by manufacturers of other elements of the EPGS must also be considered in the overall operation of the system.

3.2 Description

The principal characteristics of the major EPGS components are contained in Table 3-2. Components contained in this table include the turbine, generator, condenser, cooling tower, feedwater heaters, and water treatment equipment.

The basic turbine configuration selected for this system is a tandem compound, double-flow, extraction, condensing turbine designed to operate at a back pressure of up to 16.92 kPa (5 in-Hg). The gross heat rate for the turbine when operating at 8.46 kPa (2.5 in-Hg) has been estimated to be 8640 BTU/KWH. Machines of this type are capable of accepting a 10% overflow condition at the turbine inlet with a corresponding increase in electrical power output of $\sim$ 9%. The 50.8 cm (20 in) last stage buckets were selected to provide an adequate sized flow passage to permit the overflow capability since the last stage buckets, in general, represent the critical flow passage in determining permitted turbine flow.

From an operational standpoint, the turbine throttle valves will be controlled in an initial pressure control mode where the valves control the upstream pressure. This is a widely used control mode when using single-pass-to-superheat steam generation equipment. In order to vary the power output of the turbine generator, the sodium flow to the steam generators must first be changed which will cause a change in steam side pressure. The turbine valves then react by opening or closing, as required, in order to maintain the original set point pressure. As a result of the valve adjustment, a corresponding change in the turbine generator output occurs.

Table 3-2

ELECTRICAL POWER GENERATION SUBSYSTEM DESIGN SUMMARY

Turbine	
Type	Tandum Compound, Double-Flow, Extraction, Condensing Turbine
Rating	113,000 KWe
Heater Extractions	5
Shaft Speed	3600 RPM
Last Stage Bucket Size	50.8 cm (20 in)
Throttle Flow Control Mode	Initial Pressure Control
Generator	
Generator Rating	130,000 KVA
Power Factor	0.9
Output Voltage	13,800 Volts
Frequency	60 Hz
Cooling	Hydrogen Cooled
Exciter	Static Excitation System
Shaft Speed	3600 rpm
Condenser	
Type	Shell and Tube, 2-Pass
Surface	9431 m^2 (101,500 ft^2)
Tube Material	90-10 Copper Nickel
Tube Diameter (O.D.)	22.2 mm (.875 in)
Tube Wall Thickness	0.89 mm (.035 in) 20 BWG
Tube Length (Effect)	8.54 m (28 ft)
Condenser Pressure	8.46 kPa (2.5 in-HgA)
Heat Rejection	173 MW (590 x 10^6 BTU/Hr)
Cooling Water Flow	5.3m^3/s(84,250 gpm)

Table 3-2

ELECTRICAL POWER GENERATION SUBSYSTEM DESIGN SUMMARY

(Continued)

Condenser (Cont'd)	
Water Velocity	2.13 m/s (7.0 fps)
Cooling Water In	31.1°C (88.0°F)
Cooling Water Out	39.0°C (102.0°F)
Condenser Air Removal	Mechanical Vacuum Pump (2-full capacity)
Cooling Tower	
Quantity	One
Type	Mechanical Draft, Cross Flow
Number of Cells	5
Fan Motor Size	5-150 kW (200 HP)
Design Wet Bulb Temperature	23°C (73.4°F)
Cold Water Temperature	31.1°C (88.0°F)
Hot Water Temperature	39.0°C (102.0°F)
Circulating Water Flow	5.3 m^3/s (84,250 gpm)
Heat Rejection	173 MW (590 x 10^6 BTU/Hr)
Feedwater Heaters	
Low Pressure Heater (1)	Horizontal, Stainless Steel Tubes, Carbon Steel Shell with Drain Cooler, Max Tube Side Pressure - 2.2 MPa (320 psia)
Deaerator (1)	Stainless Steel Trays and Vent Condenser, Carbon Steel Shell, Horizontal Condensate Storage Section [75.7 m^3 (20,000 gal)] Pressure Rating - 0.45 MPa (65 psia)

Table 3-2

ELECTRICAL POWER GENERATION SUBSYSTEM DESIGN SUMMARY

Feedwater Heaters (Cont'd)	
High Pressure Heaters (3)	Horizontal, Carbon Steel Tubes, Carbon Steel Shell with Drain Cooler, Max Tube Side Pressure - 17.23 MPa (2500 psia)
Feedwater Treatment	
Equipment	
• Inline Polishing Demineralizers	2 Full-Capacity Units
• Makeup Water Demineralizers	2 Full-Capacity Units
Chemicals	
• pH Control	Ammonia
• Oxygen Scavenger	Hydrazine

The condenser design was developed in accordance with Heat Exchanger Institute Standards for Steam Surface Condensers. It was sized to condense the turbine exhaust at the daytime design point steam flow. The principal issue involved in specifying the condenser design centers on tube material selection. The standard designs use either copper alloys or stainless steel. The use of copper in the feedwater circuit can lead to possible copper deposition problems in the once through steam generation equipment or on the turbine blades since Cu can be picked up in the feedwater and carried to other parts of the system. Stainless steel on the other hand is subject to pitting failures due to impurities in the cooling tower circulating water, particularly when high solids concentrations are maintained in the circulating water system in order to minimize the blowdown requirements. Also, pitting failure in stainless steel is accelerated when systems experience frequent shutdowns. Even though the system would be shutdown for some period each day, the cooling water circulation pumps would have to be kept operating at all times if stainless steel tubes were used. In view of the apparent problems with stainless steel, it was decided to use 90-10 copper-nickel tubes in the condenser. Since full-capacity inline polishing demineralizers would be located downstream of the condenser, the possibility of copper carryover through the demineralizer units was considered minimal.

The method of heat rejection selected for this system is a mechanical draft, wet cooling tower. The specific configuration involves five cross flow cells with the air circulation in each cell being provided by a 150 kW (200 HP) fan. The tower structure would be made of redwood or treated fir, with wood or PVC being used as fill material. The water basin would be concrete. A continuous blowdown of the cooling tower circulation water would be maintained to control the level of dissolved solids. The actual blowdown rate which contributes to the makeup water requirement, is determined by the evaporation rate, the drift rate, and the number of cycles of concentration to be maintained in the tower circulating water. Typical blowdown rates of 6.3×10^{-3} m^3/sec (100 gal/min) to 1.58×10^{-2} m^3/sec (250 gal/min) would be expected, with makeup water requirements being in the range of 0.075 m^3/sec (1200 gal/min) to 0.0884 m^3/sec (1400 gal/min).

In defining the feedwater heaters, the principal issue involved tube materials selection. Carbon steel was selected for the high pressure heaters, downstream of the deaerator, to maintain a copper-free system down-stream of the polishing demineralizers. This was done to minimize the possibility of copper pickup in the feedwater loop. Stainless steel tubes were considered for the high pressure heaters, but recent reports of stress corrosion in similar devices ruled out the use of stainless steel. Stainless steel tubes were selected, however, for the low pressure heater, upstream of the deaerator, since it is the only practical non-copper material which can withstand the high feedwater dissolved oxygen content. The shells for both the high and low pressure heaters were chosen to be carbon steel since they are not in direct contact with stream or condensate with a high dissolved oxygen content. In addition, corrosion allowances are included as part of the shell design practice. All of the internal elements of the deaerator are made of stainless steel to minimize corrosion and a carbon steel shell with corrosion tolerance is employed.

The inline polishing demineralizers and makeup water demineralizers are necessary to insure that no significant suspended or dissolved solids are retained in the feedwater that can deposit in the steam generator tubes or on the turbine blades. The presence of these unwanted solids is inevitable due to corrosion in the feedwater cycle which occurs even though deaeration and pH control are maintained. The heart of the demineralizer is an ion exchange unit.

The two basic types of demineralizers employ either a deep bed or powdered resin. The deep bed unit uses bead-form strongly acidic cation exchange resins and strongly basic anion exchange resins in a mixed bed configuration to remove impurities from the water by ion exchange and filtration. The powdered resin unit employs a thin layer of powdered resin deposited on a nylon or stainless steel septum. It also removes impurities by ion exchange and filtration. In the case of the deep bed unit, regeneration is accomplished with acid and sodium hydroxide flushing. For the powdered resin unit, regeneration is accomplished by removing the old powdered resins and replacing them with new resins

From an itinial cost standpoint, the powdered resin units are less expensive because no separate regeneration equipment is required and initial resin inventory is low. Ultimate costs of the powdered resin approach depend on the frequency of resin replacement required. The powdered resin unit is somewhat more effective as a filter than the deep bed unit; however, it has very little reserve ion exchange capacity. In the event of a small condenser leak, operation could not be maintained for any significant period of time with a powdered resin unit. In addition, because of dialy startup which accentuates the problem of suspended solids, it is anticipated that use of a powdered resin unit would result in an extremely high resin consumption. Because of the anticipated high suspended solids loading and the possibility of a condenser leak, a deep bed unit was selected for this facility.

4.0 COLLECTOR SUBSYSTEM

The Collector Subsystem includes all of the equipment necessary to redirect available insolation on to the receiver absorbing surfaces. The principal elements of this subsystem are the heliostats, the field controllers, and the power distribution/data bus network. Since the principal hardware elements of the Collector Subsystem were defined in conjunction with the larger water/steam effort, the remaining task is to determine the optimum collector field layout (based on the goal of minimizing the cost of energy on an annual basis) and size which satisfies the power flow demand for the rest of the system.

The heliostat configuration assumed for this analysis is of the type shown conceptually in Figure 4-1. The reference heliostat is composed of six reflector panel assemblies, a reflector support structure, drive assembly, and pedestal with buried foundation. The reflector panel assemblies are each mounted to the supporting structure at four points. It is possible to create a large flat composite reflector, made up of six panel assemblies, or to make a heliostat with some focusing capability by tipping or canting the panels so that superimposed panel images occur at the focal point. The desired canting can be accomplished by selectively shimming the attachment points. Due to the long optical path lengths encountered with this system, the canted panel option was not used since the beam size is governed primarily by the finite size of the sun at long optical path lengths. As indicated in Figure 4-1, the panels are arranged so that a slot is created through the center of the reflector of sufficient width to permit inverting of the reflector assembly during non operating periods.

The drive unit incorporates two rotary drives which provide azimuthal and elevation tracking motions. The drives convert high rpm motor motion into the slow heliostat drive rates by means of a $\sim$ 42,000:1 gear reduction. The motors themselves are 230 V, 3-phase which are operated in a pulsed manner. Power pulses to the individual motors are controlled by the field controller which continually calculates the heliostat pointing error based on the difference between perfect orientation and the input from the sensing equipment.

HELIOSTAT AND SENSOR POLE ASSEMBLY

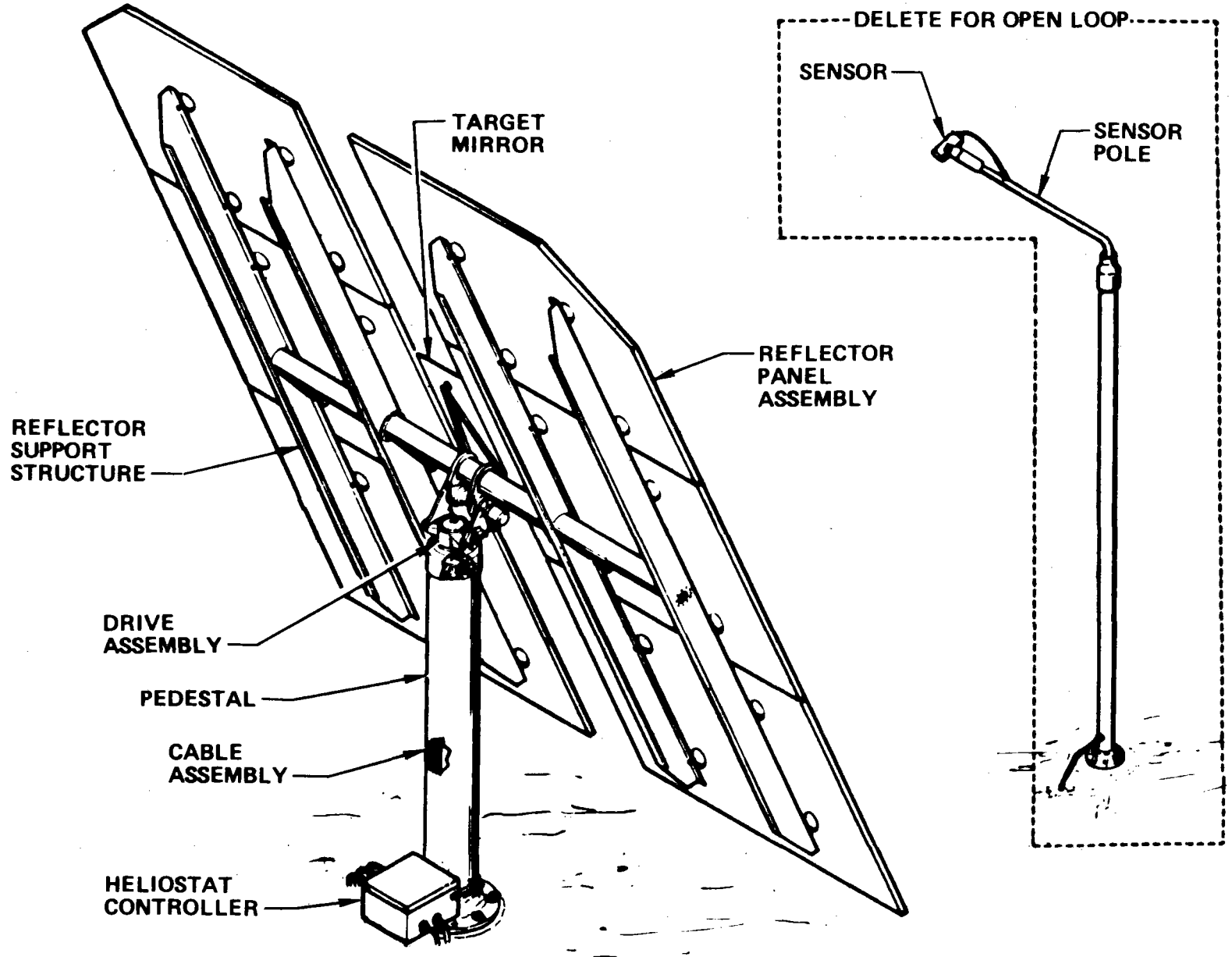

Figure 4-1 Heliostat and Sensor Pole Assembly

Either closed loop or open loop sensing control is permitted with the design. The optional beam sensor and sensor post configuration places the sensor in the line of sight to the receiver. By viewing the image of the sun and the apparent motion of that image in the target mirror, the sensor produces tracking error signals that are processed and sent to the drive motors in the form of voltage pulses. In the case of open loop control, the position of the heliostat is determined by either measuring the position of the mirror directly from the drive output or by counting motor shaft turns. By comparing the measured mirror position to the ideal position required to perfectly track the sun, which is calculated based on the sun position and heliostat location, an error signal is developed which is processed and sent to the drive motors as voltage pulses to initiate a corrective motion.

The function of the field controller is to develop pulsed voltage inputs to the drive motors of each heliostat with the duration of the pulse being determined by the measured error signal in the case of the closed loop control or the calculated error signal in the case of open loop control. Since one field controller processes information for 24 heliostats under its control, the pulsed drive signals are serialized and separated at the individual heliostat by the heliostat controller.

Before discussing the collector subsystem layout and optimization analysis, it is appropriate to review the design and performance requirements which must be satisfied by the collector subsystem hardware.

4.1 Requirements

The performance, design, and operational requirements for the overall collector subsystem and the individual hardware components were determined, for the most part, as a result of system design trade studies and site environmental factors. From an overall system standpoint, the collector field must be sized to collect sufficient thermal energy to power a 100 MWe system with a six hour storage capability in a cost effective manner. This requirement resulted in a series of performance and economic trade studies discussed in the next section.

From the environmental standpoint, two sets of subsystem requirements were established. The first set,which is termed an operational requirement, consists of a wind speed and ambient temperature limit at which the heliostats must be capable of operating within a specified accuracy. The second set of environmentally related requirements represents conditions which must be survived by the collector equipment without any degradation. A summary of the environmentally related operational and survival requirements is presented in Table 4-1. The operational conditions were determined by considering the economic impact of designing the heliostats to withstand successively more severe conditions as compared to the economic value of the energy that would be lost if the design modifications were not made. The studies were carried out using available correlations of solar insolation versus wind speed and the frequency of wind speed occurrence for 12 southwestern desert sites. The final values of operation wind speed and temperature were selected on the basis of minimum cost of energy on an annual basis. It should be pointed out that the heliostats are capable of operating at higher wind conditions and temperatures outside the indicated operational range. However, structural distortion would result in an image which is not within the specified accuracy.

From a subsystem survival standpoint, the conditions shown in Table 4-1 represent a compilation of the most severe conditions experienced at representative desert sites over a 50 year period. In general, these conditions will require the heliostat to be stowed to a minimum damage orientation which would depend on the nature of the environmental factors involved.

In addition to the requirements just discussed, the heliostats must be operated in a safe manner from the standpoint both of moving equipment and hazards associated with reflected beams. Wherever existing safety codes exist, the collector equipment will be designed to comply with such standards. In areas where no standards have been established, such as in the area of redirected beams, an effort will be made to use conservative operating practices.

Table 4-1

COLLECTOR SUBSYSTEM ENVIRONMENTAL DESIGN REQUIREMENTS

Within Operational Specification	
Temperature	0-40°C (32 - 104°F)
Wind Speed - Sustained	12.4 m/s (27.7 mph)
- Gusting	16 m/s (36 mph)
Survive	
Temperature	- 20 → 60°C (-4 → 140°F)
Wind Speed - Gusting	40 m/s (90 mph)
Seismic Acceleration	0.33 g Horizontal
Precipitation	
Rain (Average Annual)	200 mm (8 in)
(Max 24 hr Rate	75 mm (3 in)
Snow Load	250 Pa (5 psf)
Sleet Buildup	50 mm (2 in)
Hail (Any Orientation)	20 mm (.75 in) at Terminal Velocity
(Vertical Stowed Position)	25 mm (1 in) at Terminal Velocity

4.2 Collector Subsystem Analysis and Trade Studies

For the purpose of discussion, the analysis involved in defining the Collector Subsystem can be subdivided into two efforts. The first effort is related to defining the most cost effective field arrangement or shape, while the second effort involves the definition of the actual collector field capacity. This latter effort involves matching the actual collector field capacity with the capability of the turbine and thermal storage to accept the energy flow from the receiver. Although these two activities are treated separately in this report, they are actually interrelated and must be considered on a simultaneous basis during the actual analysis.

In defining the overall collection field layout, a trade study was carried out which considered all of the cost and performance aspects of the heliostats in the collector field, the receiver, and the tower/vertical piping. From a heliostat standpoint, these factors include hardware, land, and wiring costs, adjacent heliostat blocking and shadowing, reflective surface and tracking accuracies, and cosine effects. The receiver factors include hardware costs (as influenced by size and weight), heat loss, and beam interception. Tower and piping factors include cost factors as a function of tower height and power level.

The analysis starts by considering a large collector field subdivided into a series of computational cells in which locally optimum heliostat spacing arrangements are established. The cells are then ordered in terms of decreasing performance and sequentially added to the assumed tower and receiver. With the addition of each new cell, a revised figure of merit is calculated which is a measure of the annual cost of thermal energy for the composite collector field, receiver, and tower configuration existing that point in time. As more and more cells are sequentially added to the collector field, the figure of merit continues to decrease until a minimum value is reached which determines the collector field layout appropriate for the particular receiver and tower.

The resulting power output characteristics of the collector field/receiver over a complete one year cycle are compared with the ability of the balance of the system to accommodate the power flow in an economically optimum fashion. If a mismatch occurs, an adjustment in tower height and receiver size is made,and the process is repeated until the predicted output of the collector field matches the ability of the rest of the system to accept the power flow. All such collector field analyses are optimized on an annual energy basis.

A plot plan of the optimized collector field along with pertinent sizing data is shown in Figure 4-2. The collector field surrounds the central exclusion area which contains the tower, thermal storage, and balance of plant equipment. The exclusion area in turn is shifted slightly to the south of center in order to optimize the annual collection of energy. The irregular field outline results from the cell-by-cell computational approach which deletes marginally performing cells. In reality, the field outline would be defined with a smooth curve which would approach an ellipse. The heliostats within the field would be arranged in a radial stagger layout to produce the maximum performance per unit glass area on an annual basis for most areas of the field. The field would actually be laid out along complete circles or continuous arcs with alternate rows being staggered relative to their neighbors. The density of the field would vary continuously from approximately 45 percent near the tower exclusion to approximately 13 percent along the northern edge.

A summary of the energy collection characteristics for the baseline collector field is shown in Table 4-2 for representative days throughout the year. The second column indicates the total energy collection capability of the collector field/receiver for the indicated day. Implicit in these values are the period of effective collection for the indicated day and an insolation of 950 W/m^2. As indicated, the collected energy is allocated to direct turbine operation which occurs when the receiver and turbine are operating simultaneously (even though all receiver power first goes to thermal storage) or as an excess value which accumulates in thermal storage). During the summer periods of

SODIUM SYSTEM FIELD LAYOUT

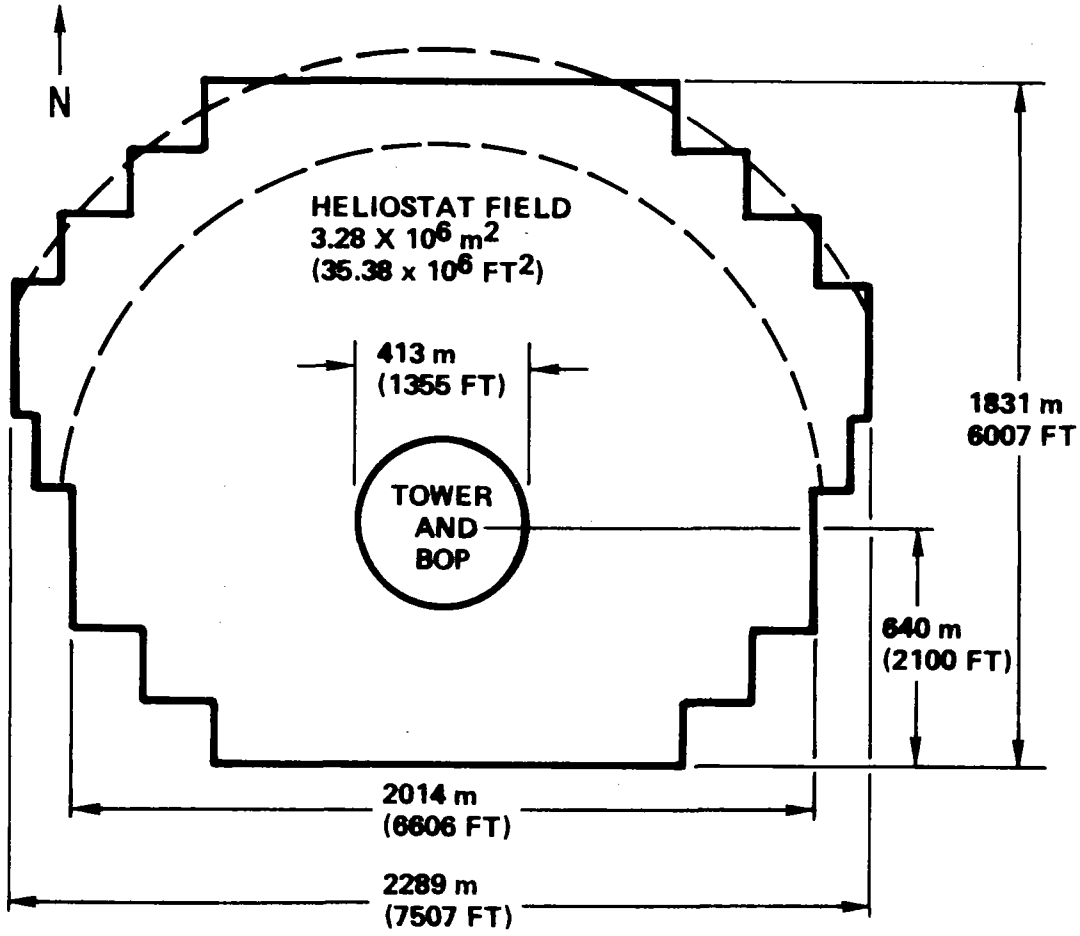

- RADIAL STAGGER ARRAY
- OPTIMUM ANNUAL ENERGY TRIM
- RECEIVER CENTERLINE ELEVATION
  258 m (846 FT)
- TOWER TOP ELEVATION
  232 m (761 FT)
- GLASS AREA
  781,000 m^2
- NUMBER OF HELIOSTATS
  20,580

Figure 4-2 Sodium System Field Layout

Table 4-2

SYSTEM PERFORMANCE SUMMARY

DAY	TOTAL COLL CAPABILITY (MWHt)	DIRECT TURBINE OPER (100 MWe)		EXCESS ENERGY (MWHt)	ENERGY TO STORAGE (MWHt)	PERIOD OF OPER FROM STORAGE - 100 MWe - (HR)	SPILLAGE	
		REQ'D ENERGY (MWHt)	PERIOD (HR)				(MWHt)	(%)
JUN 21	5035	3317	11.6	1718	1610	6	108	2.1
MAY 21/ JUL 21	4951	3233	11.3	1718	1610	6	108	2.2
APR 21/ AUG 21	4669	3006	10.5	1663	1610	6	53	1.1
EQUINOX	4209	2722	9.5	1487	1487	5.5	0	0
FEB 21/ OCT 21	3551	2325	8.1	1226	1226	4.6	0	0
JAN 21/ NOV 21	2972	2013	7.0	959	959	3.6	0	0
DEC 21	2696	1871	6.5	825	825	3.1	0	0

ANNUAL CHARACTERISTICS:

- ACTUAL THERMAL ENERGY COLLECTION* 1.32×10^6 MWHt
- MAXIMUM COLLECTION CAPABILITY* 1.33×10^6 MWHt
- ANNUAL ELECTRICAL PRODUCTION* 472×10^3 MWHe NET
- SPILLAGE 0.75%

*35 CLOUDY DAYS UNIFORMLY SPACED

operation, the excess energy actually exceeds the ability of the thermal storage subsystem to accept the energy. This condition would result in spillage of some of the collectable energy by selectively deactivating a small portion of the collector field or by increasing the heat rejection rate. During this period, it is seen that a full six hour storage charge level is accomplished. By contrast during the winter periods of operation, the shorter collection day and poorer collector field geometric factors result in an under collection capability. This is apparent from the tabulated values for winter operation. It is seen that when the turbine is operated at its design point level during the normal daylight hours, insufficient excess energy is available to completely charge the thermal storage. This type of summer over-collection and winter under-collection characteristic is an anticipated result of an optimization study based on annual energy considerations.

From an annual performance standpoint, pertinent summary data appear at the bottom of Table 4-2. The "actual thermal energy collection" entry corresponds to the thermal energy that actually passed through thermal storage and the turbine. The maximum capability corresponds to the maximum level of annual energy which could be collected by the collector field/ receiver. The annual electrical production represents the net electricity produced by the system after the system parasitic loads have been considered. Implicit in the annual energy numbers are 35 days when the system is assumed to be down either due to the occurrence of clouds or for maintenance reasons. The annual spillage estimate for this configuration is $\sim$ .75% of the total collection capability.

4.3 Collector Subsystem Description

The Collector Subsystem which is composed of 20,580 heliostats laid out in an arrangement defined in Figure 4-2 is capable of creating a variety of heat flux profiles on the receiver surface depending on heliostat aim strategy used. Due to the high heat transfer capability of the sodium, the receiver is capable of accommodating the heat flux which would result from

a one-point aim strategy, i.e., all heliostats aimed at the nearest point to the heliostat on the equator of the cylindrical receiver. The peak heat flux which results on the equator of the north facing side of the receiver is $\sim 1.67\ MW/m^2$. If excessive tube temperature conditions were to occur, it would be possible to reduce the flux peak by adopting a multiple aim strategy to distribute the flux vertically. The baseline design, as discussed in Section 5, does not require the use of a multiple aim strategy since the receiver is capable of accommodating the peak flux which results from a single aim point strategy.

From an overall field performance standpoint, the diurnal variations in absorbed power are shown in Figure 4-3 for representative days of each month throughout the year. The curves, which were developed for a constant insolation level, include both cosine and blocking/shadowing effects of the collector field in addition to receiver interception and receiver heat losses from the receiver. The curves indicate the relatively high performance of the collector field during the spring-summer-fall period with some fall-off in performance being experienced during the winter period due to reduced field cosine and blocking/shadowing effects.

Design details for the collector subsystem and the heliostat hardware are summarized in Table 4-3. The entries in the "general" category refer to the complete subsystem as it interacts with the receiver. The items specified under the "heliostat" entry refer to the characteristics of a specific heliostat which makes up the collector field.

4.4 Aiming Strategy

Aiming all heliostats at a point centered in the receiver produces disproportionately high fluxes on the lower half of the receiver and accompanying low interception factors for close in heliostats. An improved aiming strategy is to aim each heliostat at the vertical center of the nearest receiver element, i.e. at the equator or "belt" of the receiver. This produces a nominally symmetric vertical distribution and the best possible interception factor.

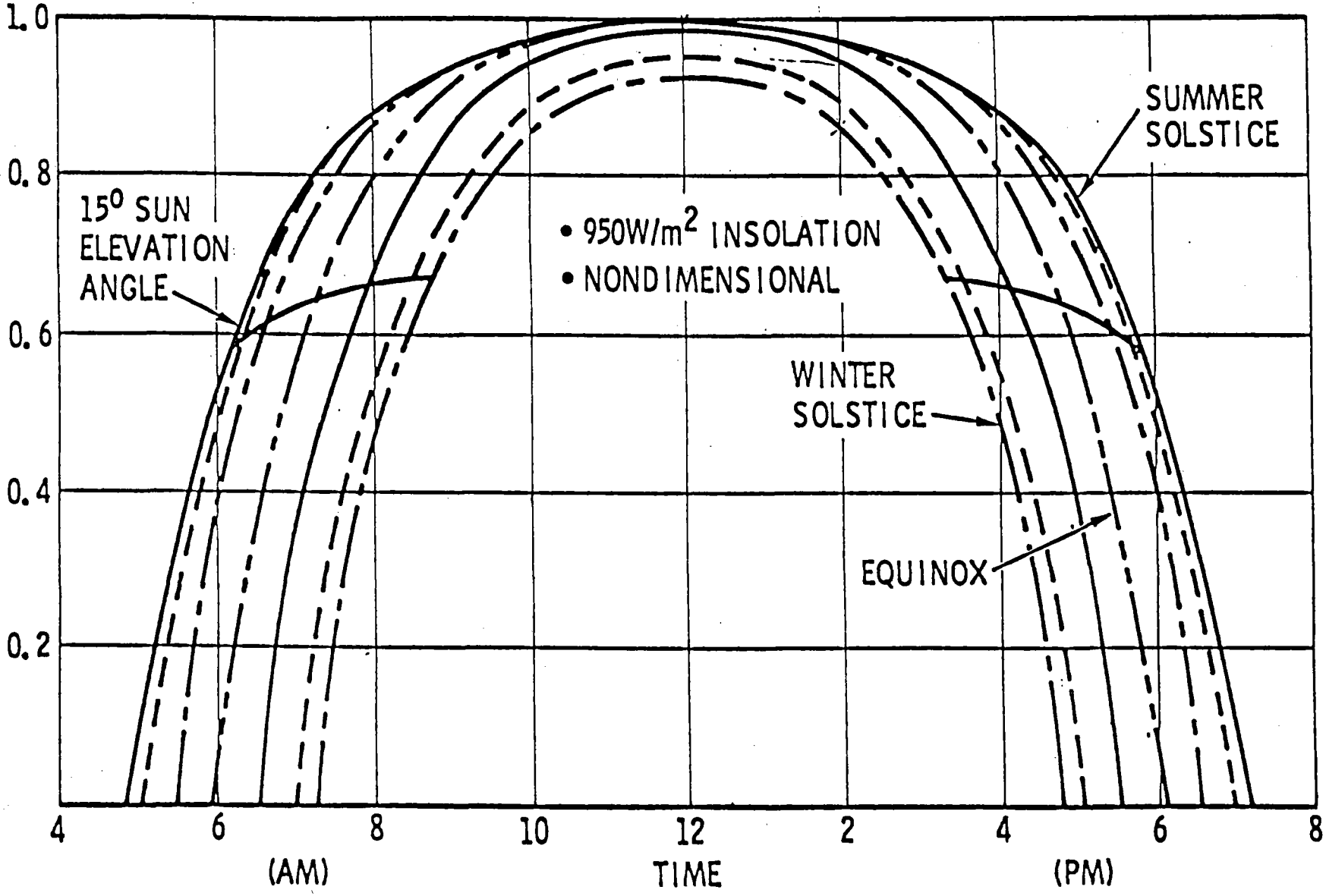

Figure 4-3 Diurnal Variations in Absorbed Thermal Power

Table 4-3

COLLECTOR SUBSYSTEM SUMMARY

General	
Total Field Area	$3.28 \times 10^6 m^2$ (35.4×10^6 ft^2)
Number of Heliostats	20,580
Total Minor Area	781,000 m^2 (8.40×10^6 ft^2)
Annual Collectable Energy	1.33×10^6 MWHt
Tower Height	232m (761 ft)
Receiver Centerline Elevation	258m (846 ft)
Heliostat Arrangement	Radial Stagger
Aim Strategy	1-point, Equator
Heliostat	
Reflector Shape	Square - 6.5 x 6.5m (21.3 x 21.3 ft)
Minor Type	Second Surface Silvered Float Glass
Minor Area	37.95m^2 (408 ft^2)
Reflectivity	0.91
Drive System	
Elevation	Orbidrive, 3ϕ 230 VAC
Azimuth	Orbidrive, 3ϕ 230 VAC
Reflected Beam Accuracy	3mr, 1σ
Drive Rate	
Elevation	15°/min
Azimuth	5°/min

The lower flux capabilities of the water/steam receiver led to the choice of a receiver height of 25.5 m and a diameter of 17 m for that case. A rather crude defocusing strategy was adequate to redistribute the flux with minimal spillage on this large receiver surface (1362 m^2). The higher flux capabilities of the liquid sodium receiver make an "aim at the belt" strategy feasible, although the resulting peak flux is marginally high. Improved receiver efficiency results from reducing the receiver length to 17 m. (surface area 908 m^2). The interception loss increases slightly, but reductions in radiation and conduction losses more than compensate. In the balance of this section, we will discuss an improved aiming strategy called the high-low aim strategy which reduces the peak flux substantially, even for this shortened receiver. This reduced peak flux makes it possible to consider further reduction of the surface area of the receiver to 801 m^2 by reducing the receiver diameter to 15 m. Associated with reduced radius is an increase in the peak flux. For the "aim at the belt" strategy the peak flux is excessive, but the high-low aiming strategy makes this 15 m dia x 17 m tall receiver a viable candidate for future consideration, having advantages of reduced weight, cost, and thermal losses.

The first completed iteration on the collector field given by our optimization program for the 100 MWe commercial baseline Solar Tower System was used for the generation of flux profiles for a 17 m diameter by 17 m high cylindrical sodium cooled receiver. This field is not the most current optimized field but is comparable in heliostat density, with 26.3 per cent ground coverage. Also, shading and blocking, which vary with heliostat spacing, have neglible effect on the images produced at noon on vernal equinox. Only .8 percent of the energy is lost at this time of day due to shading and blocking. Thus, the flux profiles of the high-low aim strategy are representative of the type of performance that may be expected from the smaller sodium receiver and a specially optimized collector field.

The high-low aiming strategy developed involves aiming alternate heliostats above and below the target utilized by the one point strategy (where the center of each image is directed to the belt of the receiver). The amount of this shift, s, is given in meters on an image plane whose normal is parallel to the incoming central ray of the image. The formulation is as

follows:

$$s = (\frac{h}{2})(\cos\phi) - C_1(R + (\alpha_L + C_2)\ \ell)\ , \text{ where}$$
$$s \geq 0$$

h is the height of the receiver and ϕ is the elevation angle of the receiver from a point in the collector field. The term after the minus sign represents the radius of the image. R is the rms radius of the heliostat. ℓ is the slant distance to the receiver. α_L is the limb angle of the sun, and C_2 represents the limb angle of an appropriate image degrading function. By adjusting the parameters C_1 and C_2, thereby controlling the estimated image size, a two point aim can be developed. The actual shift of the image on the receiver is given by s / $\cos\phi$.

Initially, C_1 = 1.0 and C_2 = .003 radians. However, subsequent executions of the receiver program demonstrated that this formulation was excessively conservative, resulting in no added beam spillage and essentially no decrease in peak flux. The best performance of those attempted resulted from

$$s = (\frac{h}{2})\ (\cos\phi) - 0.85\ (R + \alpha\ \ell)$$

where C_1 = 0.85 and C_2 = 0.0. Essentially very little energy resides in the skirts of the degraded images from these large flat heliostats. Table I shows three aiming strategies for the 17 X 17 m receiver and one for a 17 X 15 m receiver. The one point aim reveals the maximum interception factor and intercepted power that can be obtained for this configuration compared to other aiming strategies. The three point aim of the commercial steam receiver is shown to be inadequate for the shorter sodium receiver, giving an interception factor of only 90.8%. On the other hand, the high-low strategy only reduces the interception factor from 96.6% to 95.1%, while lowering the peak flux by some 14%. These three profiles of flux incident on the receiver are shown in Fig. 4.4 for a northern panel By reducing the receiver diameter from 17 m to 15 m, the interception factor is reduced from 95.1% to 93.7% for the high-low aim. Peak flux is only 7% below that of the one point aim for the 17 X 17 m receiver because of the smaller receiver area and corresponding increase in concentration.

However, reduced receiver weight, cost and thermal losses are a plus for this smaller receiver. Comparing the high-low aim as applied to the 15 m dia receiver and the 17 m dia receiver, the power loss amounts to 1.5% and peak flux is up by 8% for a 12% reduction in receiver area.

These studies demonstrate that an appropriate high-low aim can effectively reduce the peak flux of the single point aim while maintaining an acceptably high interception factor. Such studies aid in identification of the most cost effective receiver under constraints of receiver peak flux limitations.

Table 4 - 4

Aim Strategy Summary

Aim	Diameter (Meters)	Interception	Power (MW_t)	Peak Flux (MW/m^2)
one point	17	.966	548.6	1.84
three point	17	.908	516.0	1.33
high-low	17	.951	539.9	1.58
high-low	15	.937	531.6	1.72

Preliminary field configuration - 18.812 heliostats; system focal length, 232 m; receiver length, 17 m; Heliostat Reflectivity, 0.91; Insolation 1018 w/m^2
All values are incident on receiver.

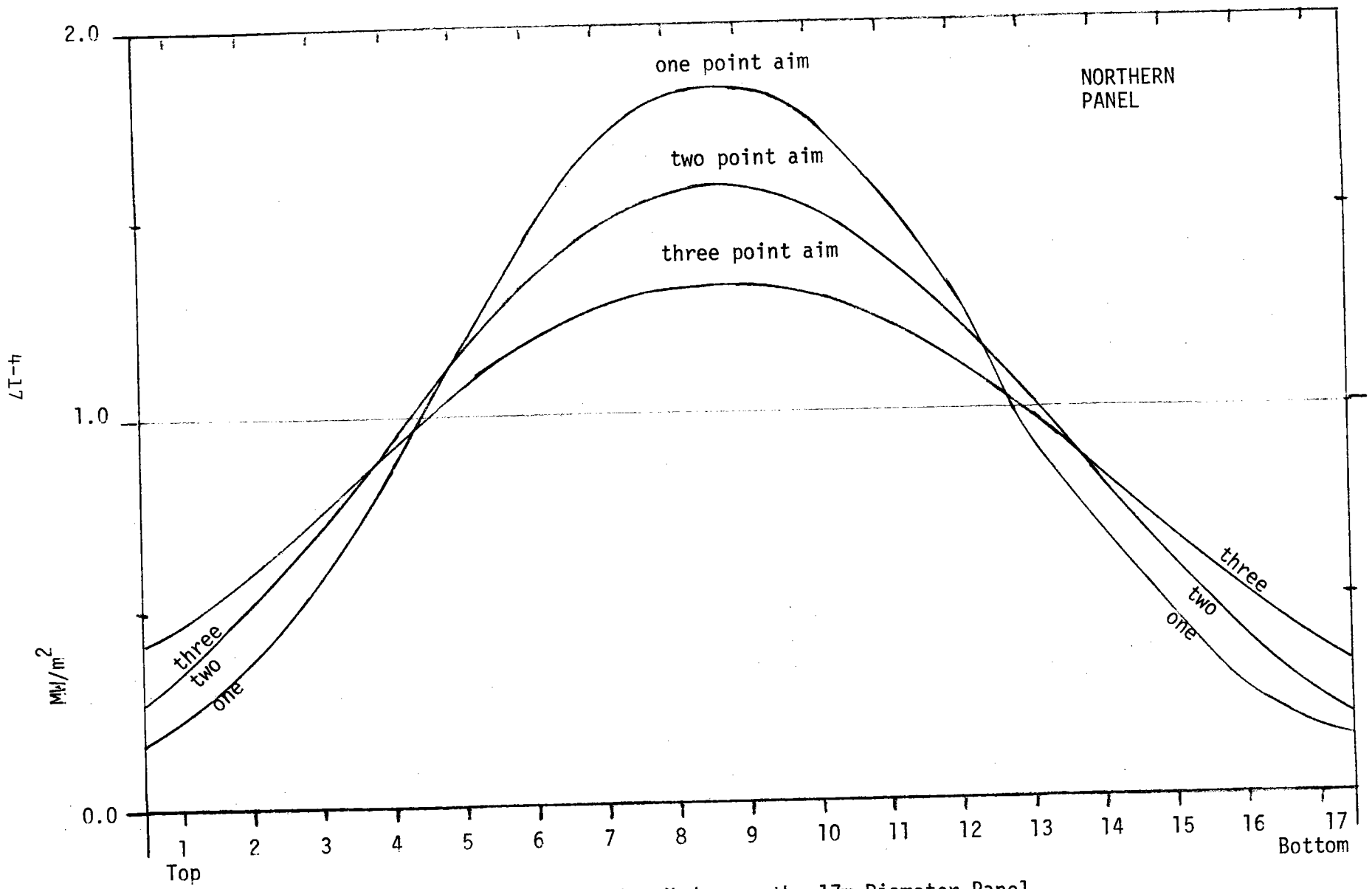

Figure 4-4. Flux distribution for several aim stratagies

5.0 RECEIVER SUBSYSTEM

5.1 Requirements

The Receiver Subsystem includes all components and piping necessary to absorb the incident thermal energy from the Solar Collector Subsystem and make it available to the turbine as superheated steam. The major components included in the Receiver Subsystem are the receiver, steam generator units and the receiver pump. For the subject configuration, Figure 5-1, operation always requires flow through the thermal storage tanks, even though these tanks are defined as part of the Thermal Storage Subsystem. The intent is to include in the Receiver Subsystem only those components necessary for direct operation.

The functional requirements for this system are given in Table 5-1. The steam generator is required to supply 286 MWt of thermal energy to yield the gross day time electric power output of 113 MWe. Maximum receiver power is identified as 475 MWt to provide for simultaneous steam turbine operation and charging of the Thermal Storage Subsystem. Required steam temperature at the turbine inlet is 538°C (1000°F) which determines the sodium operating temperature. Feedwater temperature is 205°C (400°F).

A 30-year design life with 90% availability gives a requirement for about 10,000 daily start/stop cycles. Receiver mid-point elevation is given as 258 m (846 ft). When the riser and downcomer are filled with sodium, the static pressure at the base of the tower is 2.31 MN/m^2 (334 psi). Minimum receiver size is limited by energy loss due to spillage and receiver fatigue life associated with the peak absorbed flux. The statement of work for this study specified an external type absorber surface for the receiver. Several aim strategies were considered to obtain candidate receiver flux distributions for the study.

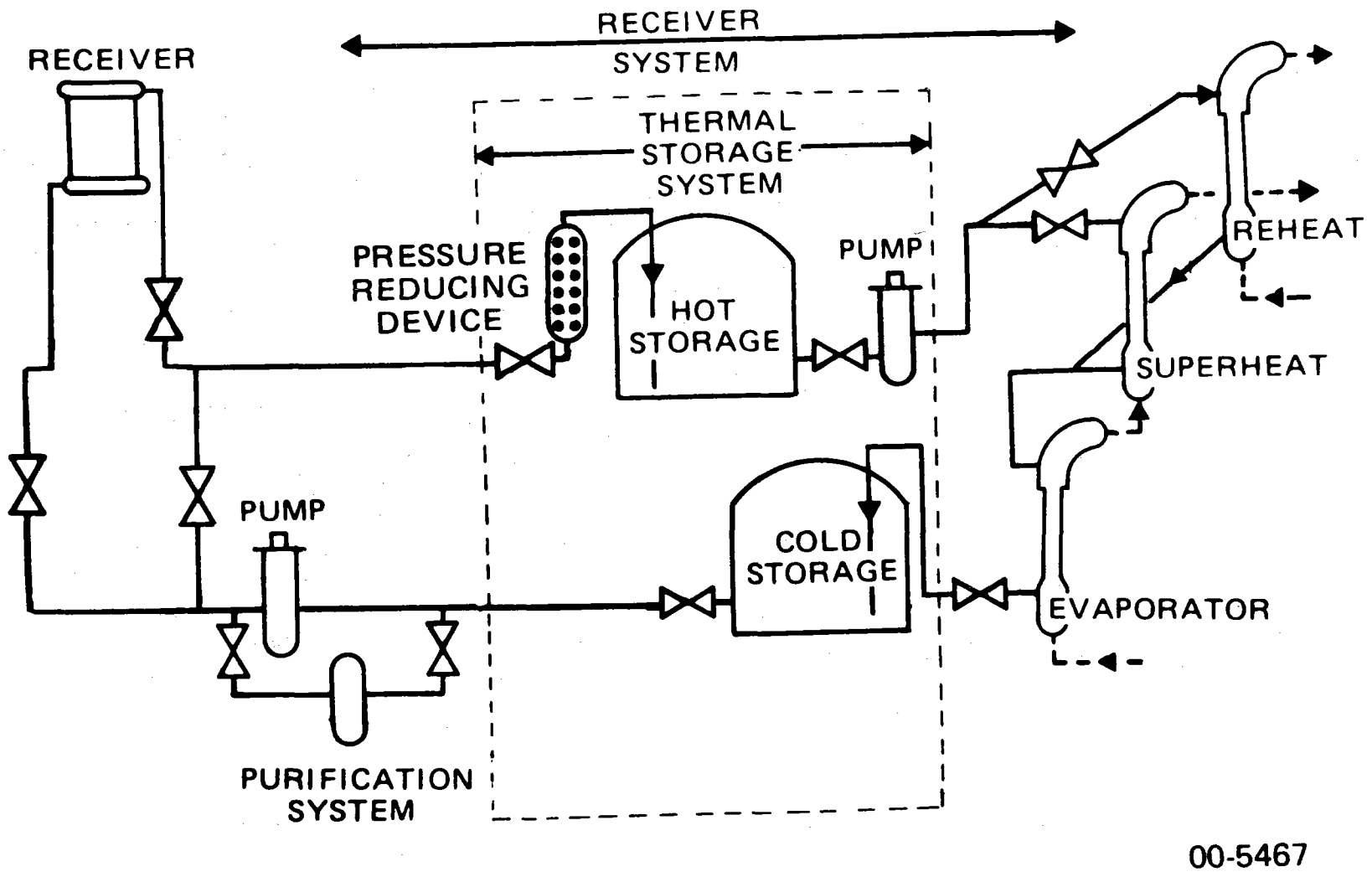

FIGURE 5-1 REVISED BASELINE CONFIGURATION

TABLE 5-1

RECEIVER SUBSYSTEM FUNCTIONAL REQUIREMENTS

Wet Cooling System

Parameter		Requirement
Nominal Thermal Power,	MWt	286
Maximum Thermal Power,	MWt	475
Receiver Temp. - In,	$^{o}C(^{o}F)$	288 (550)
- Out,	$^{o}C(^{o}F)$	593 (1100)
Flowrate	Kg/h (lb/h)	4.47×10^{6} (9.83×10^{6})
Receiver mid-point Elevation	M (ft)	258 (846)
Steam Generator Units		
Sodium Side		
Superheat - In,	$^{o}C(^{o}F)$	593 (1100)
- Out	$^{o}C(^{o}F)$	472 (882)
Reheat - In,	$^{o}C(^{o}F)$	593 (1100)
- Out,	$^{o}C(^{o}F)$	472 (882)
Evaporator- In,	$^{o}C(^{o}F)$	472 (882)
- Out,	$^{o}C(^{o}F)$	288 (550)
Water/Steam Side		
Feedwater Temp - In,	$^{o}C(^{o}F)$	205 (400)
Evaporator Temp - Out	$^{o}C(^{o}F)$	340 (643)
Steam Temp. - Out	$^{o}C(^{o}F)$	538 (1000)
Reheat Temp. - In	$^{o}C(^{o}F)$	394 (740)
- Out	$^{o}C(^{o}F)$	538 (1000)

5.2 Analysis and Trades

The initial baseline configuration established early in the study consisted of two sodium loops as shown in Figure 5-2. The primary trade studies performed around the initial baseline were as follows:

1) Use of NaK in place of sodium in the baseline primary loop.

2) Alternate Configurations.

The selection criteria were to meet the requirements of Section 5.1, minimize cost, and maximize operational flexibility. Operational flexibility included the following required operations:

1) Direct operation.

2) Direct plus storage system charge.

3) Direct plus storage system discharge.

4) Storage system charge only.

5) Storage system discharge only.

5.2.1 NaK Versus Sodium

An investigation of the desirability of using NaK in place of sodium in the receiver (primary) loop was performed. Since the main

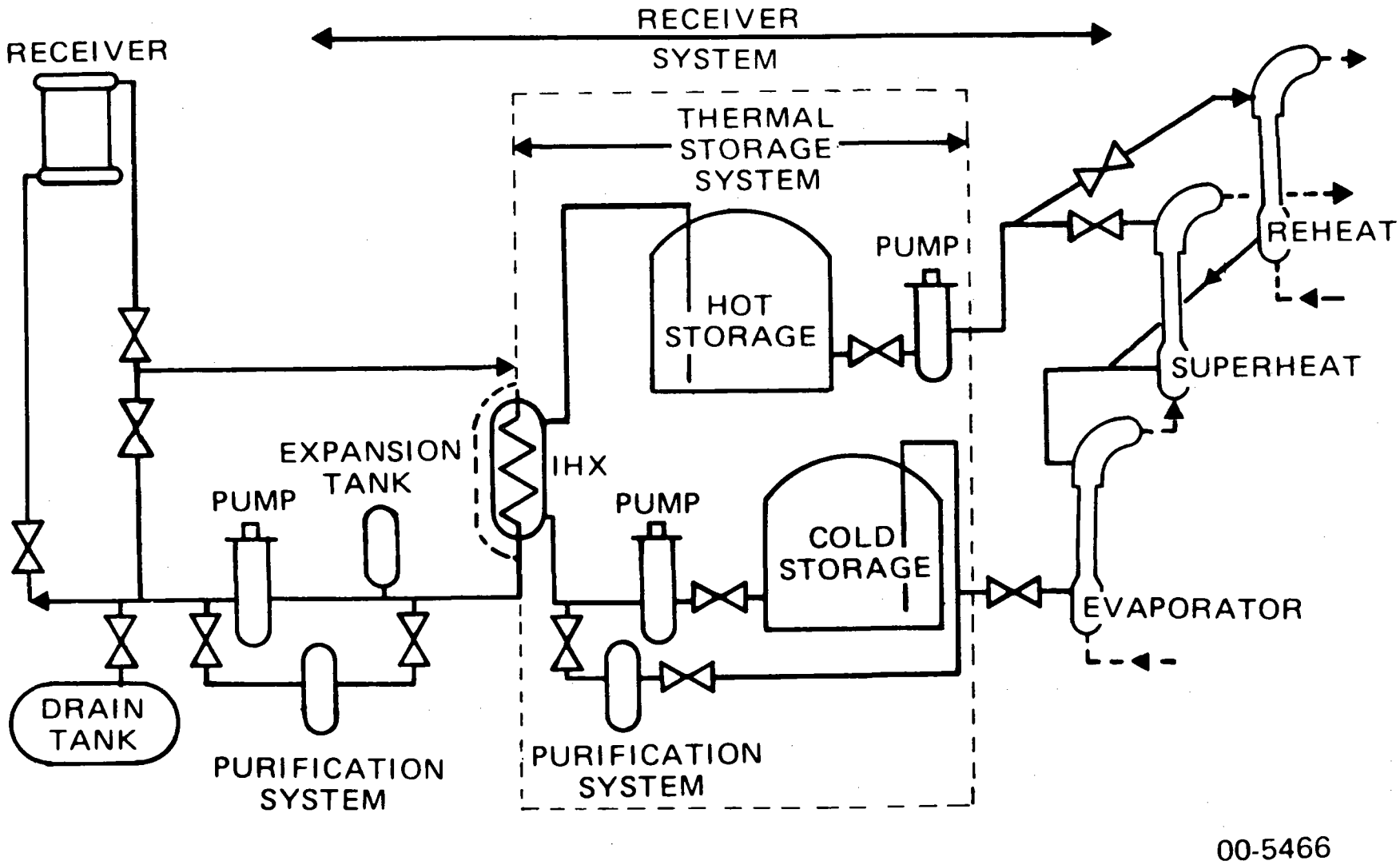

FIGURE 5-2 INITIAL BASELINE CONFIGURATION

objective in using NaK is to obtain a sufficiently low freezing point to eliminate the need for a preheat (pipe heat tracing) system, this study considered the eutectic NaK 78 in the comparison (with a potassium and sodium content of about 78% and 22%, respectively). The freezing point of pure NaK 78 is -12.7°C (9.2°F). Table 5-2 gives a comparison of the physical properties of sodium and NaK 78.

The properties affecting loop performance are primarily density and specific heat; both of these properties for NaK 78 tend to increase the flow rate required to transfer a given quantity of heat and to increase pump power. Table 5-3 compares the loop performance parameters. Using NaK 78 would require a 45% increase in flow rate.

For NaK 78, three pipe sizes are considered, 0.61-m (24 in.), 0.71 m (28 in.), and 0.76 m (30 in). Using pipe of 0.61-m (24-in.) diameter, the same as the sodium system, requires a significant increase in pump power due to the higher flow rate and the increase in head. A 0.71 m (28-in.) pipe gives approximately the same system ΔP as for the sodium system. The increase in pump power is proportional to the increase in flow rate. The 0.76 m (30-in.) pipe gives the same flow velocity of 6.1 m/sec (20 ft/sec) as the sodium system. The decrease in system pressure drop, assuming that the loop pipe length is unchanged for the larger pipe, is balanced by the increased flow rate so that pump power requirements are substantially unchanged. The pipe loop length is considered to be 671 m (2200 ft).

Table 5-4 gives the system cost comparisons. Installed pipe cost per ft is estimated to be as follows:

24 in.	$4231/m ($1,290/ft)
28 in.	$4756/m ($1,450/ft)
30 in.	$4920/m ($1,500/ft)

These costs include fittings, insulation, and hangers. The preheat costs were developed for the large pipe and tanks and doubled

REV 9/28/77

TABLE 5-2

SODIUM AND NaK 78 PROPERTIES COMPARISON

PROPERTY	UNITS	TEMP C (^{o}F)	SODIUM	NaK 78
Density	Kg/m^3 (lbm/ft^3)	260 (500)	884 (55.2)	811 (50.6)
		427 (800)	844 (52.7)	772 (48.2)
		538 (1,000)	819 (51.1)	746 (46.6)
C_p	KJ/Kg.K (Btu/lbm ^{o}F)	260 (500)	1.32 (0.315)	0.892 (0.213)
		427 (800)	1.28 (0.305)	0.875 (0.209)
		538 (1,000)	1.26 (0.301)	0.867 (0.207)
Thermal Cond.	w/m.K (Btu/hr-ft-^{o}F)	260 (500)	79.1 (45.7)	25.5 (14.75)
		538 (1,000)	65.4 (37.8)	26.1 (15.1)
Vapor Press	mN/m^2 (psia)	260 (500)		
		538 (1,000)	0.0010 (0.15)	0.0051 (0.74)
ABS Viscosity	Pa.S (lbm/hr ft)	260	3.8×10^{-4} (0.91)	2.8×10^{-4} (0.67)
		538 (1,000)	2.3×10^{-4} (0.56)	1.7×10^{-4} (0.41)
Freezing Point	^{o}C (^{o}F)	-	97.8 (208)	-12.7 (9.2)
Cost	$/Kg ($/lb)	-	0.60 (0.27)	3.52 (1.60)

TABLE 5-3

PRIMARY LOOP PERFORMANCE

T_{ave} = 427°C (800°F)

PARAMETER	UNITS	SODIUM	NaK 78		
Main Pipe Size	m (in.)	0.61 (24)	0.61 (24)	0.71 (28)	0.76 (30)
Flowrate	Kg/sec (lb/sec)	1356 (2983)		1977 (4353)	
System ΔP	MN/m^2 (psi)	1.13 (164)	2.53 (368)	1.13 (164)	0.786 (114)
Flow Velocity	m/sec (ft/sec)	6.10 (20)	9.76 (32)	7.0 (23)	6.10 (20)
Pump Power	kW	2417	7924	3525	2465
Primary Loop Vol.	m^3 (gal)	227 (60000)	227 (60000)	295 (78000)	333 (88000)

TABLE 5-4

100 Mwe LIQUID METAL SYSTEM

PRIMARY SYSTEM SODIUM VS NaK 78

PARAMETER			SODIUM		NaK 78	
Pipe Size	m (in.)		0.61 (24)	0.61 (24)	0.71 (28)	0.76 (30)
Costs:						
Preheat	10^6		.50			
Pipes	10^6		2.84	2.84	3.17	3.31
Pumping	10^6	for 20 yr	3.60	11.78	5.24	3.66
Liquid Metal	10^6		0.11	0.67	0.87	0.98
	10^6		7.05	15.29	9.28	7.95
Small Valves	Seal		Freeze		Bellows	
Large Valves (2)	Seal		Freeze		Refrig. Stem	
Safety	Fire		Not Self-Sustaining below 204°C (400°F)		Burns at Room Temp.	
Heat Transfer			Superior heat and conductivity	Heat transfer components tend to be larger		

to account for the smaller auxiliary sodium piping, giving a sodium preheat cost of $500,000. This amount is shown in Table 5-4 for the sodium system.

While this study assumes that preheat is not necessary for NaK 78, the desert site locations for a solar plant do have temperatures less than the freezing point of NaK 78, and, under long-term standby conditions, some preheat capability would probably be necessary.

Pumping costs for a 20-year life were estimated at 3¢/KW-hr. The liquid metal costs were obtained from suppliers for large bulk quantities. Table 5-4 shows the sodium system to have the lowest total cost.

Table 5-4 lists several considerations other than cost. The valves in a sodium system will, in general, have freeze stem seals. For small valves, a NaK 78 system would use bellows seal valves which generally cost more. The 0.61 m (24 in) or larger valves with bellows seals have not been developed for liquid metal service. Hence, the development of a new type of valve is required, or as an alternative, use of a freeze stem valve with a refrigerated stem to obtain a frozen plug of NaK 78. The studies to date have assumed a need for flow control capability using valves and for tower shutoff capability.

The performance of heat transfer components, such as the receiver and steam generator, are adversely affected by the use of NaK 78 in place of sodium. The tendency is for the size of the components to increase, but this is not evaluated quantitatively herein. The higher flow rate for the NaK 78 system either yields a higher pressure drop for a component of fixed size or requires a larger flow area if the component ΔP is to be maintained. The poorer conductivity of NaK 78 also tends to require a greater heat transfer surface area.

In general, the fire hazard with NaK 78 is considered to be somewhat greater than that for sodium as indicated in Table 5-4.

The preponderance of liquid metal experience is with sodium, and, since Table 5-4 shows no cost advantage for NaK 78, the recommendation is that the receiver primary loop be operated using liquid sodium.

5.2.2 Alternate Configurations

Other configurations investigated include those of Figures 5-2 and 5-3. Figure 5-2 shows the initial baseline configuration established in this study. This configuration used two sodium loops thermally coupled by an intermediate heat exchanger (IHX). The receiver loop operates at high static pressure due to the tower static head. The thermal storage loop operates at a relatively low pressure. The storage tanks are pressurized with an inert gas only to the extent necessary (<0.007 MN/m^2, (<1 psi)) to keep air (oxygen) out of the tanks. The two pumps are designed to supply about 61 m (200 ft) of head to pump from one storage tank to the other. This two loop configuration supplies all of the operating sequences listed at the beginning of this section. Figure 5-3 shows an arrangement which eliminates the pump from the hot storage tank loop. The remaining pump in the Thermal Storage System, with additional piping, and valves, is used to perform the function of both. The piping and valve arrangement is more complex and may eliminate the cost advantage of removing one pump. Moreover, the capability to simultaneously discharge thermal storage and operate the steam generators directly from the receiver is lost. For the Figure 5-3 configuration, the steam generator is coupled to the receiver through the IHX on direct operation so that thermal transients generated at the receiver may be transmitted to the steam generator rather than being buffered by the hot storage tank as is the case for the configurations of Figures 5-1 and 5-2.

Because of this lack of isolation from the receiver transients and the apparent complexity of the flow configuration, the configuration of Figure 5-3 was not considered further.

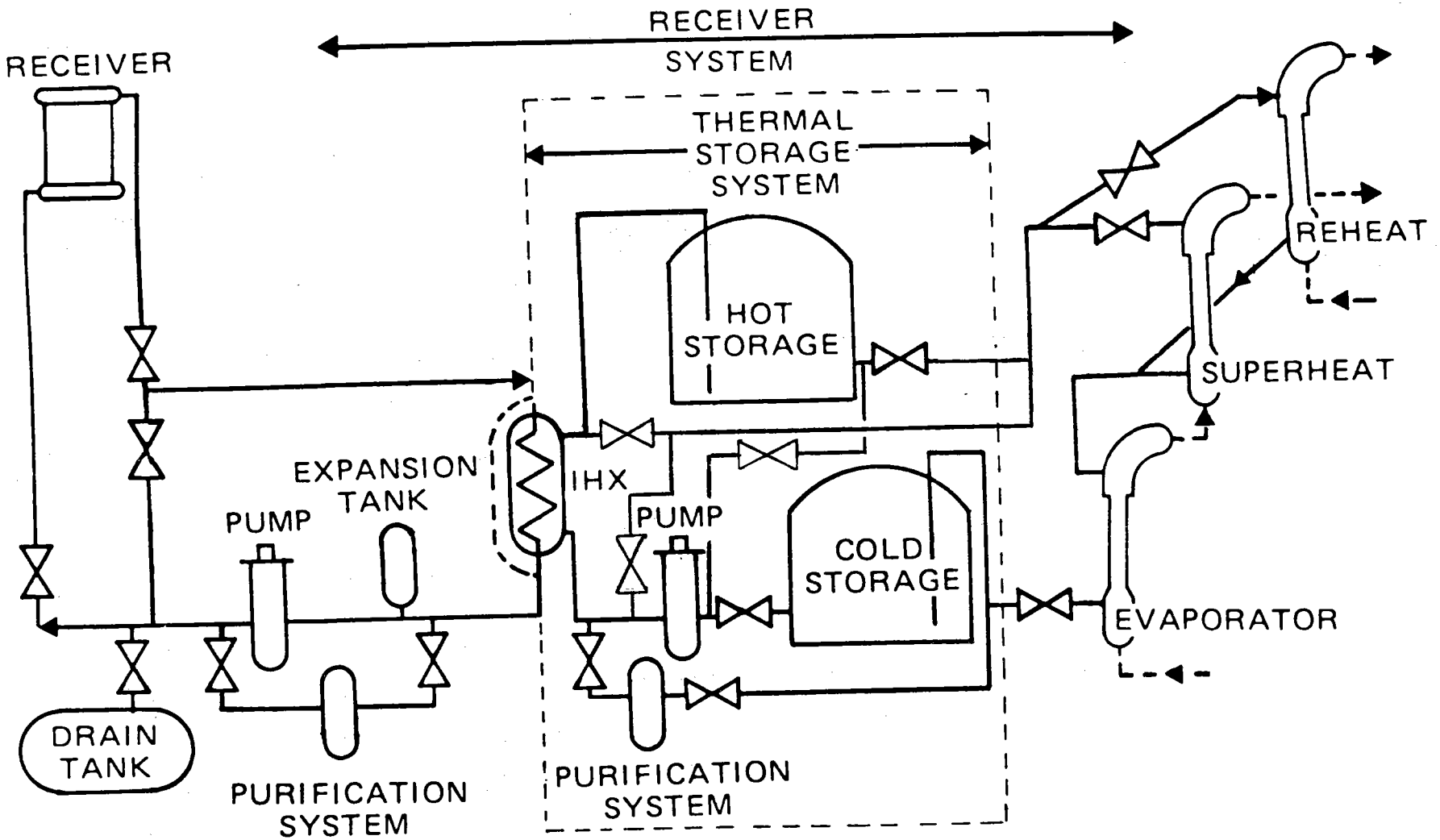

FIGURE 5-3 ALTERNATE CONFIGURATION A

After considerable study, the initial baseline configuration of Figure 5-2 was replaced with the configuration of Figure 5-1. The choice was on the basis of operational simplicity, reduced number of components, and the reduced cost.

The single loop configuration of Figure 5-1 eliminates the IHX and incorporates a pressure reducing device (PRD) such that low pressure, gravity head storage tanks may be used. This configuration requires a high head receiver pump since the tower static head is dumped by the PRD. This configuration provides all of the operating sequences listed above.

The steam generator arrangement for the initial baseline configuration consisted of ten modular units developed by AI. These units were arranged with four as evaporators, four as superheaters, and two as reheaters. While these units have been designed and tested and could be readily built, extensive interconnecting piping is required and each unit requires a flow balancing control valve. A simpler arrangement is to consider a single evaporator, a single superheater, and a single reheat unit. The piping arrangement is greatly simplified. The two larger units are similar in size to the steam generator being developed for the CRBRP, with the expectation that the technology for steam generators of this size will have been well developed. The reheat requirement is satisfied by a modified AI modular steam generator.

5.3 Design Description

The Receiver Subsystem contains the receiver, the receiver pump, the steam generator units, and the main sodium piping including the riser and downcomer in the tower. The steam generator units are included with the Receiver Subsystem on the basis that the receiver loop could be connected directly with the steam generator without the Thermal Storage Subsystem if operation were only during hours of sunshine. The Thermal Storage Subsystem includes only the added components necessary to provide six hours of storage operation at full power. With the baseline configuration, however, direct

operation of the steam generator with the receiver is by definition only since all liquid sodium passes through the storage tanks to reach the steam generators. This is a substantial advantage for this configuration since receiver operation is decoupled from the power generating activity. Hence, power generation can continue as long as hot sodium is in the storage tanks without regard for the transient conditions at the receiver due, for example, to passing cloud fronts.

The receiver is cylindrical in shape, 17 m x 17 m with an external energy absorbing surface consisting of 24 panels. Each panel has 115 stainless steel 1.9 cm (0.75 in) O.D. tubes connected to a common manifold. With a single point aim strategy, peak receiver heat flux is limited to 1.7 MW/m^2 to achieve a tube life of not less than 10,000 cycles. The above receiver size can be reduced to about 15 m x 15 m if a high-low aim strategy is used at some sacrifice in beam interception factor.

The receiver pump supplies sodium from the cold storage tank through the receiver to the hot storage tank. A pump head rise of 299 m (980 ft) at a flowrate of 1.45 m^3/S (23,000 gpm) is required to pump the sodium up the tower.

The steam generator consists of an evaporator of 177 MWt, a superheater of 79 MWt, and a reheater of 30 MWt. These units would be derived from current technology for the Clinch River Breeder Reactor program and test data available for the existing AI modular steam generator.

The Receiver Subsystem characteristics are given in Table 5-5. Each of the major components shown for the revised baseline configuration of Figure 5-1 will be described in detail in the subsections to follow. The auxiliary systems will be discussed in general terms.

TABLE 5-5

RECEIVER SUBSYSTEM CONFIGURATION

Item	Value
General	
Receiver Assembly	
Dia, m (ft)	17 (56)
Receiver Assembly	
Height, m (ft)	17 (56)
Receiver mid-point elevation	258 (846)
Receiver maximum elevation	266 (874)
No. of absorber panels	24
Volume of sodium in subsystem, m^3 (gals.)	341 (90,000)
Weight of sodium in subsystem, Kg (lbs)	291,000 (641,000)
Pump outlet pressure MN/m^2 (psia)	2.38 (345)
Pump inlet pressure, MN/m^2 (psia)	0.21 (30)
Total radiation and convection loss (%)	9% at peak power 12.5% at 50% power
Absorber Panel	
Height, m (ft)	17 (56)
Width, m (ft)	2.22 (7.3)
Dry weight, kg (lb)	2,727 (6,000)
No. of tubes	116
Tube OD, cm (in.)	1.91 (0.75)
Tube ID, cm (in.)	1.65 (0.65)
Tube material	CRES 304H
Solar surface coating	Pyromark
Panel insulation	Closed-pore fiberglass
Thermal expansion provision	Flexible tube bends
Absorptivity, minimum	0.95
Peak heat flux, MW/m^2 (Btu/in^2-sec)	1.67 (1.03)
Outlet temp, ^oC (^oF)	593 (1100)
Inlet temp, ^oC (^oF)	288 (550)

Table 5-5 (Cont.)

Tower Assembly		
Construction		Slip formed concrete
Concrete Height, m (ft)		245 (797)
	Riser	Downcomer
Nominal pipe OD, cm (in.)	61 (24)	45.7 (18)
Nominal wall thickness	TBD	TBD
Material	304H	304H
Design Temperature, ^{o}C (^{o}F)	371 (700)	593 (1100)
Design pressure ANSI B31.1	2.76 (400)	2.76 (400)
Maximum flow rate Kg/hr (lb/hr)	4.47×10^6 (9.83×10^6)	4.47×10^6 9.83×10^6)
Velocity at maximum flow rate m/sec (ft/sec)	6.1 (20)	9.2 (30)
Receiver Pump		
Physical Description		
Quantity		1
Height, w/motor, m (ft)		11.3 (37)
Tank size, m (ft)		2.1 x 6.1 (7x20)
Inlet Nozzle, m (in.)		0.91 (36)
Outlet Nozzle, m (in.)		0.61 (24)
Dry Weight w/motor, Kg (lb)		107000 (236,000)
Motor		
Size, MW (hp)		5.2 (7000)
Dimensions w/coupling, m (ft)		2.1 x 3.7 (7x12)
Voltage		4160
Cooling		TBD

TABLE 5-5 (Cont.)

Pump Operating Conditions

Developed Head, m (ft)	299 (980)
Flow Rate, Kg/hr (lb/hr)	4.47×10^6 (9.83×10^6)
Speed, rpm	1100
Temperature, ^oC (^oF)	288 (550)
Sodium volume, m^3 (gal)	6.8 (1800)
NPSH, m (ft)	12.2 (40)
Discharge Head, m (ft)	311 (1020)
Speed Control, %	20-100
Pump Power (η = 70%) MW (hp)	5.12 (6950)

Design Conditions

Developed Head, m (ft)	305 (1000)
Flowrate, m^3/s (gpm)	1.45 (23000)
Speed, rpm	1100
Temperature, ^oC (^oF)	427 (800)
NPSH (min. required), m (ft)	12.2 (40)
Code	Sect. VIII, Div. 1

Steam Generator - Evaporator

Physical Description

Quantity	1
Type	Tube & shell hockey-stick
Height, m (ft)	18.9 (62)
Width, m (ft)	4.57 (15)
Shell diameter, m (in.)	1.14 (45)
Heat Transfer Area, m^2 (ft^2)	892 (9600)
No. of Tubes	1000
Tube Size, cm (in.)	1.59 (5/8)
Tube Wall Thickness, cm (in.)	0.24 (0.095)

TABLE 5-5 (Cont.)

Material	2-1/4 Cr - 1 Mo
Sodium Nozzle O.D./Thickness, cm (in.)	91/2.5 (36/1.0)
Tubesheet Diameter/Thickness, cm (in.)	122/45.7 (48/18)
Steam Nozzle O.D./Thickness, cm (in.)	201/3.8 (8/1.5)
Operating Conditions	
Sodium Side:	
Flow, Kg/hr (lb/hr	2.68×10^6 (5.90×10^6)
Inlet Temp, ^oC (^oF)	472 (882)
Outlet Temp, ^oC (^oF)	288 (550)
Pressure Drop, MN/m^2	0.138 (20)
Duty, MWt	177
Water/Steam:	
Flow, Kg/hr (lb/hr)	3.62×10^5 (7.96×10^5)
Inlet Temp, ^oC (^oF)	205 (400)
Outlet Temp, ^oC (^oF)	339 (643)
Pressure, MN/m^2	15.86 (2300)
Pressure Drop, MN/m^2 (psi)	1.38 (200)
Design Conditions:	
Pressure-Sodium Side, MN/m^2 (psig)	2.07 (300)
Pressure-Steam Side, MN/hr^2 (psig)	16.55 (2400)
Temperature, ^oC (^oF)	510 (950)
Code	ASME Section VIII, Div. 1

TABLE 5-5 (Cont.)

Steam Generator - Superheater and Reheat

Physical Description	Superheater	Reheat
Quantity	1	1
Type	Tube & shell hockey-stick	
Height, m (ft)	18.9 (62)	18.9 (62)
Width, m (ft)	3.7 (12)	3.05 (10)
Shell Diameter, m (in.)	0.81 (32)	.508 (20)
Heat Transfer Area, m^2 (ft^2)	483 (5200)	181 (1950)
No. of Tubes	534	200
Tube Size, cm (in.)	1.59 (534)	1.59 (5/8)
Tube Wall Thickness, cm (in.)	0.24 (0.095)	0.24 (0.095)
Material	SS	SS
Sodium Nozzle O.D./Thickness, cm (in.)	76.2/2.54 (30/10)	45.7/1.9 (18/.75)
Tubesheet Diameter/Thickness, cm (in.)	86.4/30.5 (34/12)	55.9/15.2 (22/6)
Steam Nozzle O.D./Thickness, cm (in.)	20.3/3 (8/1.2)	16.8/1.5 (6.6/.6)

Operating Conditions

Sodium Side:		
Flow, Kg/hr (lb/hr)	1.97×10^6 (4.32×10^6)	0.70×10^6 (1.58×10^6)
Inlet Temp, ^oC (^oF)	594 (1100)	594 (1100)
Outlet Temp, ^oC (^oF)	472 (882)	472 (882)
Pressure Drop, MN/m^2 (psi)	0.138 (20)	0.138 (20)
Duty, MWt	79	30
Water/Steam:		
Flow, Kg/hr (lb/hr)	3.62×10^5 (7.96×10^5)	3.18×10^5 (7.01×10^5)
Inlet Temp, ^oC (^oF)	339 (643)	393 (740)
Outlet Temp, ^oC (^oF)	538 (1000)	538 (1000)
Pressure, MN/m^2 (psig)	14.5 (2100)	5.17 (750)
Pressure Drop, MN/m^2 (psi)	0.69 (100)	0.35 (50)

TABLE 5-5 (Cont.)

Design Conditions:		
Pressure-Sodium Side, MN/m^2 (psig)	2.07 (300)	2.07 (300)
Pressure-Steam Side, MN/m^2 (psig)	15.2 (2200)	6.89 (1000)
Temperature, ^oC (^oF)	593 (1100)	593 (1100)
Code	ASME, Section VIII, Division I	

5.3.1 Receiver

Requirements

Receiver requirements are discussed in this section. They are grouped as general, performance, and design requirements.

The general requirement governing receiver configuration is set by the study guideline that the receiver shall be the type that receives energy on its external surface. Secondly, the receiver design must be such that its surface area shall be minimized to the extent that losses are reduced as much as practicable. In order to accomplish this, the heat flux incident upon the receiver must be maximized within the limits of the receiver material compatibility and fatigue life.

Material selection is another general requirement governing receiver design. Receiver materials were established to be conventional alloys currently in common usage with liquid sodium. No alloys were to be chosen that had little or no empirical evidence of successful operation with the cooling medium.

The receiver performance requirements are as follows:

Peak Absorbed Power, MWe	475 - 500
Flowrate, Kg/H (lb/H)	4.47×10^6 (9.83×10^6)
Temperatures:	
Inlet, °C (°F)	288 - 316 (550-600)
Rise, °C (°F)	305 (500)
Thermal Losses	Minimize

The overriding requirements imposed upon the receiver design were that it be designed to Section VIII to the ASME Boiler and Pressure Vessel Code and that it be capable of withstanding 10,000 thermal cycles.

The limiting factor determined by the above requirements is the heat flux distribution on the north side of the receiver where the most intense heat transfer rates are encountered. These distributions are presented and discussed in detail in the Thermal Analysis section of this report.

Receiver Analyses

The section presents the thermal, hydraulic, and structural analysis performed on the sodium-cooled solar receiver. The operating characteristics and design details of the configuration chosen as the baseline are also included. Figure 5-4 presents a sketch of the receiver.

Preliminary Screening of Cooling Concept

Early in the evaluation, a preliminary analysis of cooling with liquid sodium was carried out to establish guidelines for optics field analyses relative to determination of peak heat flux conditions. Requirements for this preliminary screening were assumed as follows:

Absorbed Power, MWt	500
Inlet Temperature, ^{o}C (^{o}F)	288 (550)
Exit Temperature, ^{o}C (^{o}F)	593 (1100)

No specific heat flux profile was provided; consequently, reasonable values for peak and average heat fluxes were synthesized based on previous central receiver activities, specifically the water/steam receiver studies (ERDA Contract No. E-(04-3)-1108).

The absorbed receiver power is 500 MW or 473,383 Btu/sec. On the basis of 24 independent panels, the average panel power is 20.83 MW or 19,724 Btu/sec. In the case of the 10 MWe Pilot Plant activities, the peak panel power was experienced by the north-facing panel and was approximately twice that of the average panel.

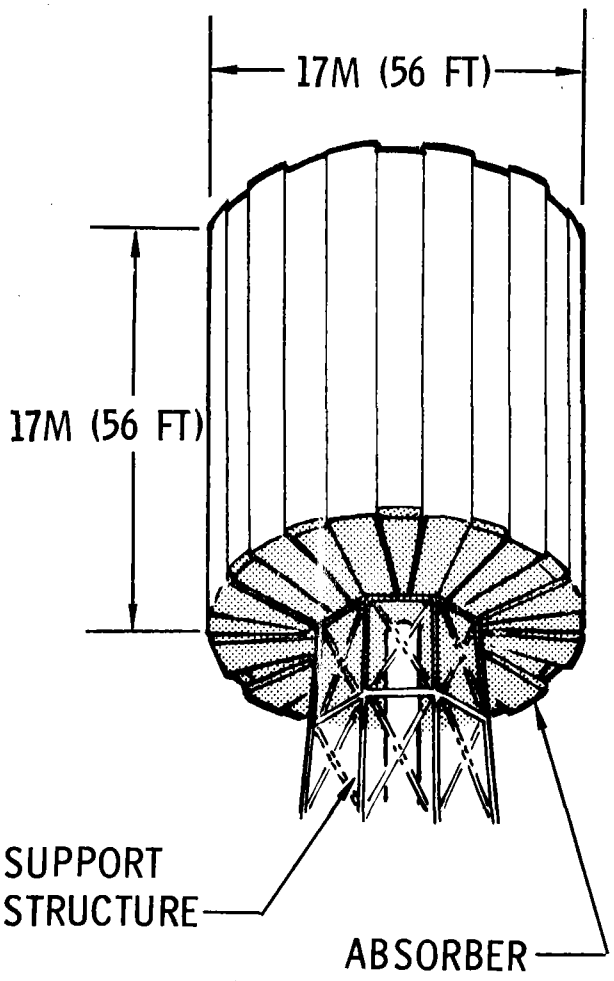

FIGURE 5-4. SODIUM COOLED RECEIVER

Therefore, the power absorbed by the maximum power sodium panel was taken as 40 MW (39,450 Btu/sec). The circumference of a 17 m cylinder is 2103 inches. This results in a 2.22 m (87.5 inch wide panel). The power per unit width of the north panel is thus .180 MW/cm (451 Btu/in-sec). The mass flow resulting is then the ratio of heat to the product of heat capacity, 1296 J/Kg °K (0.31 Btu/lb-F), and temperature rise 288°C (550°F). This results in a maximum value of mass flow per unit circumference ($\dot{m}_c$) of 0.47 Kg/cm-s (2.65 lb/in-sec). The cooling characteristics were estimated based on the above for various size tubing in a single pass configuration.

The flow per tube ($\dot{m}$) was calculated from the outer diameter (D) and the mass flow per unit circumference ($\dot{m}_c$).

$$\dot{m} = \dot{m}_c D$$

The inner diameter (d) was determined by selecting a 0.127 cm (0.05 in.) wall thickness.

$$d = D - 2 \times (\text{wall thickness})$$

The fluid velocity (V) was then calculated from

$$V = \frac{\dot{m}}{\frac{\pi}{4} d^2 \rho}$$

The convective heat transfer coefficient was estimated from the Lubarsky-Kaufman Equation (NACA TN 3336, 1955; GIEDT, "Principles of Engineering Heat Transfer,"Van Nostrum, 1957)

$$Nu = 0.625 \, (RePr)^{.4}$$

where the symbols have their usual meaning.

The coolant side film temperature differental was then estimated based on the above and a set of assumed heat flux levels. Wall temperature differential was calculated by relating the assumed heat flux to the thermal conductivity of the wall.

It was assumed that the peak heat flux would be encountered at the average bulk temperature of the coolant 441°C (825°F). This would correspond (roughly) to the midpoint of the receiver. The properties used for coolant and wall are shown in Table 5-6.

TABLE 5-6. PHYSICAL PROPERTIES AT PEAK HEAT FLUX POINT

Fluid Density	849.1 Kg/m^3 (53 lb/ft^3)
Fluid Heat Capacity	1296 J/Kg.°K (0.31 Btu/lb-F)
Fluid Dynamic Viscosity	2.54 x 10^{-4} Pa.S (0.614 lb/ft-hr)
Fluid Thermal Conductivity	69.2 w/m.K (40 Btu/hr-ft-F)
Wall Thermal Conductivity	20.8 w/m.K (12 Btu/hr-ft-F)

The calculated results are shown in Table 5-7 for the fluid parameters. The resultant wall temperatures are shown in Figure 5-5 for the assumed variation in tube size and heat fluxes ranging up to 3 MW/m^2. The ratio of film temperature drop to wall temperature drop is of interest since it explains why the temperature curves in Figure 5-5 are rather flat with respect to tube size. This is shown in Figure 5-6, which indicates that the tube is tending to be conduction-limited by virtue of the heat flux levels and the relatively thick wall 0.127 cm (0.050 inch) assumed.

Based on the pressure drop information and the total flow in the receiver 1264 Kg/S (2780 lb/sec), the pumping power required was estimated. This is shown in Figure 5-7. As shown, the power required becomes very high for tubes less than 1.52 cm (0.6-inch O.D.). Another parameter of interest is the wall temperature at the receiver exit. For numerous values of assumed heat flux, this parameter is shown in Figure 5-8.

TABLE 5-7. FLUID CALCULATION RESULTS FOR PRELIMINARY THERMAL ANALYSIS

Tube Dia. cm(in)	Flowrate, Kg/s (lb/sec)	Velocity, m/s (fps)	Mass Velocity, Kg/m^2-s (lb/ft^2-sec)	Reynolds No.	Heat Transfer Coefficient KW/m^2-K (Btu/ft^2-hr-F)	Pressure Drop, MN/m^2(psi)
3.0 (1.2)	1.45 (3.18	2.8 (9.1)	2348 (481)	258659	26.4 (4647)	0.062 (9)
2.5 (1.0)	1.20 (2.65)	3.45 (11.3)	2924 (599)	263445	32.8 (5787)	0.11 (16)
2.0 (0.8)	0.96 (2.12)	4.57 (15.0)	3876 (794)	271521	42.4 (7474)	0.21 (30)
1.3 (0.5)	0.60 (1.32)	8.72 (28.6)	7381 (1512)	295505	76.6 (13500)	1.25 (182)
0.76 (0.3)	0.36 (0.79)	20.9 (68.5)	17722 (3630)	354695	1647 (290110)	13.86 (2010)

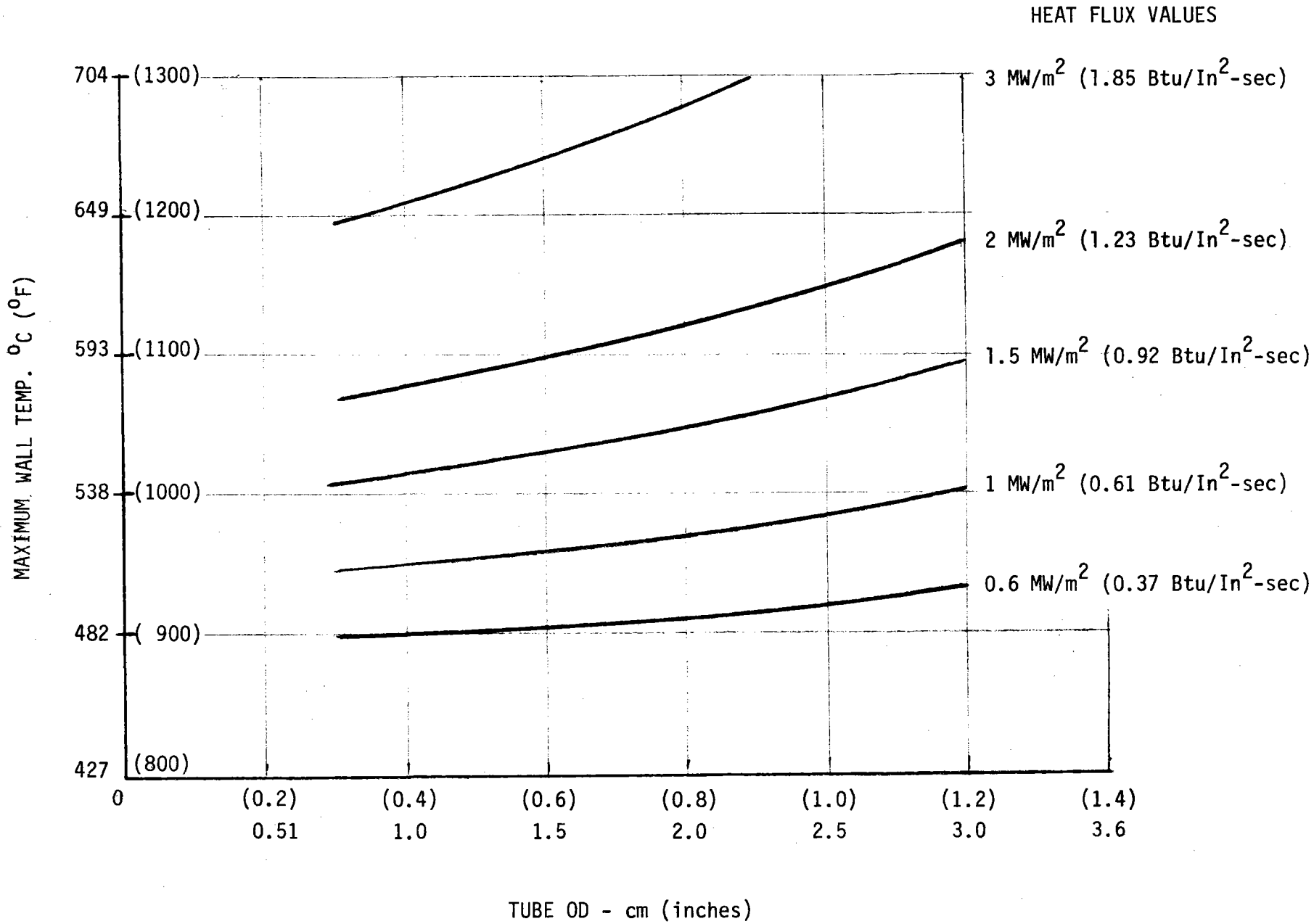

Figure 5-5. Peak Receiver Wall Temperature (North Side)
Fluid Temperature - 441 C (825 F) - Single Pass

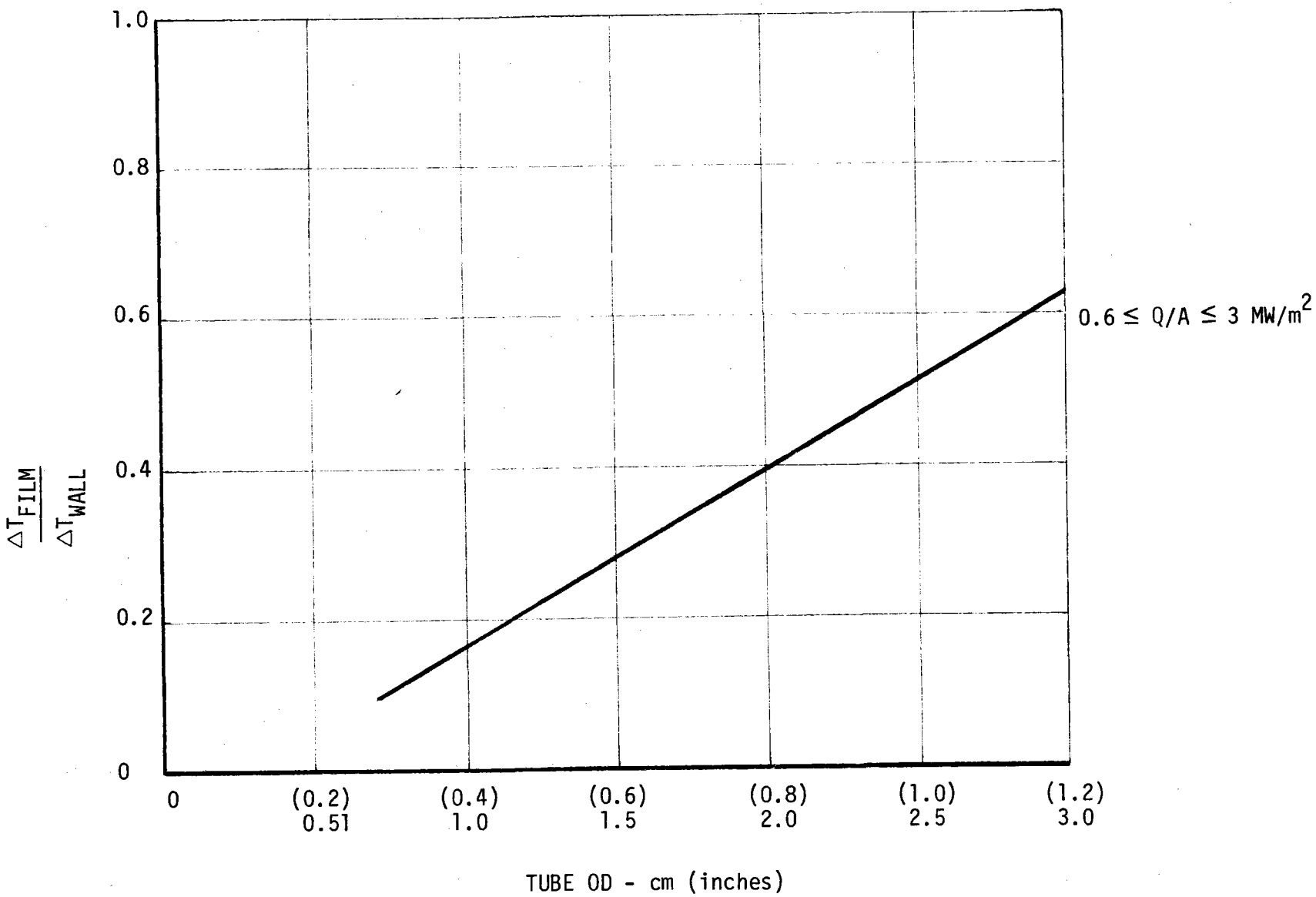

Figure 5-6. Ratio of Film Temperature Drop to Wall Temperature Drop at Peak Heat Flux Point Single Pass

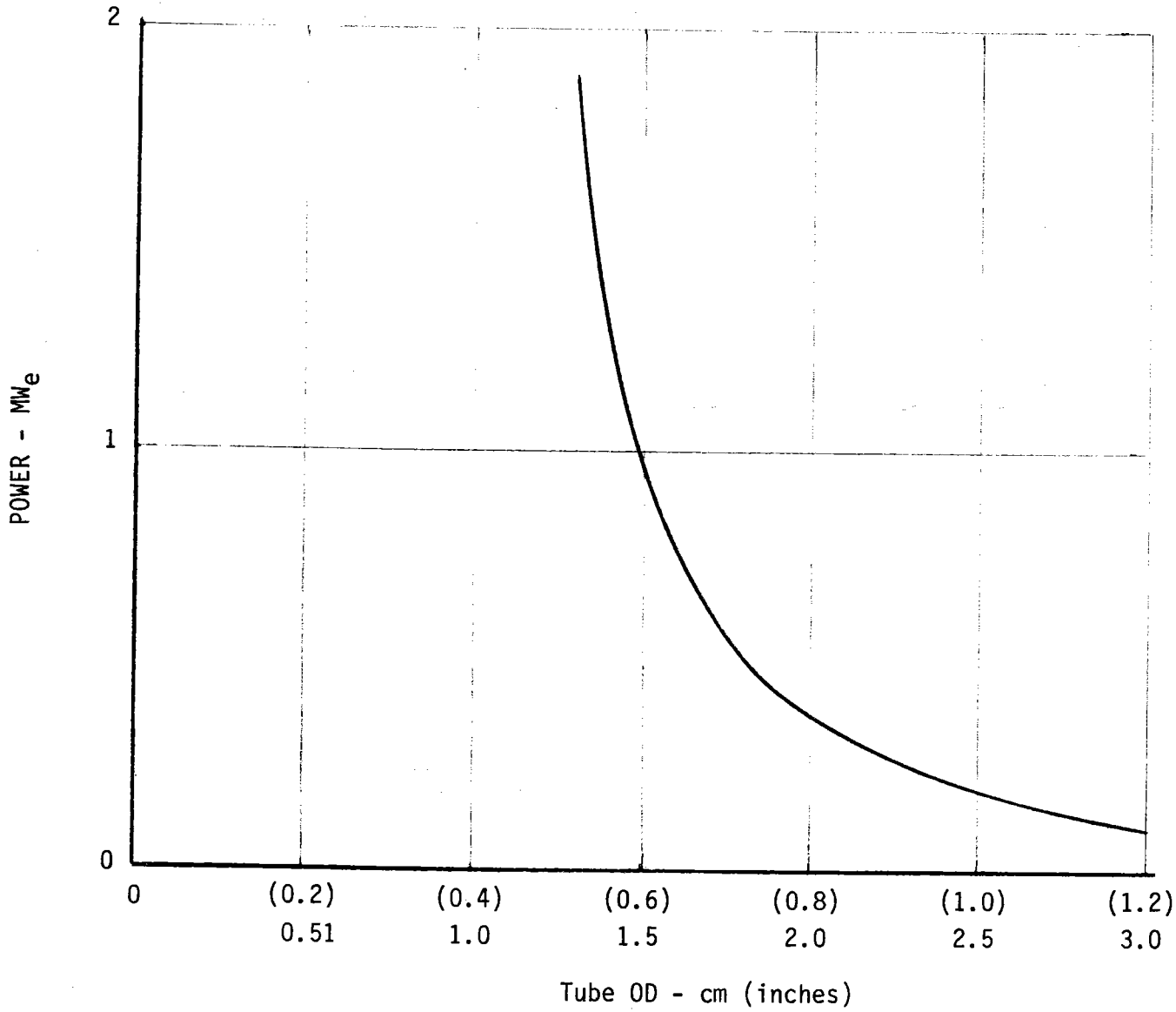

Figure 5-7. Pump Power to Cool Peak Heat Flux Panel Single Pass

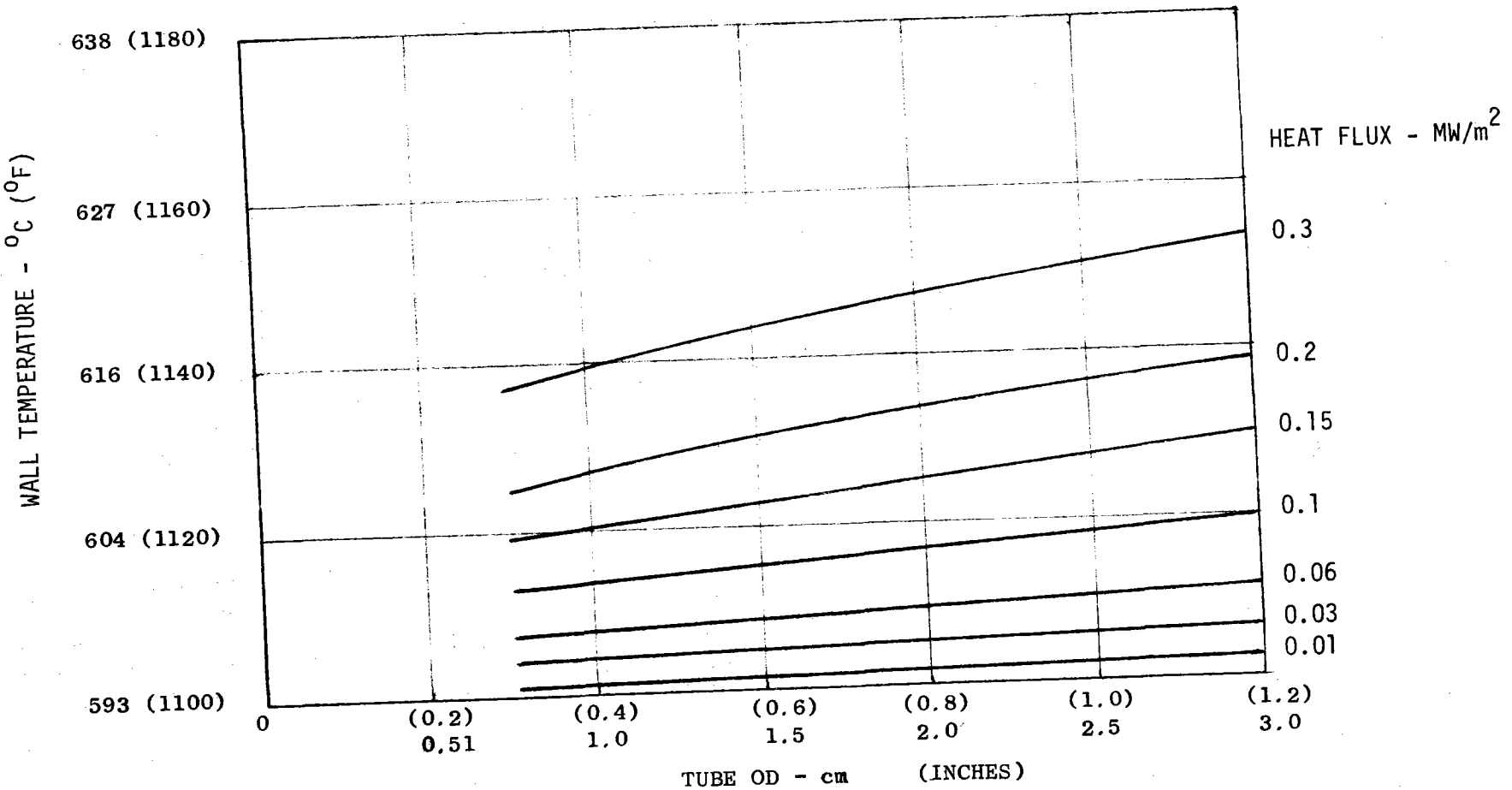

Figure 5-8. Receiver Wall Temperature at Exit (North Side)
Fluid Temperature - 593° C (1100 F) - Single Pass

The question of tube material relates to the wall temperature by virtue of allowable stress levels. Considering hoop stress as the controlling parameter, a calculation was made for a pressure of 2.07 MN/m^2 (300 psia). The values are shown in Table 5-8.

TABLE 5-8. HOOP STRESS FOR 2.07 MN/m^2 (300 psia) IN RECEIVER TUBING

Tube Diameter		Hoop Stress	
cm	(in)	MN/m^2	(psi)
3.0	(1.2)	24.8	(3600)
2.5	(1.0)	20.7	(3000)
2.0	(0.8)	16.5	(2400)
1.27	(0.5)	10.3	(1500)

These values may then be related to the allowable stress values for candidate materials.

Stainless Steel 304H is a common containment material for liquid sodium. At a temperature of 593°C (1100°F), its allowable stress is approximately 51.7 MN/m^2 (7500 psi) (ASME Code). At 649°C (1200°F), this value reduces to 31.0 MN/m^2 (4500 psi). At the peak heat flux location, the average wall temperature is below 593°C (1100°F), while at the exit of the tube bundle the average wall temperature can be as high as 604°C (1120°F). Stainless 304H is a viable candidate as the tube material. Alternate materials are available which would allow a higher heat flux that in turn would lead to a more compact receiver design.

One particularly interesting possibility is Inconel 625, which has an ultimate tensile strength of 503 MN/m^2 (73,000 psi) at 760°C (1400°F) (typical). The allowable stress will probably be 103 MN/m^2 (15,000 psi). Additionally, Inconel 625 has an elongation of 60 percent from room temperature to peak operating temperature.

The foregoing analysis has demonstrated the feasibility of single-pass cooling with reasonable tube sizes (1.5-2.5 cm) (0.6-1-in. O.D.) using conventional materials or advanced materials (i.e., Inconel 625) that have been used in aerospace applications.

Heat Flux Environment

Heat flux profiles for a 17m-diameter - 17m-high (56 x 56 ft) receiver were calculated by the University of Houston for the case of Equinox noon. The profiles are shown in Figure 5-9. Corresponding integrated panel powers are shown in Figure 5-10. All these are incident power levels. The integrated power level is approximately 550 MWt, which corresponds approximately to an absorbed power level of approximately 500 MWt. As noted in Figure 5-9, the peak heat flux is below 2 MW/m^2 which was previously indicated as the target maximum value for receiver peak heat flux.

The preliminary analysis of receiver cooling previously discussed indicated that the receiver tubing was tending to become conduction-limited; at the north side the wall temperature differential was far greater than the coolant film temperature differential. Consequently, ensuing analyses concentrated on determination of wall temperatures and fatigue life at the north side. This approach is further justified by the fact that the sodium heat transfer film coefficient follows the 0.4 power of flowrate which is proportional to power (or heat flux). Thus for a panel away from the north, as the heat flux and power reduce, the film coefficient will reduce to a lesser extent. In view of the foregoing,

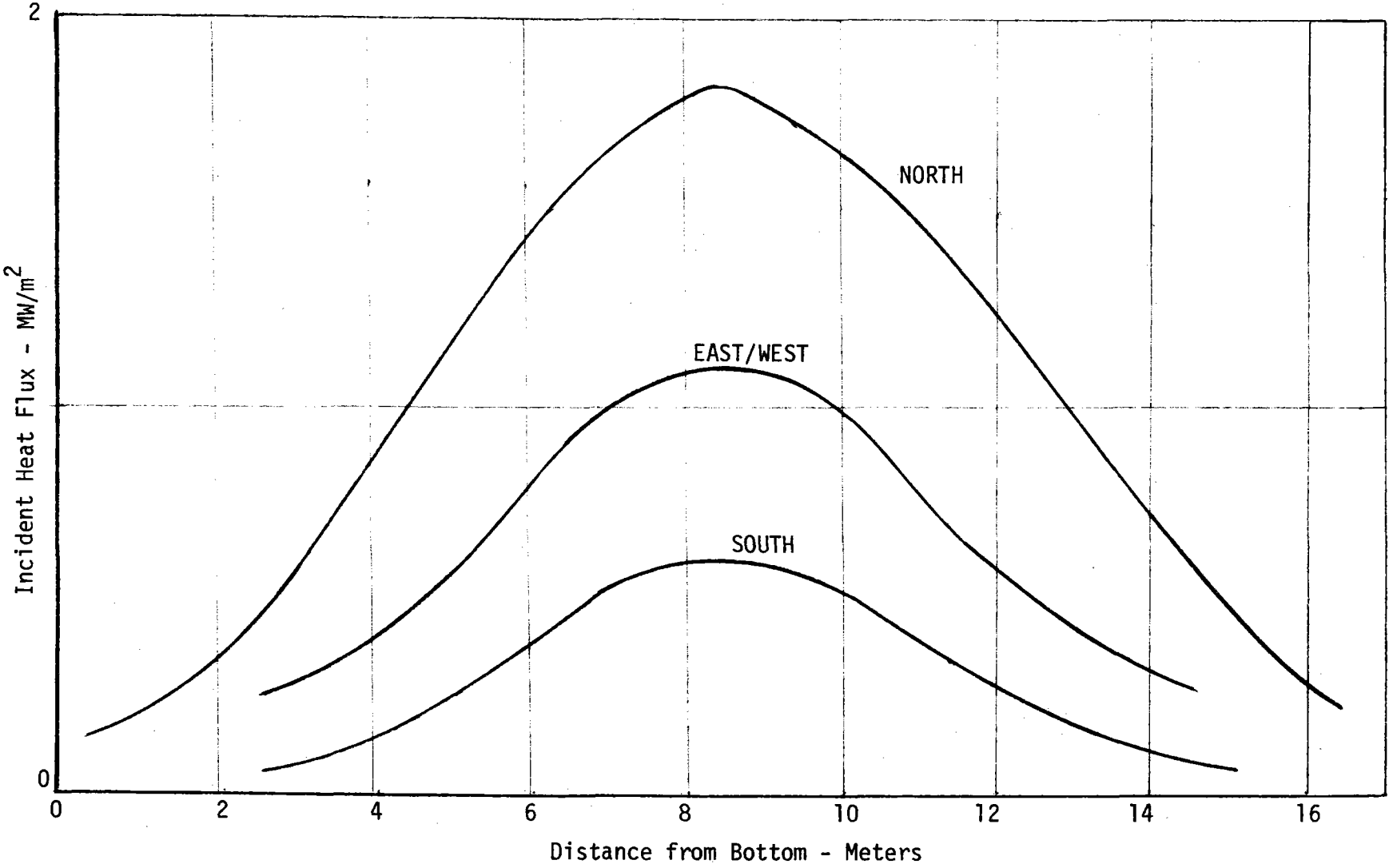

Figure 5-9. Receiver Heat Flux Profiles Equinox Noon

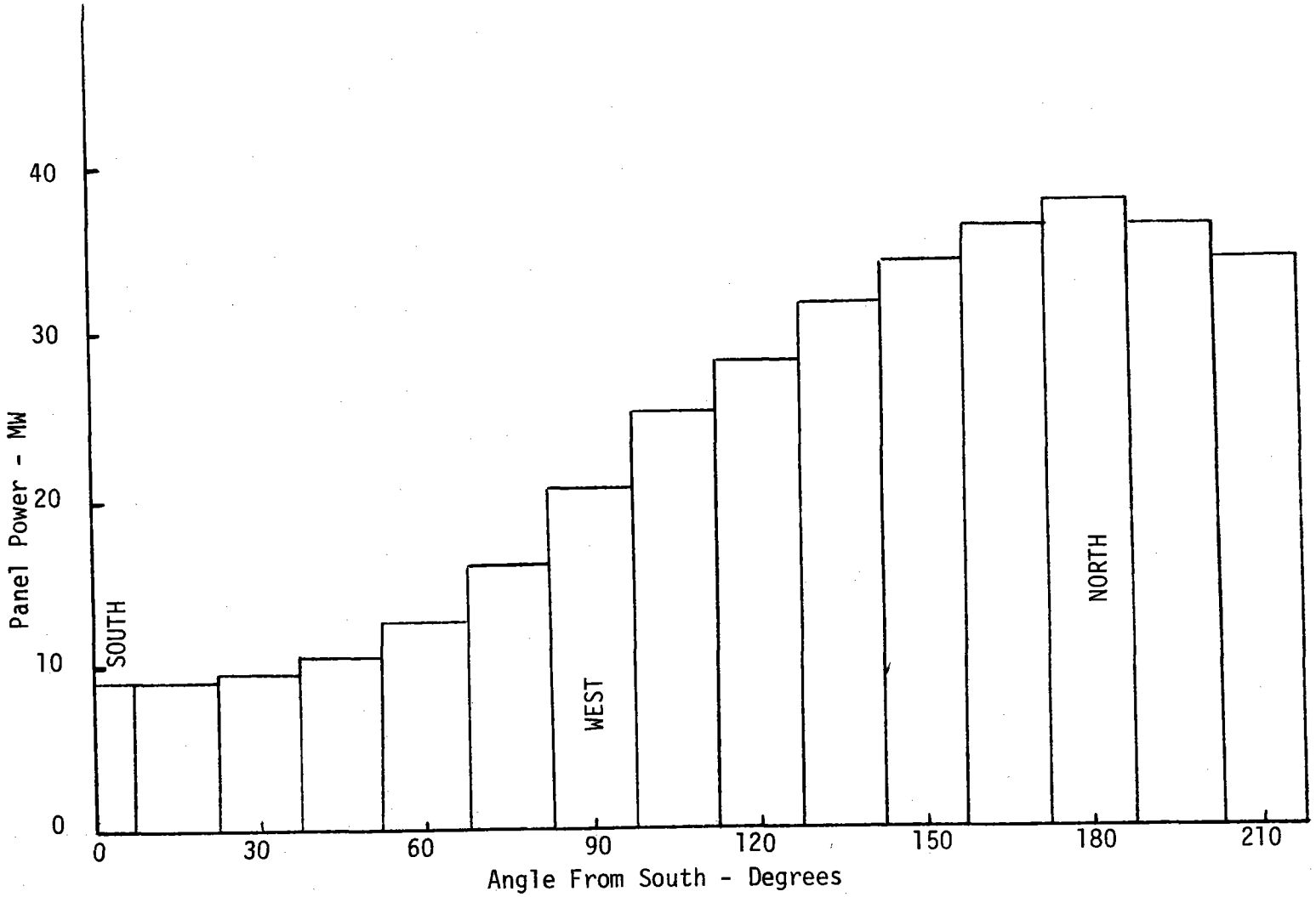

Figure 5-10. Receiver Heat Load Distribution - Equinox Noon

the north-facing panel is the controlling factor in the determination of receiver heat flux limits, tubing material, and size selection.

In addition to the heat flux profile shown in Figure 5-9, profiles were obtained for the cases of a smaller size receiver (15m x 15m) as well as other aiming strategies which included dual (high-low) point aiming and three-point aiming. Peak heat fluxes for these configurations are shown in Table 5-9. The values shown in Table 5-9 are absorbed values of heat flux rather than incident values. It is upon this basis that cooling calculations are performed.

TABLE 5-9. PEAK HEAT FLUXES ABSORBED BY RECEIVER

Diameter (m)	Aim Strategy	Peak Heat Flux MW/m^2
17	Single-Point	1.67
17	High-Low	1.43
17	Three-Point	1.14
15	Single-Point	2.15

These values were obtained by evaluation of University of Houston computer program output for the various aim strategies used, corrected to a consistent absorbed power level (500 MWt).

Detailed Thermal Analysis

Wall temperatures were calculated for the north panel considering the heat flux profile shown in Figure 5-9. These are shown in Figure 5-11, which indicates that the peak wall temperature point does not occur at

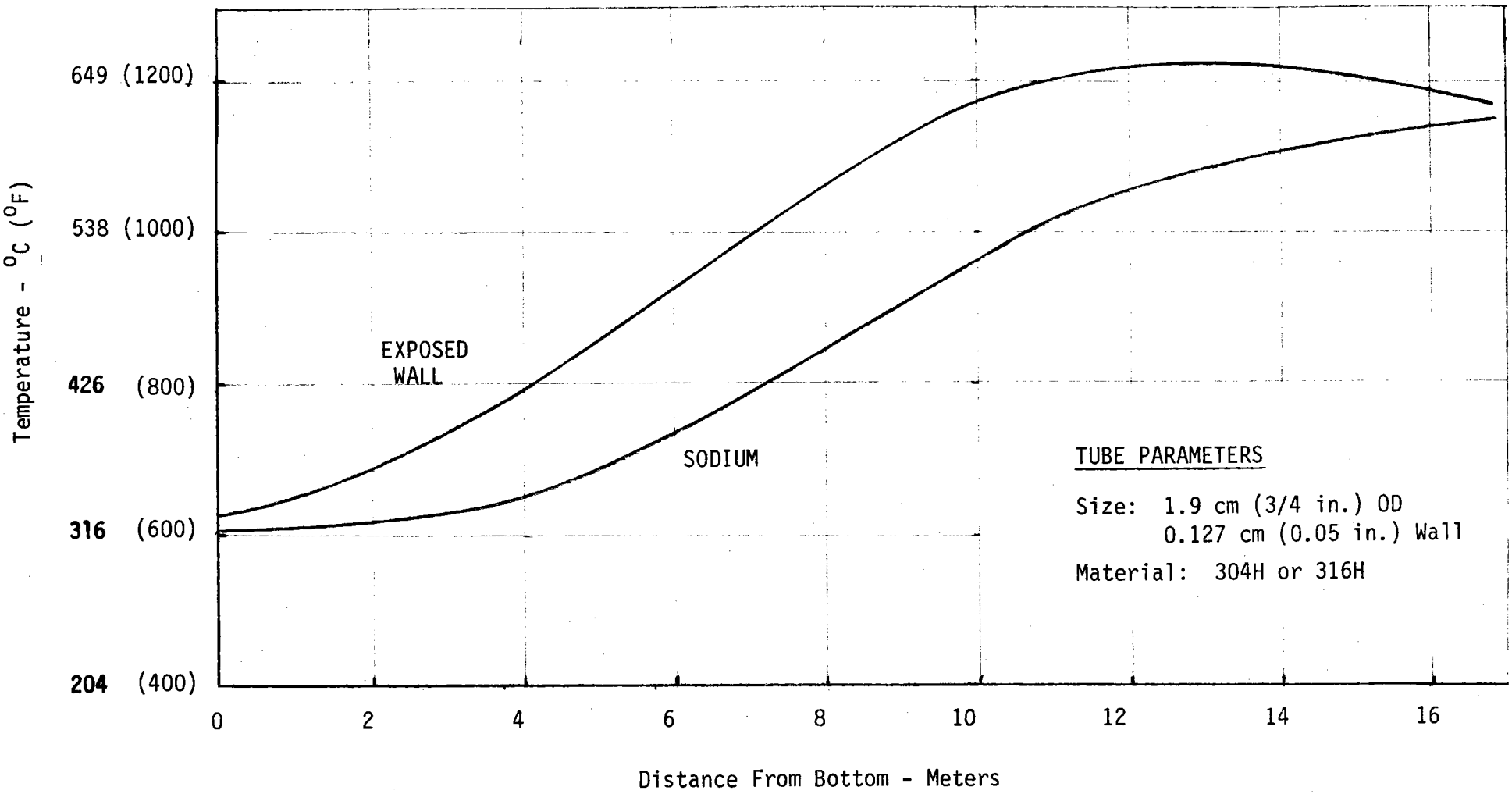

Figure 5-11. Receiver Temperature Profile, Equinox Noon, North End

the point of maximum heat flux. The determination of what, in fact, is the most critical structural position was studied (described in a subsequent section) and was found to be the point of maximum heat flux. The apparent reason is that material property degradation between 482 and 593^{o}C (900 and 1100^{o}F) for 304H stainless steel is not significant; consequently, the peak strain point controls fatigue life.

Two-dimensional temperature profiles for the 17m receiver with single-point aim are shown in Figures 5-12 to 5-16 for various axial locations along the receiver. These results are for a 1.9 cm (3/4-inch) O.D. tube with a 0.127 cm (0.05-inch) wall thickness.

Temperatures for the other aim strategies are shown in Figures 5-17 to 5-19 for a 1.9 cm (3/4-inch) tube. Figure 5-20 shows the temperature profile for the single-point aim condition with an Inconel 625 tube. Temperature profiles were also calculated for cases with smaller tubing. The peak temperatures for all cases are shown in Table 5-10. As indicated therein, changing tube size is not very significant in reducing wall temperature due to the wall resistance which tends to control the temperature balance.

Hydraulic Analysis

Pressure drops and pumping power requirements were estimated for the receiver designs synthesized previously. Power was estimated by assuming that all the flow had to be pumped through the same pressure drop, namely the north panel value. These results are shown in Table 5-11.

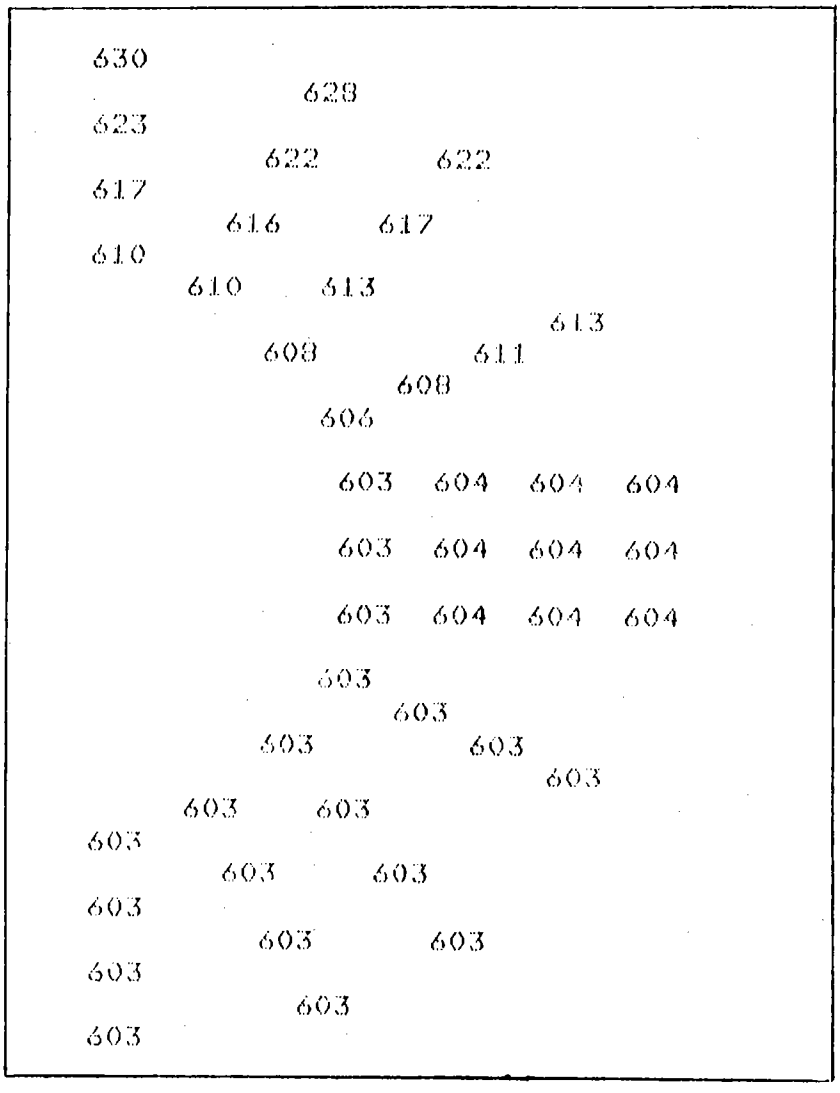

Figure 5-12. Advanced Receiver Tube Temperature Profile
Equinox Noon - North Side
1.9 cm (3/4-in.) OD - 0.127 cm (0.05-in.) Wall
Elevation 0.5 m, Heat Flux at Crown 0.154 MW/m^2
17m Receiver, Single-Point Aim

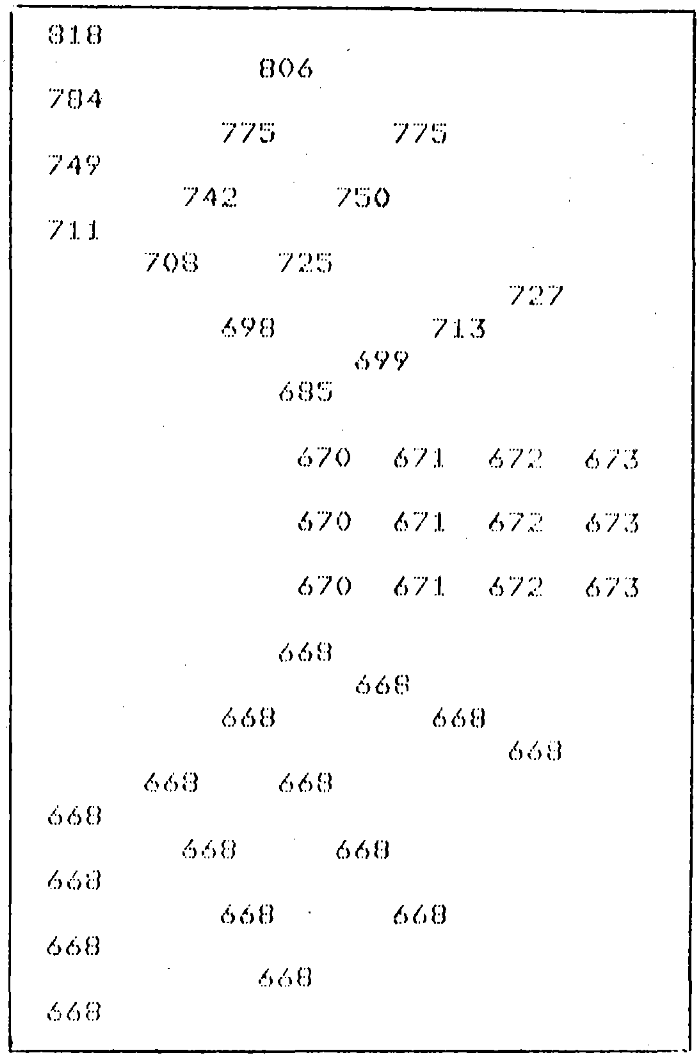

NOTE:
Temperatures in Degrees F

Figure 5-13. Advanced Receiver Tube Temperature Profile
Equinox Noon - North Side
1.9 cm (3/4-in.) OD - 0.127 cm (0.05-in.) Wall
Elevation 4.5 m, Heat Flux at Crown 0.903 MW/m^2
17 m Receiver, Single-Point Aim

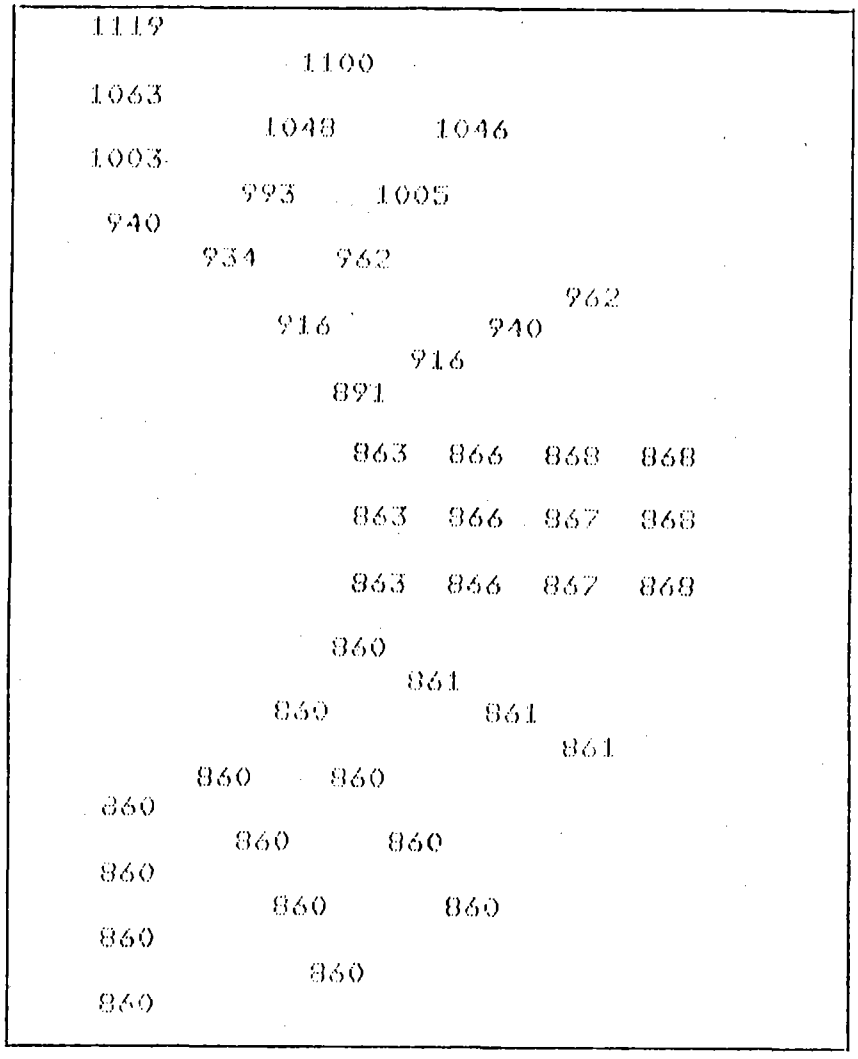

NOTE:
Temperatures
in Degrees F

Figure 5-14. Advanced Receiver Tube Temperature Profile
Equinox Noon - North Side
1.9 cm (3/4-in.) OD - 0.127 cm (0.05-in.) Wall
Elevation 8.5 m, Heat Flux at Crown 1.673 MW/m^2
17m Receiver, Single-Point Aim

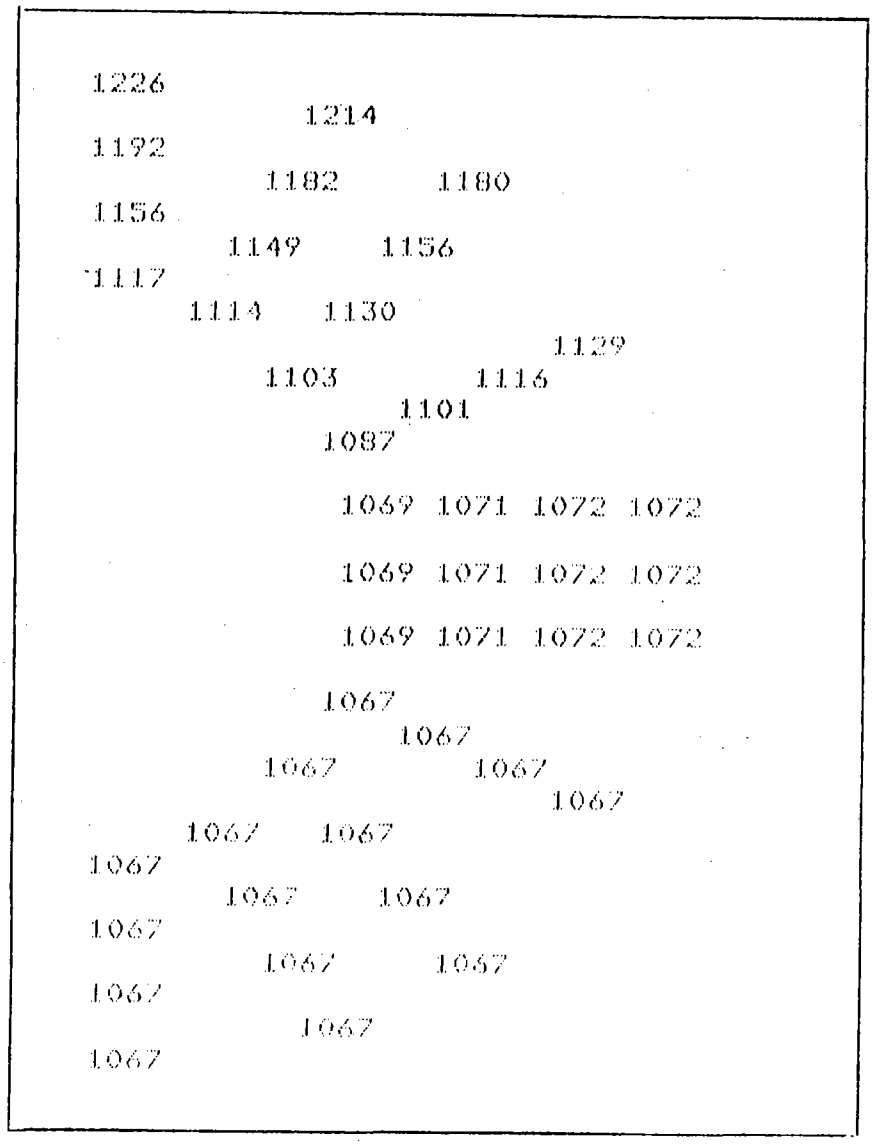

Figure 5-15. Advanced Receiver Tube Temperature Profile
Equinox Noon - North Side
1.9 cm (3/4-in.) OD - 0.127 cm (.05-in.) Wall
Elevation 12.5 m, Heat Flux at Crown 1.060 MW/m^2
17m Receiver, Single-Point Aim

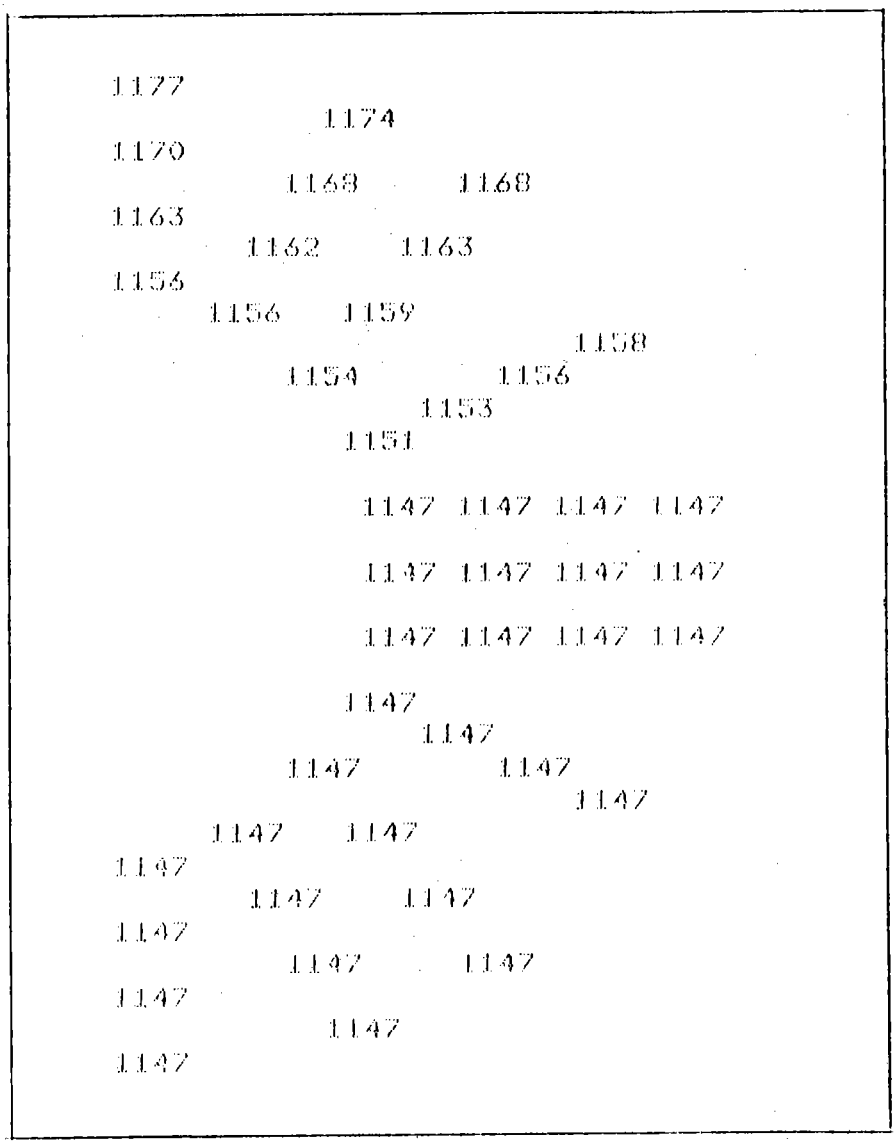

Figure 5-16. Advanced Receiver Tube Temperature Profile
Equinox Noon - North Side
1.9 cm (3/4-in.) OD - 0.127 cm (0.05-in.) Wall
Elevation 16.5 m, Heat Flux at Crown 0.200 MW/m^2
17m Receiver, Single-Point Aim

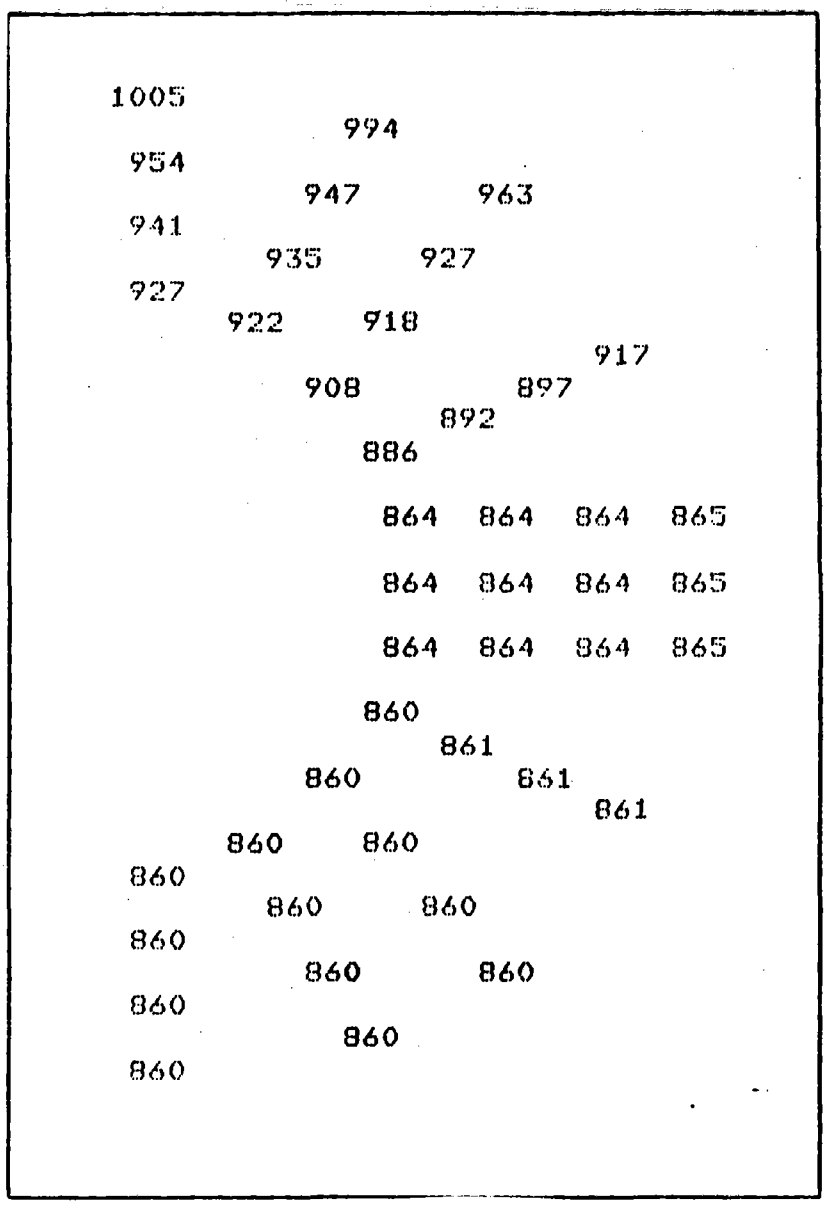

Figure 5-17. Advanced Receiver Tube Temperature Profile
Equinox Noon - North Side
1.9 cm. (3/4-In.) OD - 0.127 cm. (0.05-In.) Wall,
Elevation 8.5 m, Heat Flux at Crown 1.433 MW/m^2
Two-Point Aim Strategy, 17 m Receiver, CRES 304 Tubes

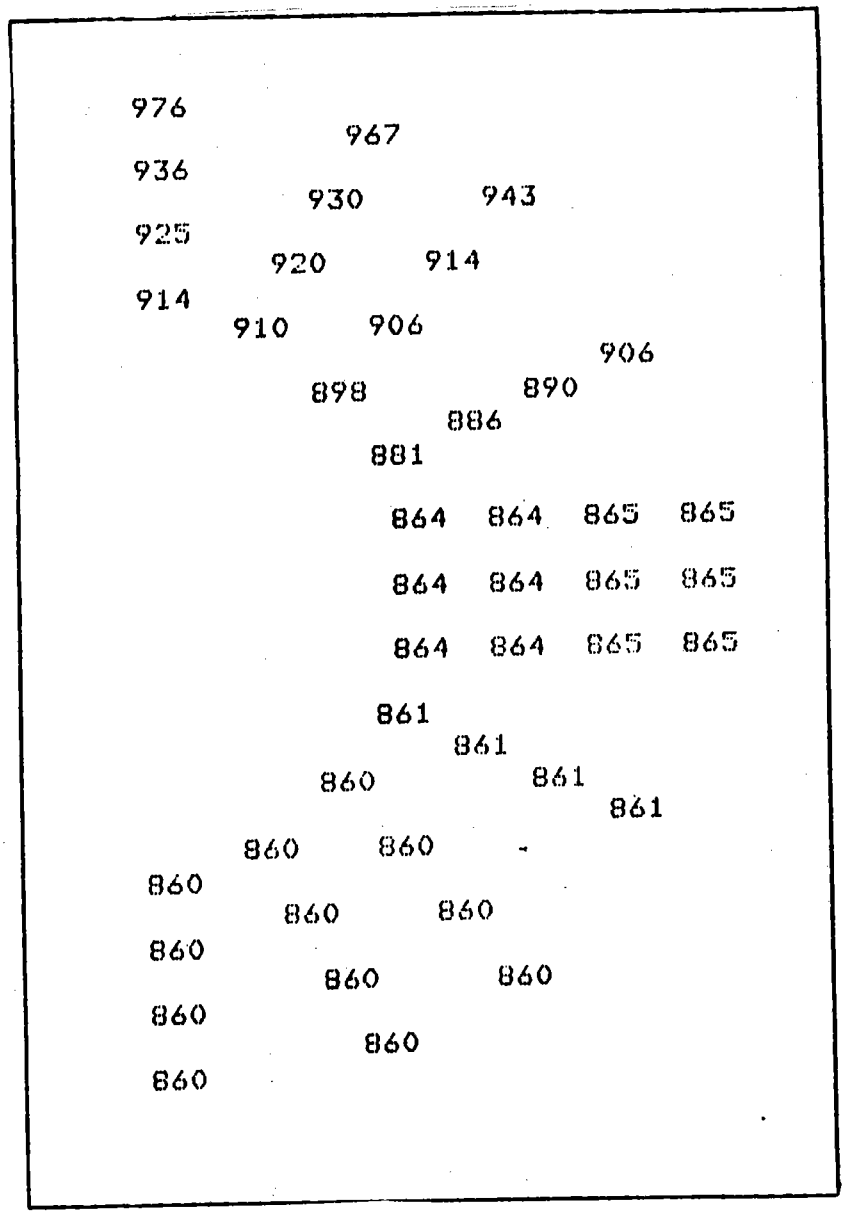

Figure 5-18. Advanced Receiver Tube Temperature Profile
Equinox Noon - North Side
1.9 cm. (3/4-In.) OD - 0.127 cm. (0.05-In.) Wall
Elevation 8.5 m, Heat Flux at Crown 1.143 MW/m^2
Three-Point Aim Strategy, 17 m Receiver, CRES 304 Tubes

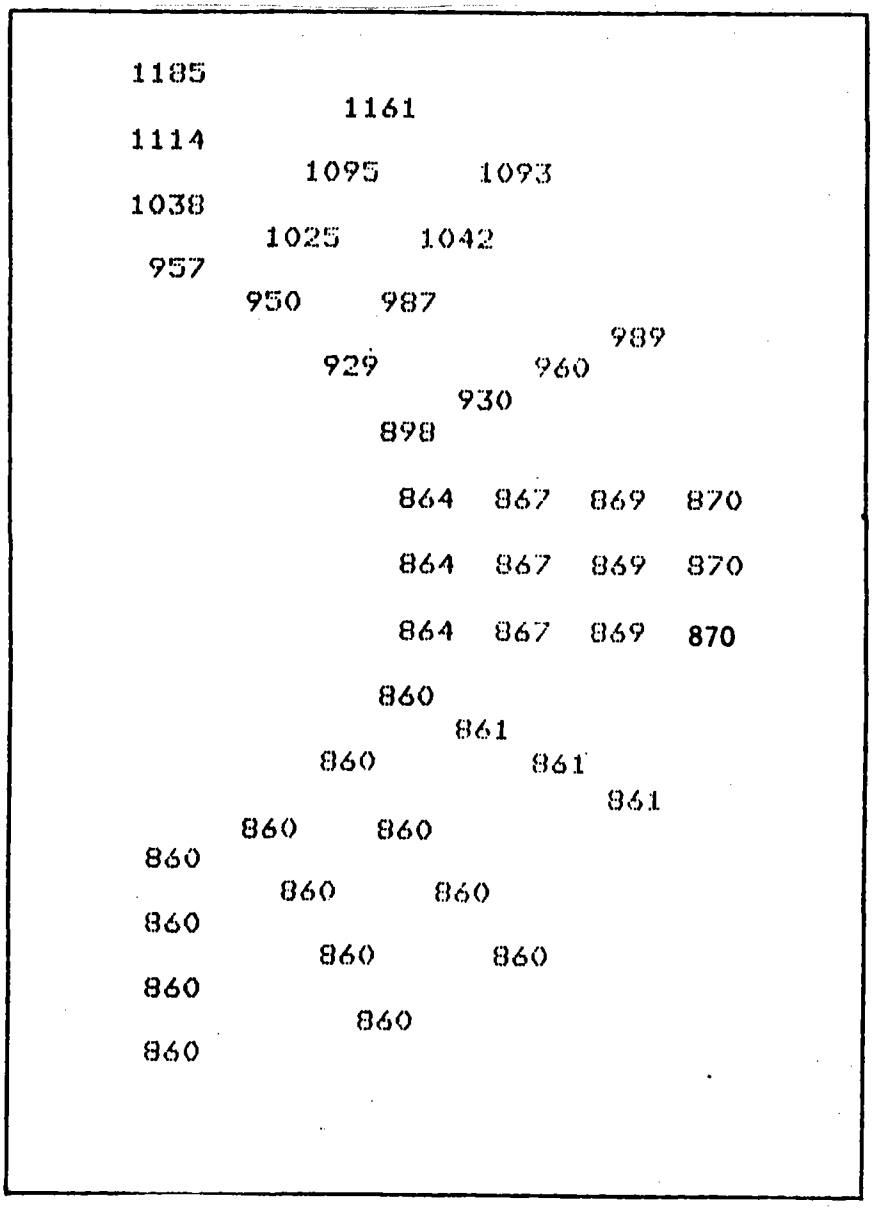

Figure 5-19. Advanced Receiver Tube Temperature Profile
Equinox Noon - North Side
1.9 cm (3/4-In.) OD - 0.127 cm. (0.05-In.) Wall
Elevation 8.5 m, Heat Flux at Crown 2.15 MW/m^2
One-Point Aim Strategy, 15 m Receiver, CRES 304 Tubes

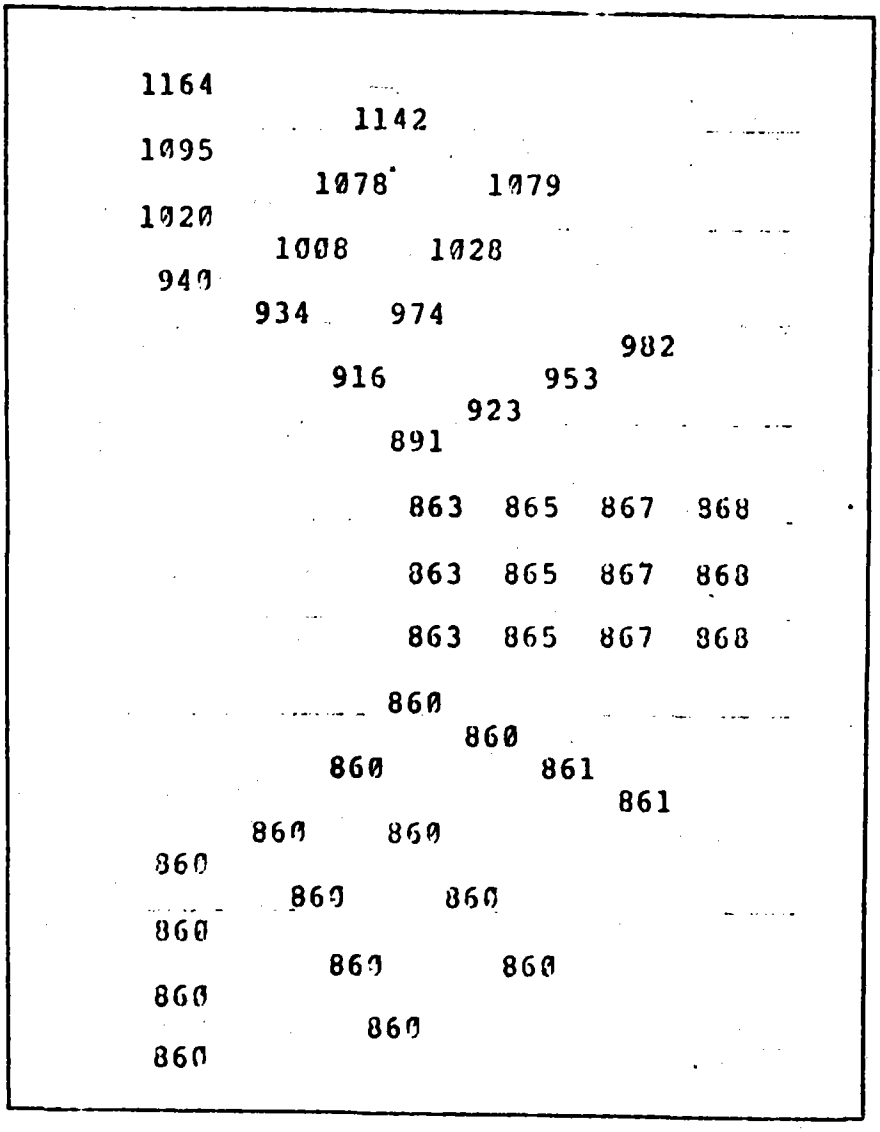

NOTE:
Temperatures
in Degrees F

Figure 5-20. Advanced Receiver Tube Temperature Profile
Equinox Noon - North Side
1.9 cm. (3/4-In.) OD - 0.127 cm. (0.05-In.) Wall
Elevation 8.5 m, Heat Flux at Crown 1.673 MW/m^2
One-Point Aim Strategy, 17 m Receiver, INCO 625 Tubes

TABLE 5-10. SUMMARY OF RECEIVER HEAT TRANSFER RESULTS

Receiver Diameter (Meters)	Collector Aim Strategy	Peak Heat Flux (MW/m^2)	Tube Material	Tube Size cm	Tube Size (in)	Crown Temperature ^oC	Crown Temperature (^oF)
17 x 17	Single Pt	1.67	SS 304H	1.9	(3/4)	604	(1119)
				1.6	(5/8)	598	(1108)
				1.3	1/2	598	(1097)
17 x 17	Single Pt	1.67	Inco 625	1.9	(3/4)	629	(1164)
				1.6	(5/8)	623	(1153)
				1.3	(1/2)	617	(1143)
17 x 17	High-Low	1.43	SS 304H	1.9	(3/4)	541	(1005)
				1.6	(5/8)	534	(993)
				1.3	(1/2)	528	(982)
17 x 17	Three Pt	1.14	SS 304H	1.9	(3/4)	524	(976)
				1.6	(5/8)	519	(967)
				1.3	(1/2)	514	(958)
15 x 15	One Pt	2.15	SS 304H	1.9	(3/4)	640	(1185)
15 x 17	High-Low	1.64	SS304H	1.9	(3/4)	596	(1105)(est)

TABLE 5-11. RECEIVER COOLING POWER REQUIREMENTS

Tube Size cm	(in)	Pressure Drop MN/m^2	(psi)	Fluid Horsepower MW	(hp)	Pump Power* MW
1.3	(1/2)	0.690	(100)	1.015	(1361)	2.03
1.6	(5/8)	0.276	(40)	0.406	(545)	0.81
1.9	(3/4)	0.138	(20)	0.203	(272)	0.41

*Assuming 50% pump efficiency

Alternate Cooling Medium

A brief and very preliminary evaluation of NaK-78 as a receiver coolant was performed relative to the use of sodium currently baselined. It was found that for the current receiver configuration (17m dia x 17m Ht) and a peak heat flux of approximately 1.75 MW/m^2, the tube size to obtain equivalent wall temperatures 649°C (1200°F) with NaK-78 would be two-thirds the size of the sodium-cooled tube. Additionally, the pumping power required would be more than 10 times greater with NaK-78 due to a combination of the higher pressure drop and higher flowrate.

The data base for this evaluation is contained in previous sections of this report. Only the north or peak power panel was evaluated. This panel absorbs 37.5 MW of thermal power. With this power level and a temperature rise of 260°C (500°F) for the coolant, the corresponding flows on the panel are:

Sodium: 96.4 Kg/sec (212 lb/sec)
NaK-78: 140.5 Kg/sec (309 lb/sec)

Using these flowrates as the available coolant and an assumed set of tube sizes, the parameters shown in Table 5-12 were generated. Based on these and the physical properties of the coolants shown in Table 5-2.

the wall temperatures shown in Figure 5-21 were generated. The coolant side heat transfer coefficient was estimated from the Lubarsky Kaufman Equation. The wall temperature differential was calculated considering a thermal conductivity of 10.4 w/m K (10 Btu/ft-hr-F) and a gauge of 0.127 cm (0.05 inch) with one-dimensional heat transfer.

TABLE 5-12. COMPARISON OF RECEIVER COOLING PARAMETERS*
Na vs NaK-78

Tube Size cm	(in.)	Number of Tubes	Mass Velocity (lb/ft^2-sec) Na	Mass Velocity (lb/ft^2-sec) NaK-78	Linear Velocity (gps) Na	Linear Velocity (gps) NaK-78	Heat Transfer Coefficient (Btu/ft^2-hr-F) Na	Heat Transfer Coefficient (Btu/ft^2-hr-F) NaK-78
2.54	(1)	87	447	651	8.5	13.5	5109	2835
1.9	(3/4)	116	793	1156	15.1	24.0	7813	4336
1.3	(1/2)	175	1338	2023	26.3	42.0	13079	7257

*Based on 2.22 m (87.5 inch) panel width and 0.127 cm (0.05 inch) wall thickness on all tubes.

Pumping power to cool the receiver was calculated by estimating the pressure drop from a standard turbulent flow equation and multiplying the head by the total receiver flows, 1301 Kg/sec (2862 lb/sec) sodium, 1896 Kg/sec (4171 lb/sec) NaK-78. Also, an efficiency of 50% was used for the pumping. The pump power is shown in Figure 5-22.

One may derive a meaningful interpretation from Figures 5-21 and 5-22 by considering the current baseline heat flux (1.75 MW/m^2) and an assumed temperature limit of 649°C (1200°F). From Figure 5-21 the required tube sizes are 2.3 cm (0.9 inch) for sodium and 1.42 cm (0.56 inch) for NaK-78. From Figure 5-22, the difference in power to cool the receiver can be seen to be an order of magnitude. Upon this basis, NaK-78 as a potential receiver coolant is seen to be vastly inferior to sodium.

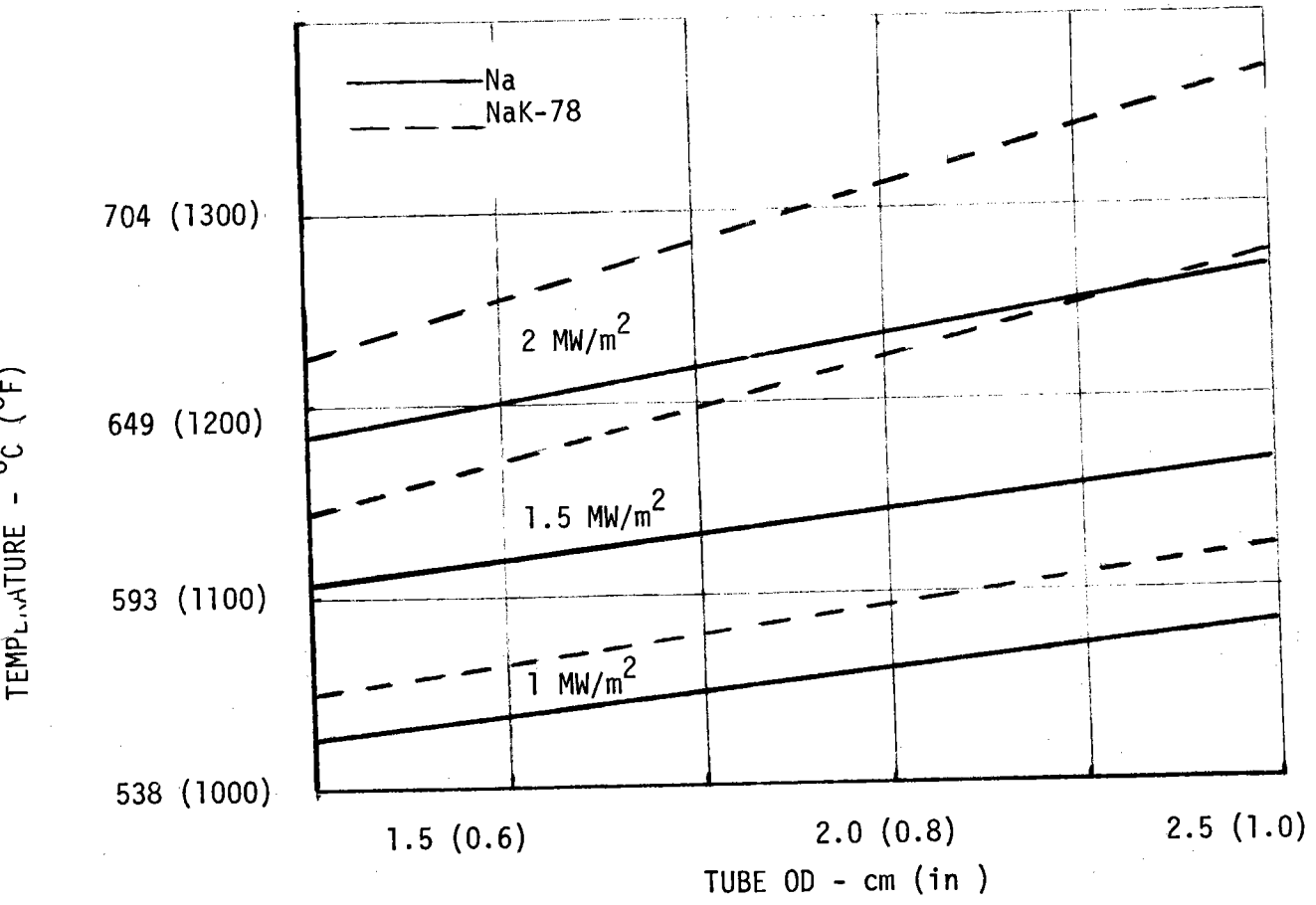

Figure 5-21. Alternate Cooling Medium Evaluation, Peak Wall Temperature

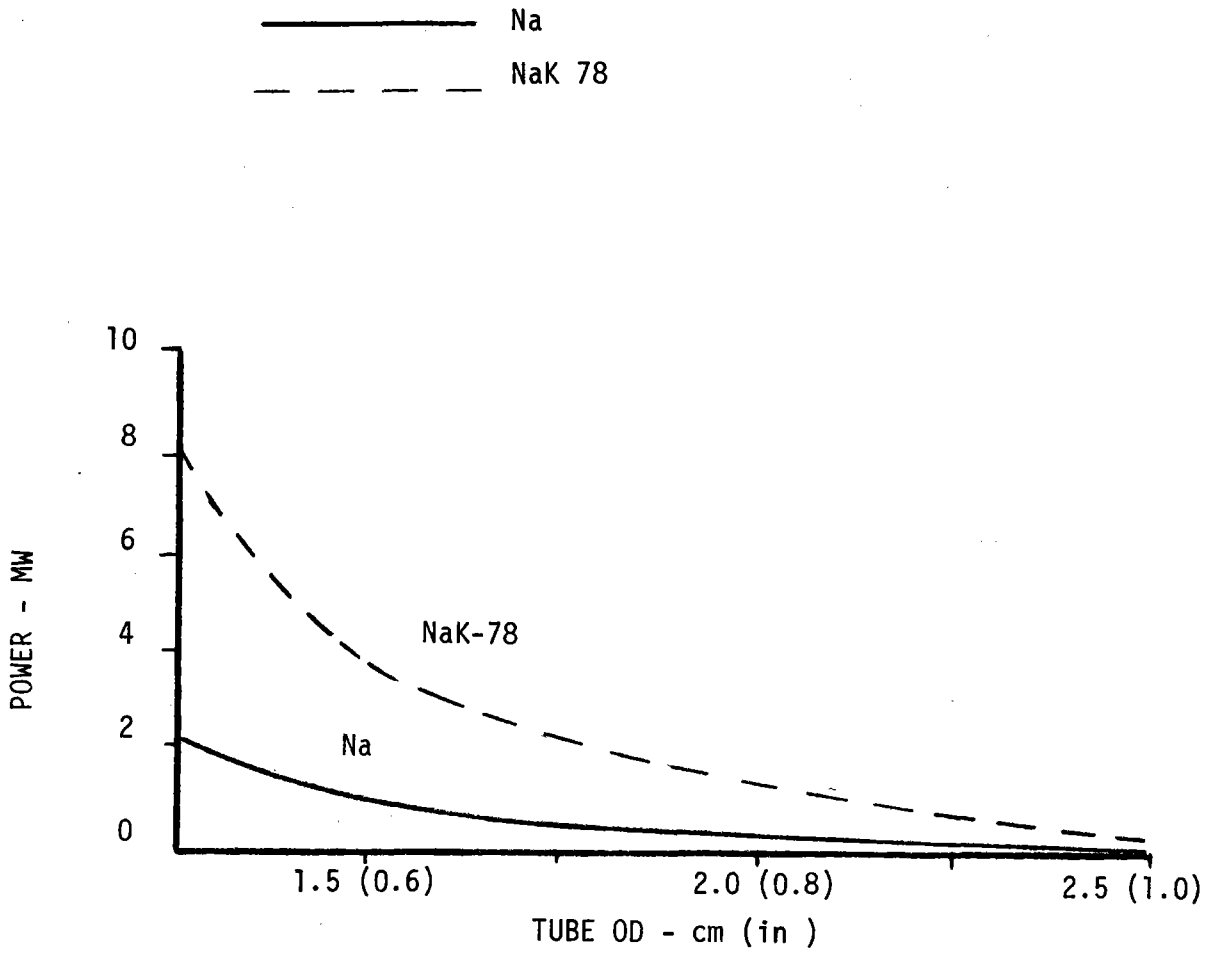

Figure 5-22. Alternate Cooling Medium Evaluation, Power for Cooling

Structural Analysis

With reference to the temperatures shown in Table 5-10, reducing tube size from 1.9 cm (3/4 inch) to 1.3 cm (1/2 inch) does not have a significant impact on operating temperature. This is due to the fact that the tube wall temperature is more controlled by the conduction within the wall. As such, in order to maintain higher heat fluxes and at the same time realize a significant reduction in wall temperature, one must consider reduction of the 0.127 cm (0.05 inch) gauge limit established for the tubing. Inconel 625 is capable of higher operating temperatures at equivalent life than Austenitic stainless steels (i.e., 304H), and consequently can be considered as a viable alternative considering the fact that its wall temperatures for equivalent heat fluxes and wall thickness are higher than those for stainless steel. If the necessity to reduce wall temperatures is of great importance, then one must consider a two- or three-point aim strategy and accept the higher losses caused by spillover or increased thermal losses due to a longer receiver length. These conclusions naturally are dependent on what wall temperatures are acceptable, and for that determination a low cycle fatigue analysis was performed. A preliminary analysis of low cycle fatigue was based on the analytically determined wall temperatures previously discussed and a fatigue life curve presented in Section III (Code Case 1592-7) of the ASME Boiler and Pressure Vessel Code for Austenitic stainless steels. Section III pertains to nuclear power plant components and, as such, is highly conservative. Because this subsystem will not be incorporated into a nuclear power plant system, it need not meet Section III requirements. Therefore, the following procedure was developed to ascertain the low cycle fatigue design curve for 304H stainless steel for the advanced solar receiver design.

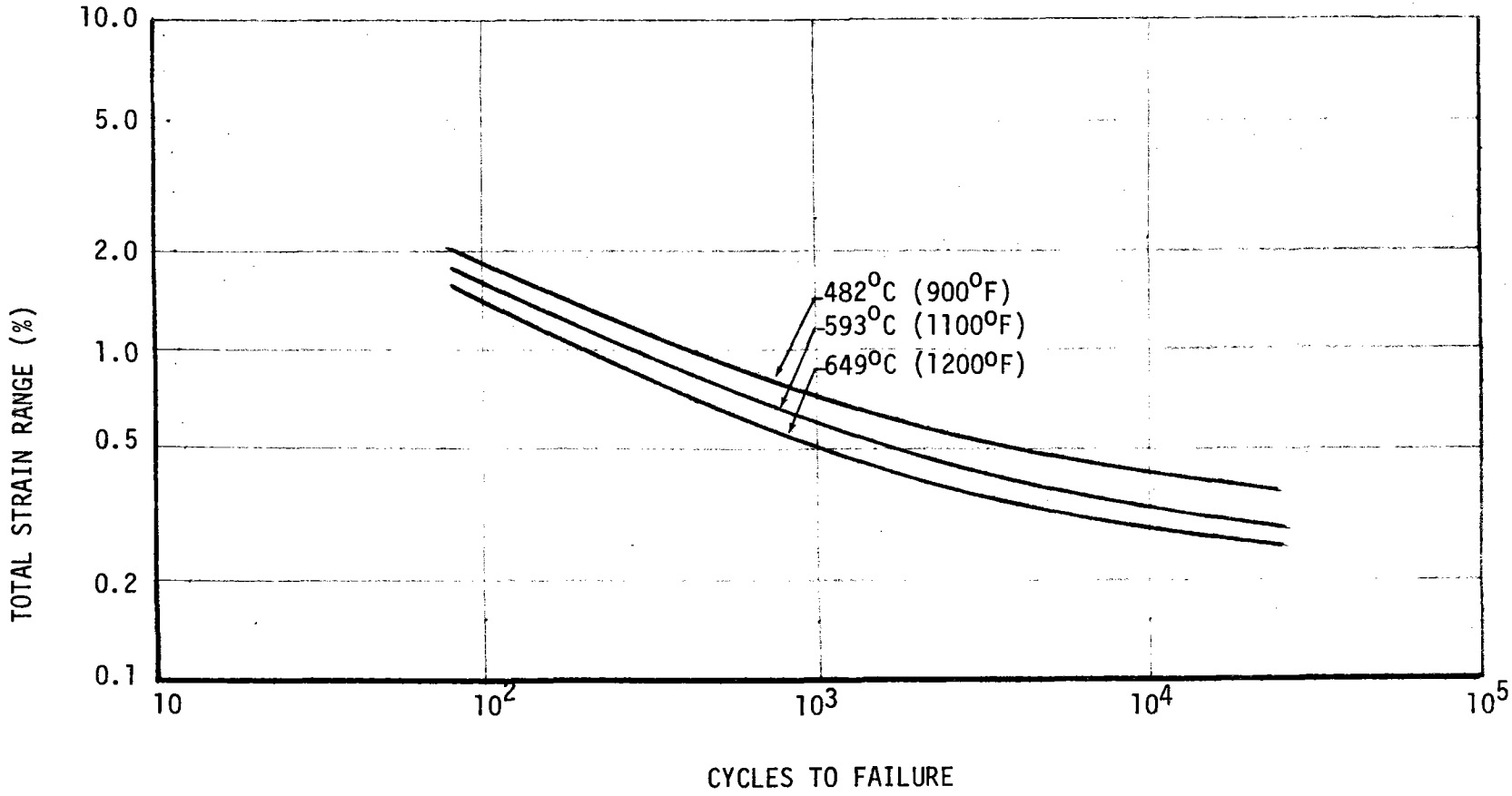

NOTES:

1. Based on "Argonne National Lab" data, R. W. Weeks
2. Factor of 3 on cycles to determine minimum expected life curve
3. Safety factor of 4 on cycles of minimum expected life curve to determine design curve

Figure 5-23. Advanced Solar Receiver Low Cycle Fatigue Design Curve, 304H Stainless Steel

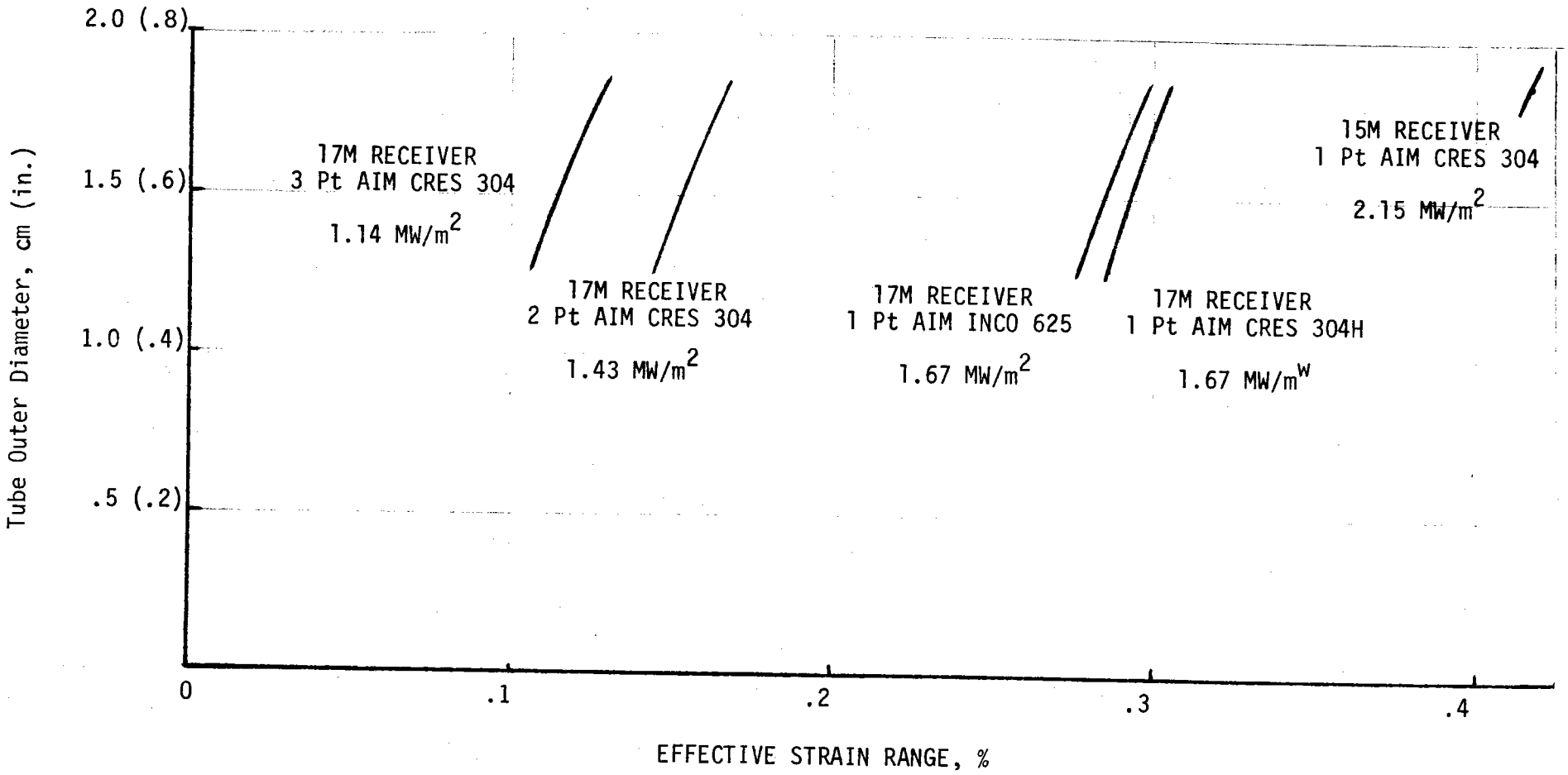

NOTE: All tubes are 0.127 cm (0.05-inch) thick

Figure 5-24. Sodium-Cooled Receiver Tube Strain

Low cycle fatigue data for the referenced material was provided by the Argonne National Laboratories. A factor of 3 was applied to the typical data curve and is defined as the minimum expected data curve. A safety factor of 4 was subsequently applied to cycles to determine the low cycle fatigue design curve. This procedure is consistent with and generally more conservative than that resulting in most design curves used at Rocketdyne for aerospace components. The recommended design curve for the solar receiver is shown in Figure 5-23. This curve was used to determine fatigue life of the receiver for the various temperature cases shown in Table 5-10.

Analysis Results

An analytic model of the stresses within the tube was developed. The results of this calculation were compared with finite element model results as to the accuracy of the strain calculation. Comparison was carried out with materials similar to those being used in this study but under heat flux conditions typical of a water/steam-cooled receiver. The comparison was generally favorable. The results of the strain analysis are shown in Figure 5-24. This figure is a plot of effective strain range vs tube size for various combinations of tube material, receiver size, and aiming strategy. As one might gather, changes in aim strategy and receiver size can result in a fourfold change in strain range within the tubes. The effect of tube size is quite small. This may be gathered from inspection of the temperature profiles previously submitted. Most of the temperature gradient is due to the conduction limit in the walls as opposed to the cooling medium. The main variable in Figure 5-24 affecting strain is therefore heat flux. Heat flux is grossly affected by receiver size and aiming strategy and, as shown in Figure 5-24, this has an overriding effect on strain.

The design life is shown in Figure 5-25, which indicates that the 17-meter receiver with a single-point aim utilizing 304H stainless steel tubing has life in excess of 10,000 cycles for the range of tube

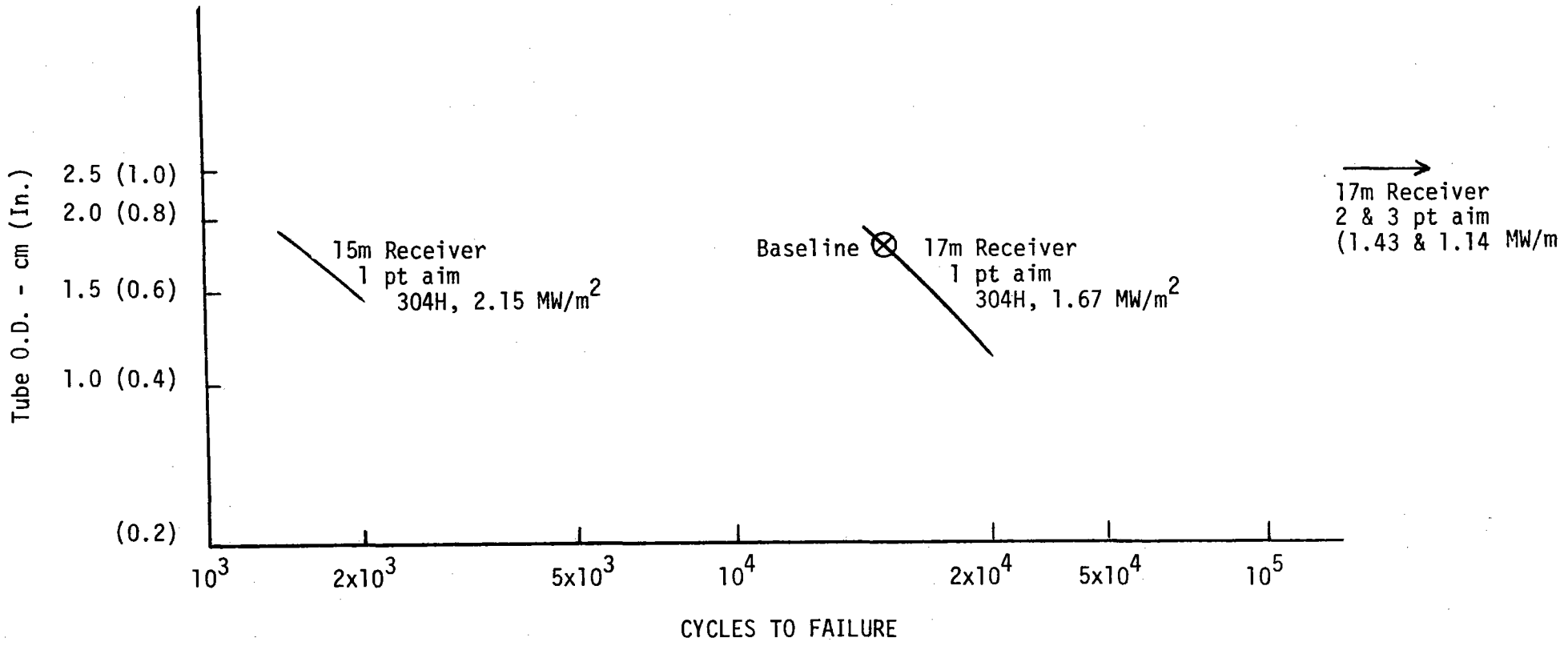

Figure 5-25. Sodium-Cooled Receiver Fatigue Life, 304H Stainless Steel Tubes 0.127 cm (0.05-Inch) Wall Thickness

sizes being considered. Increased life may be obtained by going to two and three aim points. This naturally increases receiver length to hold spillover losses constant. In all cases, as indicated on Figure 5-25, the life exceeds 100,000 cycles. Reducing receiver size to 15 meters with the single-point aim reduces the life well below the design goal, and is therefore not recommended at this point. All the information shown on Figure 5-25 is for 304H stainless steel. Using data for Inconel 625 can be expected to change the expected life, and in our judgment, for the better; however, insufficient data exist on this material to result in a valid comparison with 304H stainless. The preliminary calculation for the Incoloy 625 results in Figure 5-24 was performed using the law of universal slopes, and this resulted in reduction in life as compared with 304H stainless. Obviously, this comparison is not a valid one since the stainless calculation utilized actual test data. It was thus determined that, based on current technology, the 17-meter receiver utilizing 1.9 cm (3/4 inch) stainless steel tubing be utilized as the baseline for the sodium-cooler receiver and that any consideration of smaller receiver sizes be postponed until further data on more advanced materials is available.

Thermal Losses

Calculations of heat losses from the sodium receiver have been carried out. Receiver thermal efficiency was calculated from:

$$\text{Eff} = \frac{\alpha_s}{1 + \frac{q_R + q_c}{q_{ABS}}}$$

where α_s = Surface Solar Absorptance
q_R = IR Radiation Loss
q_c = Convection Loss
q_{ABS} = Absorbed Energy

The reflected insolation loss was calculated from the solar absorptance of Pyromark (0.95). The infrared loss was calculated from an average surface temperature for the receiver. Convective losses were estimated using a high Reynolds number heat transfer coefficient for a roughened cylinder in cross-flow.

This data was published by Achenbach, "Heat Transfer from Smooth and Rough Surfaced Cylinders in a Cross-Flow," in Germany. Calculations were carried out for two cases, namely, 315°C (600°F) and 288°C (550°F) coolant inlet temperatures with a 306°C (550°F) temperature rise. A wind velocity of 6.3 M/S (14 mph) was used in the calculation.

The individual heat loss components are shown below with the overall results plotted in terms of efficiency shown in Figure 5-26.

Power Absorbed MW	Inlet Temp. °C (°F)	Losses			
		Conv. MW	IR MW	Refl. MW	Tot. MW
500	288 (550)	6.4	16.0	27.5	49.9
300	288 (550)	6.1	14.7	16.9	37.7
100	288 (550)	5.9	13.4	6.3	25.6
500	315 (600)	6.7	18.5	27.7	52.9
300	315 (600)	6.5	17.0	17.0	40.5
100	315 (600)	6.3	15.6	6.4	28.3

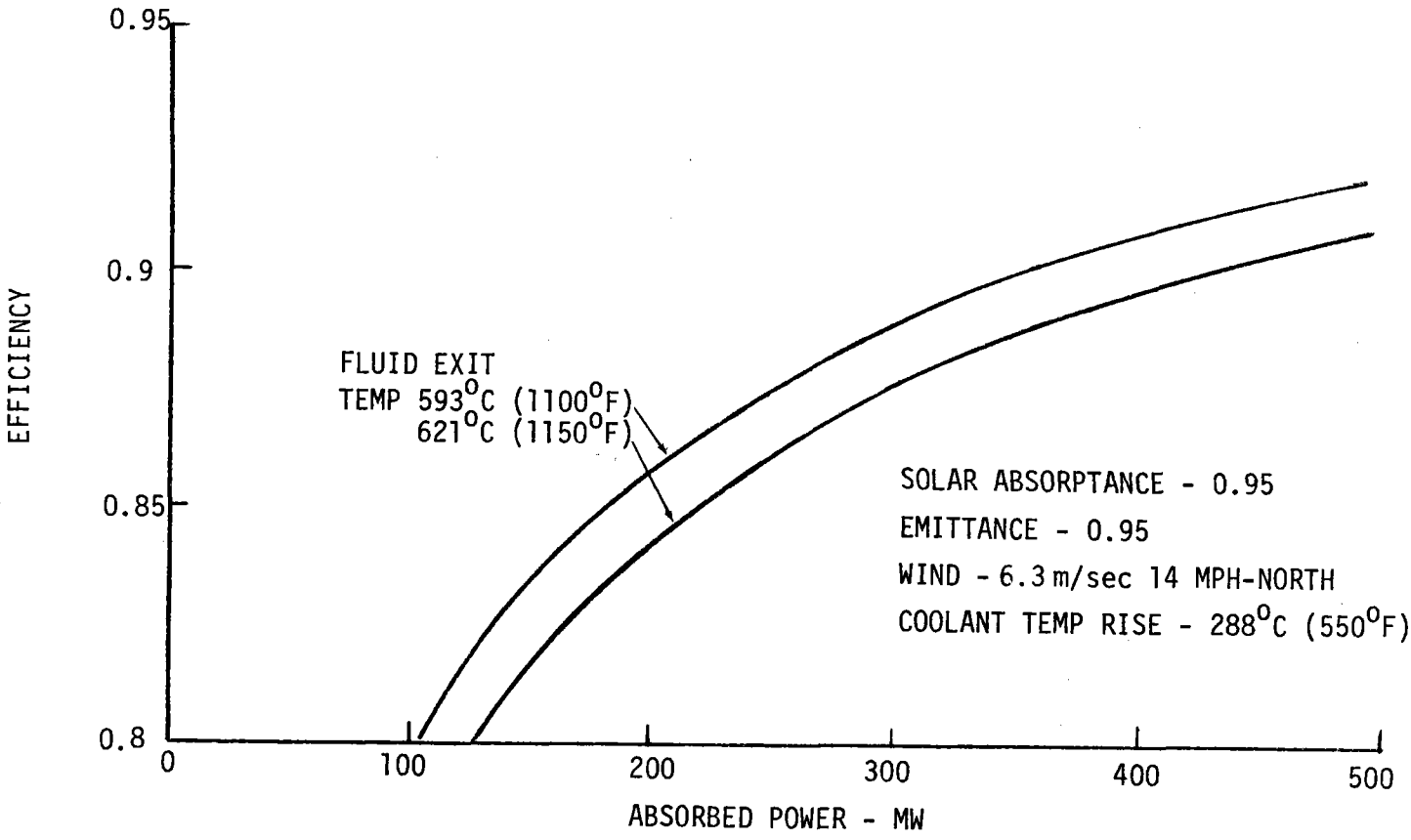

Figure 5-26. Advanced Receiver Thermal Efficiency

Receiver Design

A preliminary design layout is shown in Figure 5-27. The receiver is comprised of the following items:

1. Structural steel tower structure.
2. Coolant riser and distribution manifold.
3. Riser to downcomer crossover piping and control valve.
4. Solar panel inlet piping and coolant flow control valves.
5. Solar panels (24) with inlet and outlet manifolds and panel backup structure.
6. Solar panel outlet piping and downcomer.
7. Cover gas accumulator and vent lines.
8. Heaters, insulation, and instrumentation (temperature and pressure)
9. Miscellaneous equipment and facilities (lights, power, hoists, catwalks, passive shields, lightning protection, water, first aid, etc.).

The structural steel tower is similar to that derived for the water/steam system with the inner core the main support and the outer structure to support the panels. Eight columns on a 7-meter diameter are used as the main support.

The coolant riser and distribution manifold is 0.61 m (24 in.) pipe with 24 outlets, one for each panel. The riser to downcomer crossover

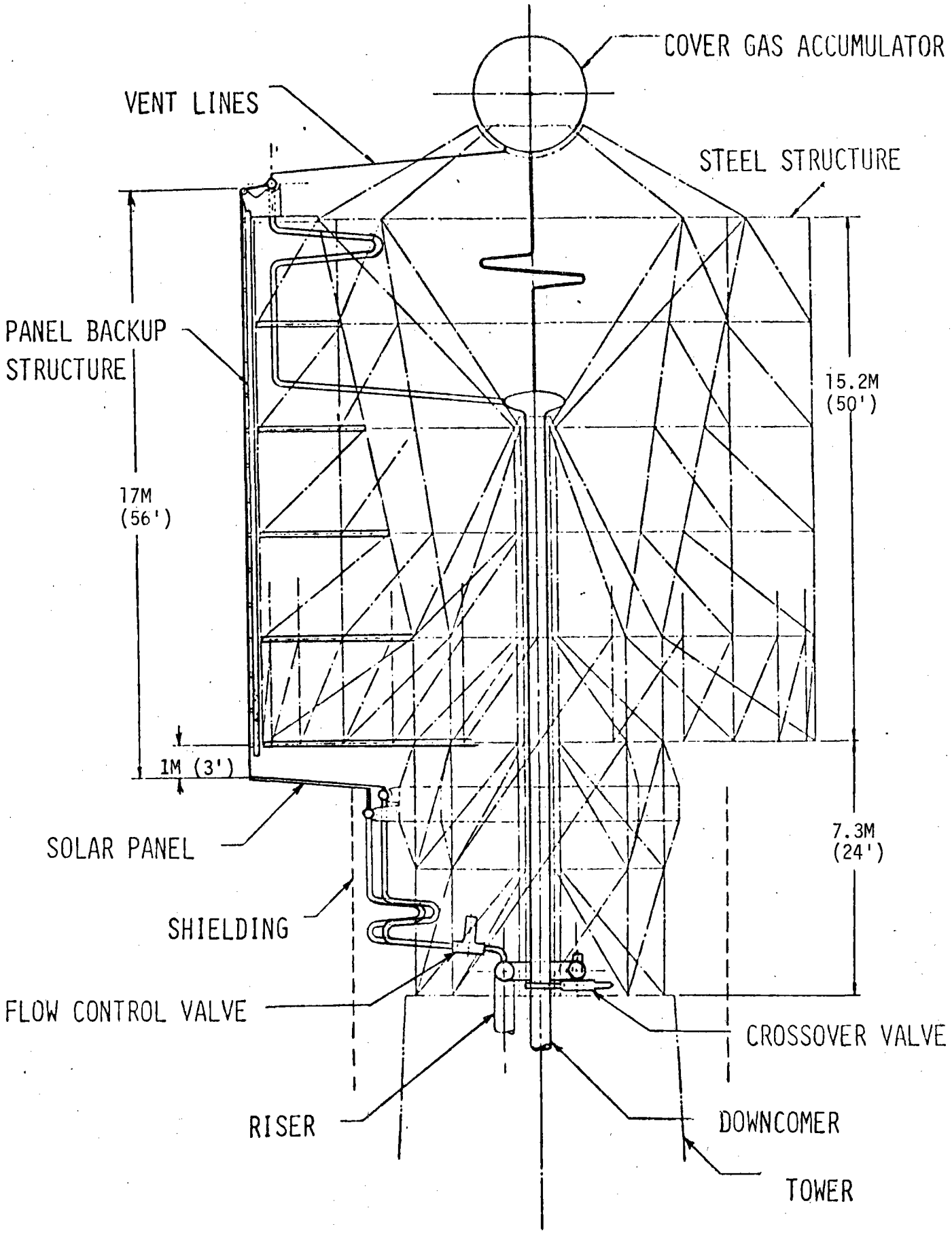

Figure 5-27. **Preliminary Design Layout**

is a 15.2 cm (6-inch) pipe which includes the shutoff valve. This is to be used while filling the system and recirculating hot sodium during standby. The inlet piping for each panel, as well as the control valve, is nominally 15.2 cm (6 inches). Both pipe and valve are free-draining back to the riser. Sodium-cooled panels are the same basic design as those used in the water/steam system, with the exception that both inlet and outlet headers are fixed and the longitudinal thermal growth is absorbed by bending in the panel at the folded back inlet end. Each panel has 115 tubes (1.9 cm (3/4-inch) O.D., 0.127 cm (0.05-inch) wall). The tubes are brazed or welded on the back side. The headers are nominally 25.4 cm (10 inches) in diameter, with staggered tubes welded and rolled. The backup structure includes two 15.2 cm (6-inch) I-beam rails with 10.2 cm (4-inch) transverse box beams approximately 0.9 m (3 feet) on centers. These will slide on clips welded to the tubes. Tube bundles and inlet headers are free-draining through the inlet plumbing. The outlet piping is 15.2 cm (6-inch) O.D. pipe and the downcomer is a 0.61 m (24-inch) O.D. pipe.

A cover gas accumulator of approximately 3.3 m (11 feet) in diameter is the high point in the receiver system. It is used to retain the cover gas during receiver operation, and to fill the void when the sodium level is lowered for standby. Trace heaters are to be used to heat all hardware with the exception of the panels. The panels will be heated by solar radiation prior to addition of coolant. The back side of the panels, as well as all plumbing and valves, will be covered with insulation.

The start and stop sequence has been developed as follows for the receiver:

1. Prior to sunup, the receiver is passivated with an inert cover gas atmosphere. Upon sun acquisition, panel temperatures are monitored until temperatures are found to exceed the riser temperature of the liquid sodium. At that point, the sodium is pumped into the receiver to displace the cover gas.

2. Following this, the receiver flowrate is slowly increased until rated outlet temperature is achieved. The temperature set point for the flow control valves is ramped from the initial set position to the rated operating condition. The receiver is then operating under automatic control.

3. At the onset of sundown, a reverse approach is utilized. Receiver flow is maintained at a 5-10% level as power reduces below this value. When receiver temperature reaches the riser temperature, the sodium is drained into the trace-heated sections of the riser and downcomer. The sodium is replaced with inert gas. At this point, the system is said to passivated.

In the event of passing clouds, the sodium outlet temperature control system will attempt to maintain outlet temperature by throttling flowrate. If sodium outlet temperature cannot be maintained at some minimum power level, say 25%, a temporary standby mode will be instituted by circulating cold tank sodium (at approximately 288°C [approximately 550°F]) to maintain the receiver at this temperature. With the passing of the clouds, a normal startup from the riser temperature will be instituted. If the cloud cover continues, a nighttime shutdown would be instituted.

The above receiver activities are decoupled from the steam generator operation since the steam generator units operate from the hot storage tank. Hence, as long as hot sodium is available, power production can continue without regard for the input transients being experienced at the receiver.

5.3.2 Receiver Pump

Requirements

The receiver pump is required to supply the flowrate of 4.47 x 10^6 Kg/hr (9.83 x 10^6 lb/h) as given in Table 5-1 to the receiver. Operating temperature of the pump is 288°C (550°F). A pump speed control range of at least 5 to 1 is required to match flowrate with the absorbed energy at the receiver to maintain receiver outlet temperature.

Design Characteristics

The receiver pump performance characteristics are listed in Table 5-1 as part of the receiver subsystem description. The required flowrate, equivalent to 1.45 m^3/sec (23,000 gpm) is well within the current flowrate capability of sodium pumps, such as the sodium pump for the Clinch River Breeder Reactor Program (CRBRP). The developed head requirement of 249 m (980 ft) is substantially higher than for existing designs and may necessitate using a two-stage centrifugal impeller design.

An alternative way of achieving the high developed head is to run two lower head pumps of 149 m (490 ft) each in series. With this arrangement, existing pump designs such as for the Fast Flux Test Facility or for the CRBRP could be used. This arrangement is expected to be more expensive, however, than a single two-stage centrifugal pump.

The concept of two pumps in series could require that the second pump accept relatively high inlet pressures. This condition was investigated as part of the analysis of the initial two loop baseline configuration, as discussed in Section 5.2. The high inlet pressure mainly influences the pump upper seal design, as is discussed in the paragraphs below. An alternative design solution would be to locate the second pump in the tower at a location high enough to reduce the inlet pressure to an acceptable level.

Pump Seals

The primary sodium pump operation at inlet pressures to 400 psi has been raised as a concern, particularly the seal between the cover gas and the upper bearing lubricating oil.

Figure 5-28 shows a schematic arrangement of the CRBRP pump with a flow capacity of 33,400 gpm at a developed heat of 450 ft. Maximum design inlet pressure for the CRBRP secondary pump is 115 psig. For the subject application, inlet pressure at the base of a 874-ft tower is 334 psig.

A cover gas seal is at the shaft upper end of the pump in the region of the floor flange. The cover gas pressure must be equal to the inlet pressure for level control. A schematic arrangement of the seals is shown on Figure 5-29. Oil is pressurized by a built-in pump to a pressure slightly greater than cover gas pressure. Oil leakage across the seal face is collected in drainage cavities and returned to the sump. Note that the seal is between the cover gas and the oil, and therefore is not exposed to liquid sodium.

A similar seal arrangement is used on pressurized water reactor pumps (Figure 5-30) which operate at inlet pressures to 2500 psig.

While some modification of current seal design may be necessary in order to optimize the design for a higher pressure, the change is expected to be well within the state of the art.

5.3.3 Steam Generator

Requirements

The steam generator arrangement is required to supply 286 MWt of thermal power to the turbine. Other system parameters that define

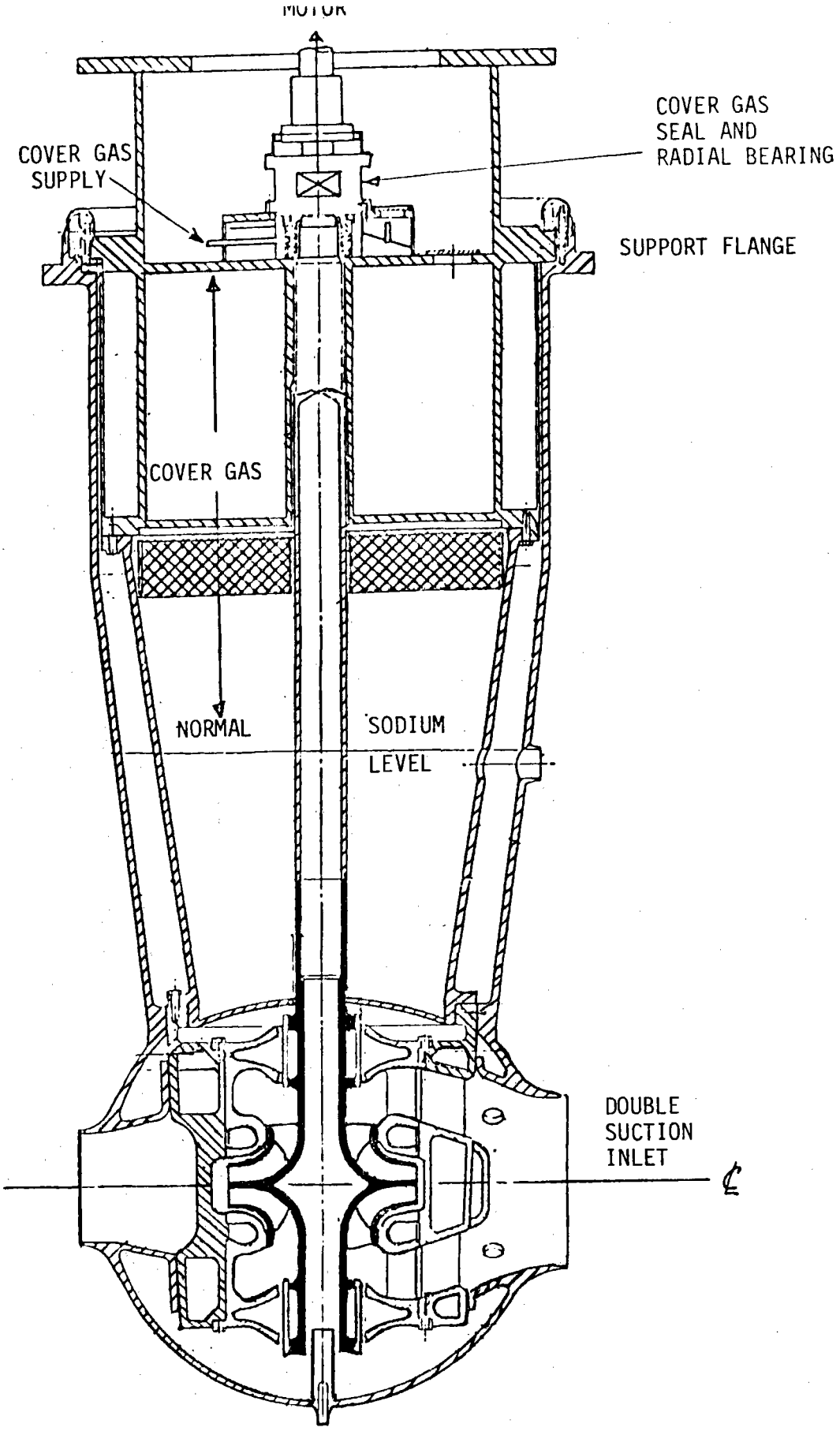

FIGURE 5-28
CRBRP PUMP SCHEMATIC

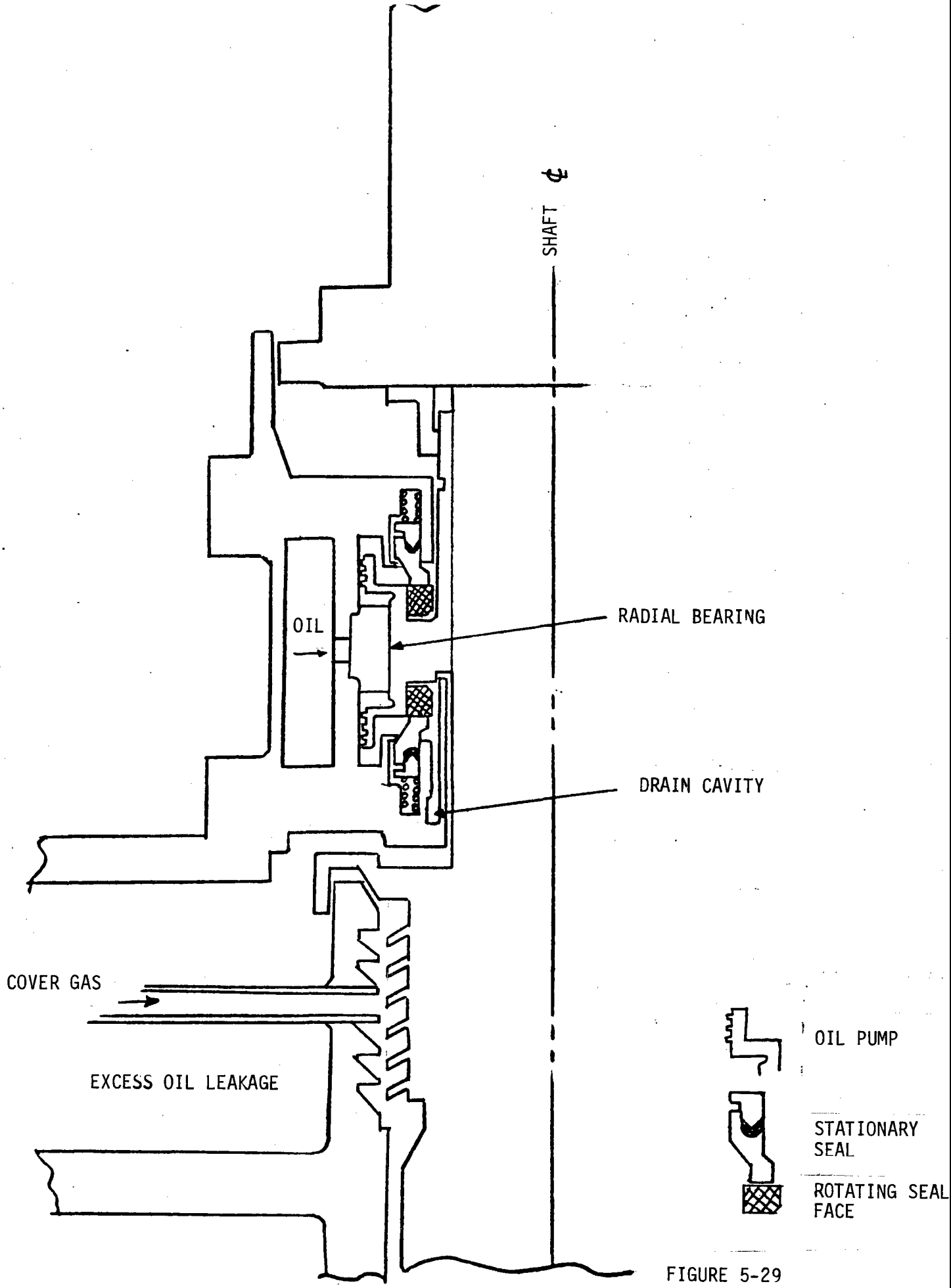

FIGURE 5-29
CRBRP PROTYPE PUMP SEAL

PRELIMINARY OPERATING PARAMETERS		
SEAL	INLET PRESSURE	FLOW RATE
NO. 1	2250	3 GPM
NO. 2	50	3 GPH
NO. 3	6	100 CC/HR

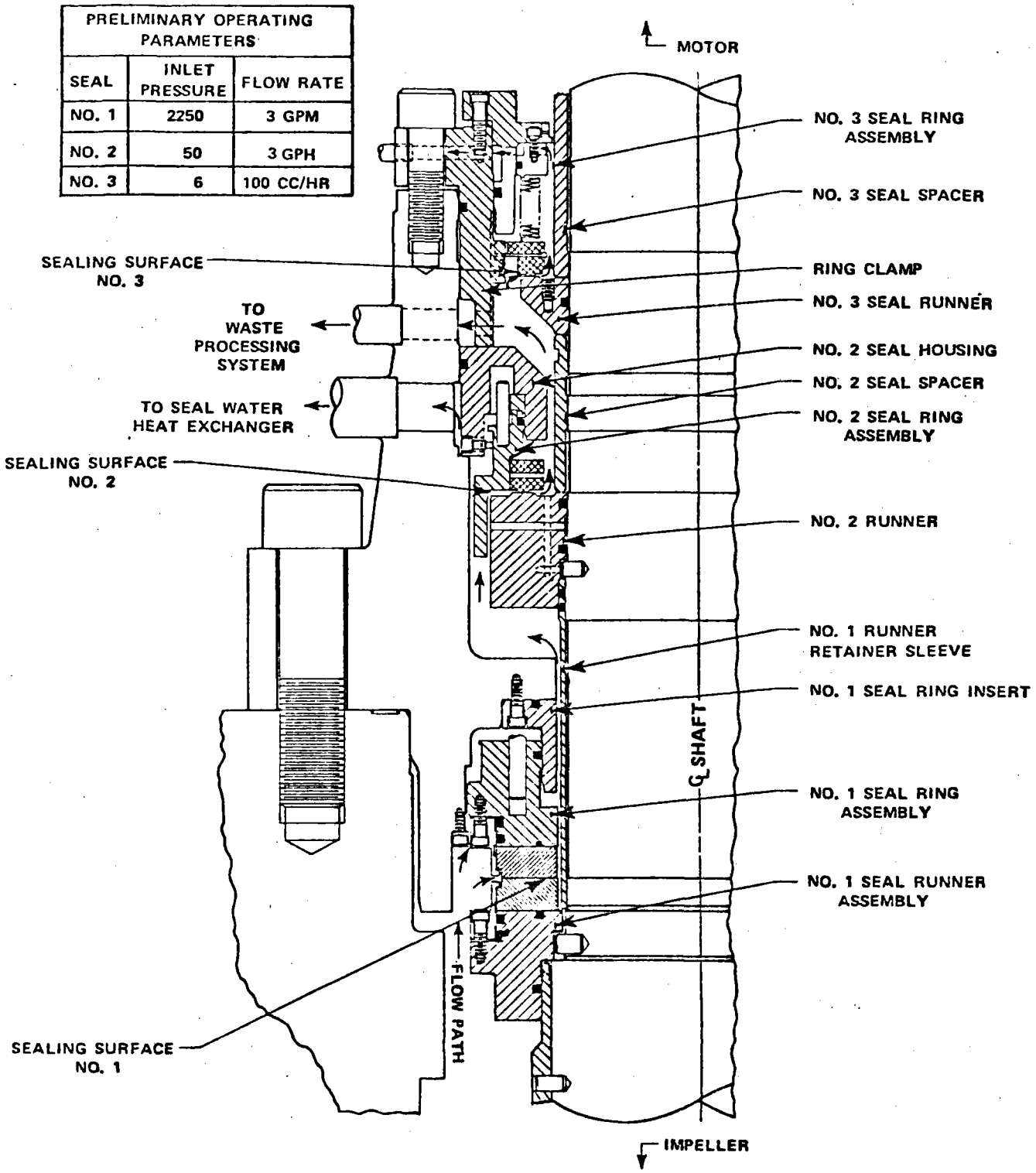

FIGURE 5-30 RCP TYPICAL SHAFT SEAL ARRANGEMENT

the steam generator operating requirements are given in Table 5-1. The turbine in temperature of 538°C (1000°F) and the feedwater temperature of 205°C (400°F) establish the sodium temperature operating range of 593°C (1000°F) inlet and 288°C (550°F). Water/steam side cycle efficiency dictates a feedwater pressure into the evaporator unit of 16.6 MN/m^2 (2400 psi). Pressure drop on both the water/steam side and the sodium side is to be minimized to reduce the required pump parasitic power. The steam cycle requires reheat as identified in Table 5-1.

Design Characteristics

The cycle requirements given above together with the large sodium temperature difference across the steam generator are best satisfied by separate units performing the evaporator, superheat, and reheat functions. By separating these functions, the ΔT across the evaporator unit is 184°C (332°F) and across the superheater or reheat is 121°C (218°F). This range of temperature difference eases the structural design of the units and more closely matches the current experience with sodium service steam generator design. Two approaches were considered in providing the steam generator function.

The initial approach used the Atomics International modular steam generator unit (AI/MSG). This unit, pictured in Figure 5-31 was built and tested in liquid sodium at power levels up to 33.8 MWt. For this application, a total of ten units were arranged as four evaporators, four superheaters, and two as reheaters. This arrangement has a reasonably good match of load requirements for each function but with the reheaters operating at a slightly derated condition. The extensive interconnecting piping for this arrangement contained control valves for flow balancing purposes. The evaporator units would be built using 2-1/4 Cr - 1 Mo, identical to the test unit. For the higher temperature application as the superheater or reheater, the units would be constructed of 316H stainless steel. Stainless steel was selected as the most suitable material after a review of high temperature operating experience with different materials.

The experience acquired in the U.S. as well as in other countries relative to the use of liquid metals for heat transport in power producing systems is summarized in Table 5-13. Operating temperatures up to 704°C (1300°F) have been successfully demonstrated. As can be seen, the material of construction for piping, core vessels, and for intermediate heat exchangers (IHX) has generally been one of the 300 series stainless steels. One of the major components in these power systems is the steam generator. A great many studies and tests on this component have been conducted over the last twenty years or so and a great amount of progress has been made. The results of small-scale and large-scale liquid metal loop tests as well as the experience gained in power reactor systems are delineated in Table 5-14. The problems identified do not seem to be associated with temperature. Most of the experience, however, has been acquired at temperatures less than 538°C (1000°F). One of the most successful steam generator development and test efforts has been carried out at Atomics International on the Modular Steam Generator (MSG). The salient features of this component are summarized in Figure 5-31. This is the design recommended for solar applications. At temperatures at or below 510°C (950°F), no change in material of construction is necessary. However, at temperatures above 510°C (950°F), the recommended material of construction is Type 316H SS. The status of the MSG for solar application is given in Table 5-15. The recommended change in material will require a structural analysis effort in order to confirm the adequacy of the current design using stainless steel Type 316H.

The modular approach appears attractive for early plants, but for a large number of standardized plants, evaporator, superheaters, and reheater units designed for the specific purpose would greatly simplify the system flow configuration and result in a cost reduction. This simpler arrangement for the power requirements of the revised configuration would consist of an evaporator of 177 MWt, a superheater of 79 MWt, and a reheat unit of 30 MWt. The larger evaporator unit could be a scale-up based on the Clinch River Breeder Reactor (CRBR) design ($\sim$120 MWt). The superheater would be very similar to the current CRBR since with the

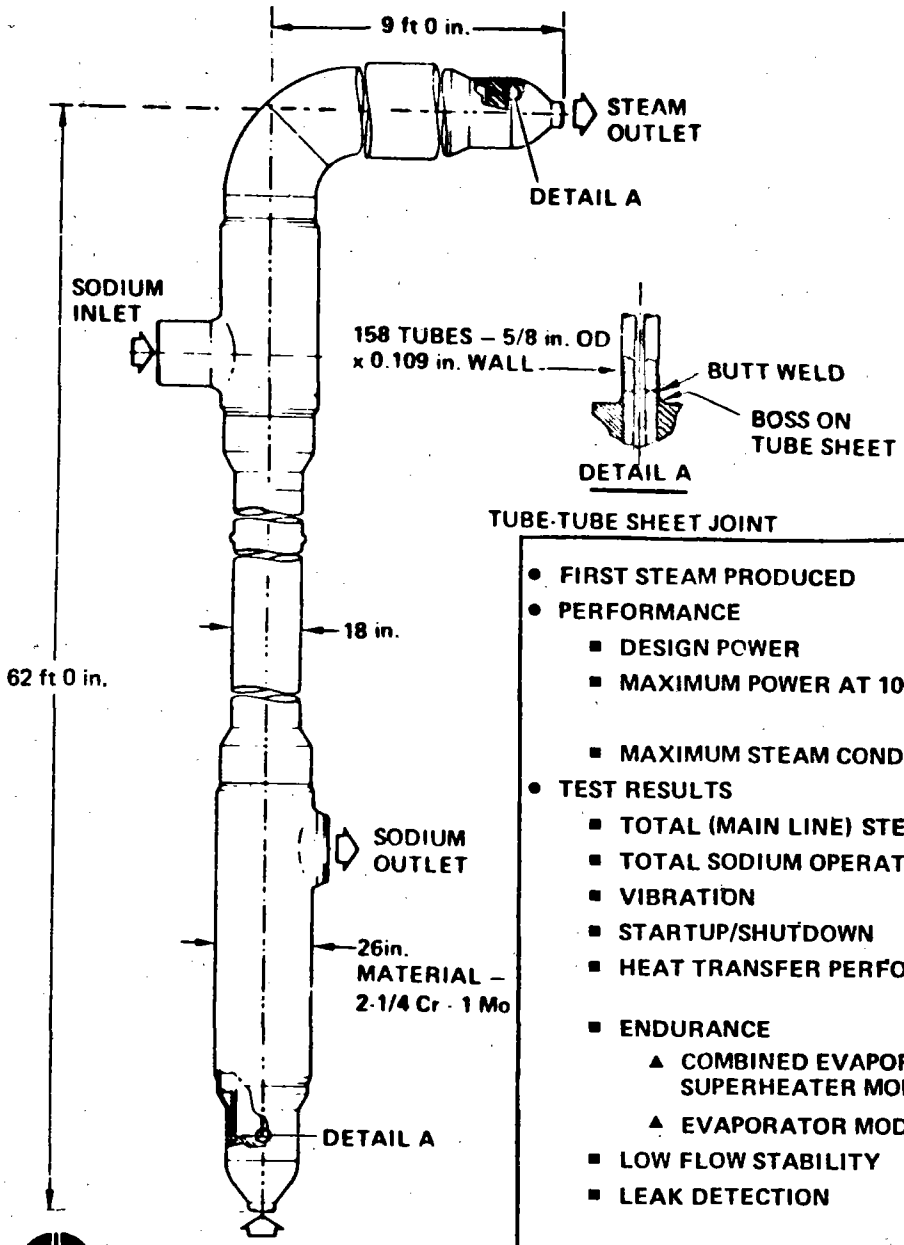

• FIRST STEAM PRODUCED	7-9-72
• PERFORMANCE	
■ DESIGN POWER	28.4 Mwt
■ MAXIMUM POWER AT 100% FLOW	32.1 Mwt (FOR 2400 psig STEAM)
	33.8 Mwt (FOR 1450 psig STEAM)
■ MAXIMUM STEAM CONDITIONS	2430 psig/930°F
• TEST RESULTS	
■ TOTAL (MAIN LINE) STEAMING TIME	4015 hr
■ TOTAL SODIUM OPERATING TIME	9305 hr
■ VIBRATION	LEVELS LOW, SAFE
■ STARTUP/SHUTDOWN	37 CYCLES, STABLE
■ HEAT TRANSFER PERFORMANCE	PARAMETRIC DATA OBTAINED FROM 1450 TO 2450 psig
■ ENDURANCE	
▲ COMBINED EVAPORATOR/ SUPERHEATER MODE	500 hr
▲ EVAPORATOR MODE	500 hr
■ LOW FLOW STABILITY	STABLE, ALL CONDITIONS OF INTEREST
■ LEAK DETECTION	DETECTABILITY OF 10^{-6} lb/sec H_2O DEMONSTRATION
■ TRANSIENTS	INTEGRITY MAINTAINED

Figure 5-31. Highlights of AI Modular Steam Generator Testing

74-M20-15-44

TABLE 5-13

LIQUID METAL REACTOR EXPERIENCE

Facility	Location	Power (MWt)	Coolant	Component	Material	Temperature (°F) Design	Temperature (°F) Maximum Operational	Operation
EBR-II	Idaho	45	Na	Core Vessel	304 SS	1000	880	1964 to Present
				Piping	304 SS	1000	880	
				IHX Shell	304 SS	1000	880	
Fermi	Michigan	100	Na	Core Vessel	304 SS	1000	825	1963 to 1966
				Piping	304 SS	1000	825	
				IHX Shell	304 SS	1000	825	
Sefor	Arkansas	24	Na	Core Vessel	304 SS		820	1968 to Present
DFR	Scotland	60	NaK	Core Vessel	321 SS		780	1962 to 1967; 1969
				Piping	321 SS		780	
				IHX Shell	321 SS		620	
Rapsodie	France	24	Na	Core Vessel	316 SS		1000	1967 to Present
				Piping	316 SS		1000	
				IHX Shell	316 SS		950	
SRE	California	20	Na	Core Vessel	304 SS	1500	1030	1957 to 1964
				Piping	304 SS	1200	1030	(> 37,000 hr)
				IHX Shell	304 SS	1200	1000	
HNPF	Nebraska	240	Na	Core Vessel	304 SS	1000	945	1963 to 1965
				Piping	304 SS	1000	945	
				IHX Shell	304 SS	1000	895	
BR-5	USSR	5	Na Primary	Core Vessel	321 SS		840	1959 to ?
			NaK Secondary	Piping	321		840	(38,000 hr to
				IHX Shell			800	July 1967)

TABLE 5-13 (Continued)

LIQUID METAL REACTOR EXPERIENCE

Facility	Location	Power (MWt)	Coolant	Component	Material	Temperature (^{o}F) Design	Temperature (^{o}F) Maximum Operational	Operation
EBR-1	Idaho	1.4	NaK	Core Vessel Piping IHX Shell	347 SS 347 SS A-Nickel		610 610 580	1961 to 1963
SNAP 2 (DR & ER)	AI	0.06	NaK	Core Vessel Piping IHX Shell	316 SS 304 SS 316 SS	1300 1300 1300	1200 1200 1200	~3000 hr Each
SNAP 8 (DR & ER)	AI	0.6	NaK	Core Vessel Piping IHX Shell	316 SS 316 SS 316 SS	1400 1400 1400	1300 1300 1250	S8ER - 10,000 hr S8DR - 10,000 hr
SNAP 10 (FS-3, FS-4)	AI	0.03 0.04	NaK	Core Vessel Piping	316 SS 316 SS	1050 1050	1010 1010	FS-3 - 10,000 hr FS-4 - 1,000 hr
ANL	Tennessee	2.5	Na	Core Vessel Piping	Inconel Inconel		1300	220 hr

TABLE 5-14

SUMMARY OF "COMPACT TUBE" STEAM GENERATOR EXPERIENCE

TYPE OF TEST	SMALL-SCALE TESTS			
FACILITY	W-HTMI	GRAND QUEVILLEY	INTERATOM KNK MODEL	MONJU 2-TUBE MODEL
POWER (MWt)	1	5	5	1
CONFIGURATION	SINGLE-WALL SERPENTINE TUBE WITH COVER GAS	SERPENTINE TUBE AND SHELL, HELICAL TUBE, AND Z-TUBE	SERPENTINE TUBE AND SHELL	SINGLE-WALL HELICAL TUBE
MATERIALS	ALLOY 800	2-1/4 Cr – 1 Mo EVAPORATOR, TYPE 321 SS SUPERHEATER	STABILIZED 2-1/4 Cr – 1 Mo	2-1/4 Cr – 1 Mo
TYPE OF OPERATION	ONCE THROUGH	ONCE THROUGH	ONCE THROUGH	ONCE THROUGH
LIQUID METAL INLET TEMPERATURE (°F)	960	1020	790	1000
EXIT STEAM CONDITIONS (psi/°F)	2400/950	2470/955	1160/790	2545/955
OPERATING TIME (h)	800	8000	5600	3600
PROBLEMS	INSTABILITY	MINOR FLOW MALDISTRIBUTION	NONE	TWO SMALL WELDS IN HAZ OF WELDS WHICH HAD NOT RECEIVED PWHT

TABLE 5-14 (Continued)

SUMMARY OF "COMPACT TUBE" STEAM GENERATOR EXPERIENCE (CONTINUED)

TYPE OF TEST	LARGE-SCALE TESTS					
FACILITY	PHENIX	SUPER-PHENIX FIVES-CAIL BABCOCK	SUPER-PHENIX STEIN INDUSTRIES	SNR HELICAL TUBE	MONJU	AI-MSG
POWER (MWt)	45	45	45	50	50	33.8
CONFIGURATION	SERPENTINE TUBE AND SHELL	HELICAL TUBE	Z-TUBE	HELICAL TUBE	HELICAL TUBE	HOCKEY STICK
MATERIALS	2-1/4 Cr – 1 Mo EVAPORATOR, TYPE 321 SS SUPERHEATER-REHEATER	INCOLOY 800 TUBES, TYPE 304 SS SHELL	2-1/4 Cr – 1 Mo EVAPORATOR, TYPE 316 SS SUPERHEATER	STABILIZED 2-1/4 Cr – 1 Mo	2-1/4 Cr – 1 Mo	2-1/4 Cr – 1 Mo
TYPE OF OPERATION	ONCE THROUGH	ONCE THROUGH	ONCE THROUGH	ONCE THROUGH	ONCE THROUGH	ONCE THROUGH
LIQUID METAL INLET TEMPERATURE (°F)	1020	975	975	970	940	950
EXIT STEAM CONDITIONS (psi/°F)	2545/955	2705/915	2705/915	2470/932	1940/910	2430/930
OPERATING TIME (h)	7000	1000	~1000	~1000	~4000	4,000
PROBLEMS	NONE	NONE	NONE	NONE	FLOW IN-STABILITY BELOW 30%, LIQUID LEVEL CONTROL (SODIUM SIDE)	NONE

TABLE 5-14 (Continued)

SUMMARY OF "COMPACT TUBE" STEAM GENERATOR EXPERIENCE (CONTINUED)

TYPE OF TEST	REACTOR PLANT OPERATION				
FACILITY	EFAPP	DFR	KNK	PHENIX	BOR 60
POWER (MWt)	143	3	28	15	30
CONFIGURATION	SERPENTINE TUBE	SERPENTINE SHAPE – SEPARATE H_2O AND Na TUBES IN Cu LAMINATIONS	SERPENTINE SINGLE TUBE IN SHELL	7-TUBE SERPENTINE UNITS	SERPENTINE TUBE
MATERIALS	2-1/4 Cr – 1 Mo	TYPE 321 SS	2-1/4 Cr – 1 Mo	2-1/4 Cr – 1 Mo EVAPORATOR, TYPE 321 SS SUPERHEATER	LOW-ALLOY STEEL
TYPE OF OPERATION	ONCE THROUGH	ONCE THROUGH	ONCE THROUGH	ONCE THROUGH	ONCE THROUGH
LIQUID METAL INLET TEMPERATURE (°F)	820	570	790	1020	900
EXIT STEAM CONDITIONS (psi/°F)	910/780	147/518	1160/790	2400/955	-430
OPERATING TIME (h)	2000		5200+	6000+	20,000+
PROBLEMS	SEE NOTE 1	CHLORIDE STRESS CORROSION	LEAK IN HAZ OF SPACER TAB ON TUBE	NONE	NONE

NOTE 1

CAUSTIC STRESS CORROSION; TUBE VIBRATION; WEAR; TUBE-TUBESHEET WELD LEAKS; FLOW INSTABILITY, CORRECTED BY ORIFICING

TABLE 5-15

STEAM GENERATOR MATERIAL SUMMARY

Evaporator (with temperatures under 950°F): 2-1/4 Cr-1 Mo

1. Material is essentially immune to stress corrosion cracking
2. Good thermal conductivity
3. Low coefficient of expansion
4. Analytical techniques verified
5. Experience and economics

Superheater & reheater (with temperatures over 950°F): Type 316H SS

1. Analytical techniques verified
2. Welding procedures qualified - 2-37 tube bundles made but not tested
3. SNAP - Operation at 1300°F air blast heat exchanger exposed to weather ~1300°F
4. Feedwater dissolved solids should be less than 50 ppb

poorer heat transfer characteristics of steam, the unit is estimated to operate at about 79 MWt as a superheater. As indicated above, 316H stainless steel would be selected for both the superheater and the reheater. The reheat unit would be similar to the current AI/MSG though scaled-up slightly. While the AI/MSG is rated at about 32 MWT as a combined evaporator and superheat unit, as a superheat only the power would be reduced to about 25 MWt, necessitating a modest scale-up.

5.3.4 Auxiliary Systems

The auxiliary systems that support the main flow system are as follows: (1) fill and drain, (2) purification, (3) preheat, (4) instrumentation and control, (5) inert gas, and (6) sodium-water reaction relief. The scope of the subject effort did not include significant study of these auxiliary systems. In the discussion below, general characteristics are presented based on common practice with sodium systems.

Fill and Drain

The fill and drain system provides for the initial fill of the storage tanks with sodium, the fill of the piping system from the storage tanks prior to operation, sodium bulk storage, and drain provisions to the storage tanks. For the revised baseline configuration, the thermal storage tanks are also the bulk storage tanks when the system is drained for hold periods. The hot storage tank would be designated as the prime storage tank with the cold tank as backup. Either tank would be sized to contain the entire sodium volume.

Initial fill would be accomplished at a temperature of 204°C (400°F) from railroad type tank cars each containing 36,400 Kg (80,000 lb) of sodium. A melt station is required to melt the sodium in the tank cars and a pressure source of inert gas such as nitrogen to move the sodium from the tank car to the storage tank.

The riser and downcomer lines are filled using the receiver pump. Both lines are filled simultaneously up to the receiver. The receiver is also filled if adequate preheat of the receiver tubes has been attained using the collector field. A filled system is detected by a sodium level in the cover gas accumulator, at the top of the receiver.

Purification

The usual purification system for sodium systems contains one or more cold trap units for removal of oxides of sodium. While early plants may have such units, it is expected that such units may be unnecessary for the Nth plant. If reasonable precaution is taken during construction to maintain a clean system, the initial contamination of the very large quantity of sodium used is not expected to be beyond an acceptable 10 ppm.

The source of initial contamination in a sodium system is the oxides and foreign material on the interior walls of the system. These contaminants are absorbed due to the excellent cleaning action of liquid sodium. In this system, the quantity of sodium used is very large compared to the wetted surface area of the pipes and components; hence the contamination is diluted to acceptable levels.

Purification systems frequently contain sodium sample stations and sodium characterization equipment for on-line measurement of oxides, hydrogen, etc. Such monitoring for the Nth plant would be minimal except for hydrogen. Monitoring for hydrogen will continue for all plants as an indication of water leaks in the steam generator units.

Preheat

All sodium containing pipes and components will be electrically trace heated and insulated. However, the electric trace heaters would not be used during plant operation with flowing sodium except dead-ended lines (without flow) or drained lines. Certain lines used to enhance system drainage may normally be empty but must be heated in the event of a need for a rapid drain.

Most of the lines will depend on flow circulation during plant operation to maintain line temperature (i.e., a small thermal loss is acceptable). During shutdown for night, a small flow will be maintained wherever possible using hot tank or cold tank fluid for pipes and components of the hot leg or cold leg, respectively. The storage tanks would depend on the thermal inertia of the contained sodium. A filled hot tank with 30 cm (12 in) of calcium silicate insulation would lose about 2.2°C (4°F) temperature over a 12-hour period.

Electric preheat would be used prior to filling the pipe and components with sodium. The receiver and steam generator units would not be trace heated. The receiver is preheated using the solar collector field. The steam generator is preheated using hot water and steam from an auxiliary boiler.

Instrumentation and Control

The sodium instrumentation and control (I&C) system must be integrated through the master control center with the collector field system and with the electric power generating system. Because of the isolation between receiver operation and steam generator operation afforded by the storage tanks, the sodium system I&C is essentially two systems--one for the receiver end and one for the steam generator end, each operating relatively independent of the other. This relative independence of operation between the receiver and the steam generator is a strong advantage of this system. The steam generator control

system will respond primarily to load demand. The receiver control system will respond to maintain sodium outlet temperature. Details of the sodium system I&C remain to be determined.

Inert Gas

Argon is the inert gas used most commonly with sodium systems. Nitrogen is less expensive but is generally not used in order to avoid possible nitriding of stainless steel materials.

The inert gas system contains a high pressure or liquid supply tank, a distribution system to each component, and generally includes the vent and relief function. The system is constructed of carbon steel material except for those connections to sodium service components that may be exposed to high temperature liquid sodium or sodium vapor (including inadvertant exposure). These will be made of stainless steel.

The inert gas system will maintain an inert cover on all sodium free-surfaces and in all components washed with sodium in order to avoid exposure to atmospheric oxygen.

Sodium-Water Reaction Relief

This system consists of a tank and separator connected through burst diaphragms to the sodium system as near as possible to the steam generator units.

The function of the reaction products system is to reduce pressures in the main sodium system, to contain liquid and solid reaction products, and to vent safely the gaseous products resulting from a major failure in the steam generator.

All piping and components downstream of the burst diaphragms are made of carbon steel, and are without trace heating or insulation.

In the event of a sodium-water reaction in the steam generator, the pressure pulse generated is clipped at a predetermined level by the rupture of the burst diaphragms. The resulting discharge is routed to a cyclone-type separator tank. The gaseous products, mainly hot hydrogen, and entrained particles are discharged from the center of the separator through a burn stack to atmosphere. The liquid and solid materials exit the separator through a bottom drain to the contaminated sodium tank.

The system is sized to contain the steam generator inventory, tower downcomer volume, and the flow during pump coastdown. After a pump coastdown period of ~30 seconds, the main flow block valves are closed to eliminate flow to the steam generator and reduce the amount of contaminated flow downstream of the steam generator.

714-D.10/pag

6.0 THERMAL STORAGE SUSBYSTEM

6.1 Requirements

The system requirements given in Section 2 establish the requirements for the Thermal Storage Subsystem. Six hours of storage operation are required at 100 percent of rated power. The cycle efficiency with wet tower cooling is estimated to be 39.5 percent and the nighttime parasitic power demand is considered to be 6 MWe. With these characteristics, the thermal storage requirements are 1610 MWt.

As indicated in the previous section, the sodium side steam generator temperatures are 593^{o}C (1100^{o}F) inlet and 288^{o}C (550^{o}) outlet. These conditions determine the hot tank storage temperature of 593^{o}C (1100^{o}F) and cold tank storage of 288^{o}C (550^{o}F). Figure 6-1 shows a schematic of the thermal storage subsystem together with the major performance parameters.

6.2 Analysis

The Thermal Storage System consists of a hot sodium storage tank, cold sodium storage, a pump and interconnecting piping as shown in Figure 6-1. The steam generator pump supplies sodium from the hot storage tank through the steam generator to the cold sodium tank.

The thermal storage requirement of 1610 MWt is satisfied with 15.3 x 10^{6} Kg (33.6 x 10^{6} lb) of sodium operating with a temperature change from the hot storage to the cold storage of 305^{o}C (550^{o}F).

Storage system costs are dominated by the cost of the tanks and the sodium. For this reason, the tank height versus diameter relationship was examined as well as the number of tanks.

THERMAL STORAGE SUBSYSTEM SUMMARY

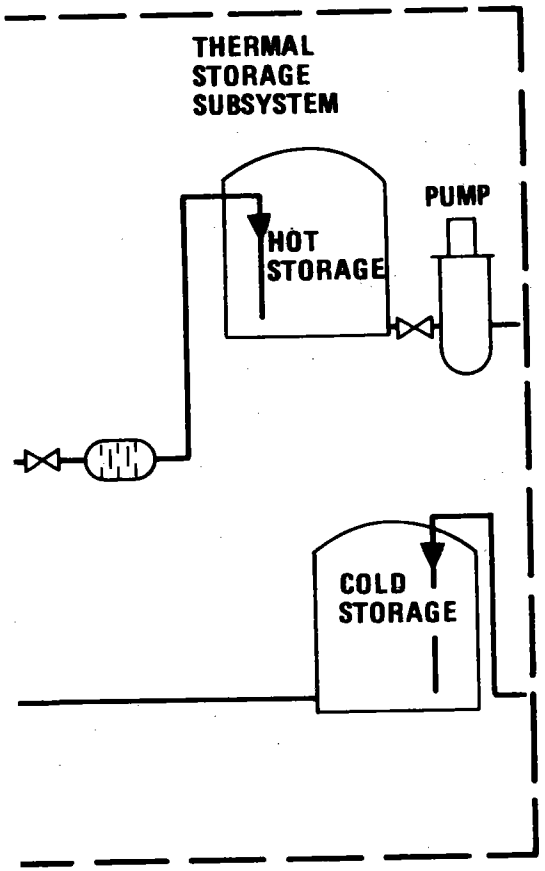

	HOT TANK	COLD TANK
ENERGY IN STORAGE, MWT-H	1,600	
TEMPERATURE °C (°F)	593 (1,100)	288 (550)
WEIGHT OF SODIUM KG (LB)	15.3 X 10^6 (33.6 X 10^6)	
VOLUME OF SODIUM M^3 (GAL)	18,925 (5.0 X 10^6)	17,910 (4.6 X 10^6)
STORAGE TANK SIZE M (FT)	38.14 X 17.2 (1.25 X 56)	38.14 X 15.6 (1 25 X 51)
MATERIAL	SS	CS
MAXIMUM FLOW RATE KG/H (LB/H)		
IN	4.47 X 10^6 (9.83 X 10^6)	2.68 X 10.6 (5.90 X 10^6)
OUT	2.68 X 10^6 (5.90 X 10^6)	4.47 X 10^6 (9.83 X 10^6)

Figure 6-1 Revised Sodium System Baseline

Figure 6-2 shows the effect of height-diameter ratios of 1/2 and 1 and number of tanks. The total installed cost of the system is shown with n hot tanks of stainless steel and n cold tanks of carbon steel. The cost of the cold tank of equivalent size is about 40% that of the hot tank due to the use of carbon steel. These parameteric costs include material and labor, insulation, electrical preheat, and interconnecting piping and valves for multiple tank systems. Single tanks with a height to diameter ratio of 1/2 gave the lowest cost system. An examination of the several cost parameters shows that the bare tank costs decrease with an increasing number of tanks with minimum at about 10 tanks. However, the increasing surface area and resulting insulation/preheat costs as well as the interconnecting pipe costs outweigh the decrease in metal costs so that one tank (one hot and one cold) is a minimum cost system.

An alternative tank arrangement is to consider an n + 1 tank system. With this arrangement, n hot tanks are sized for the entire storage system sodium inventory plus one cold tank. As the cold tank is filled, a hot tank becomes available for cold storage and so on until there are n tanks with cold sodium and one hot tank. A possible schematic arrangement of tanks is shown in Figure 6-3. Figure 6-4 shows the storage system costs for this arrangement. A shallow minimum is indicated at n = 3 without the cost of the sodium valves required to make the system function. Three full flow 0.61 m (24 in.) valves are required for each added tank. The cost of 0.61 m (24 in.) sodium service valves is somewhat uncertain, but $100,000 each is used in Figure 6-4. The upper curve of Figure 6-4 now shows a small minimum at n = 2, but the apparent cost savings of $200,000 compared to a single hot tank system is within the accuracy of the estimating procedure. In addition, the above evaluation did not include analyses of the added structural effects upon those tanks that see the dual use service. The apparent cost savings would probably be eliminated by the special design considerations required for the pipes and those tanks subjected to the thermal transients resulting from the dual use concept.

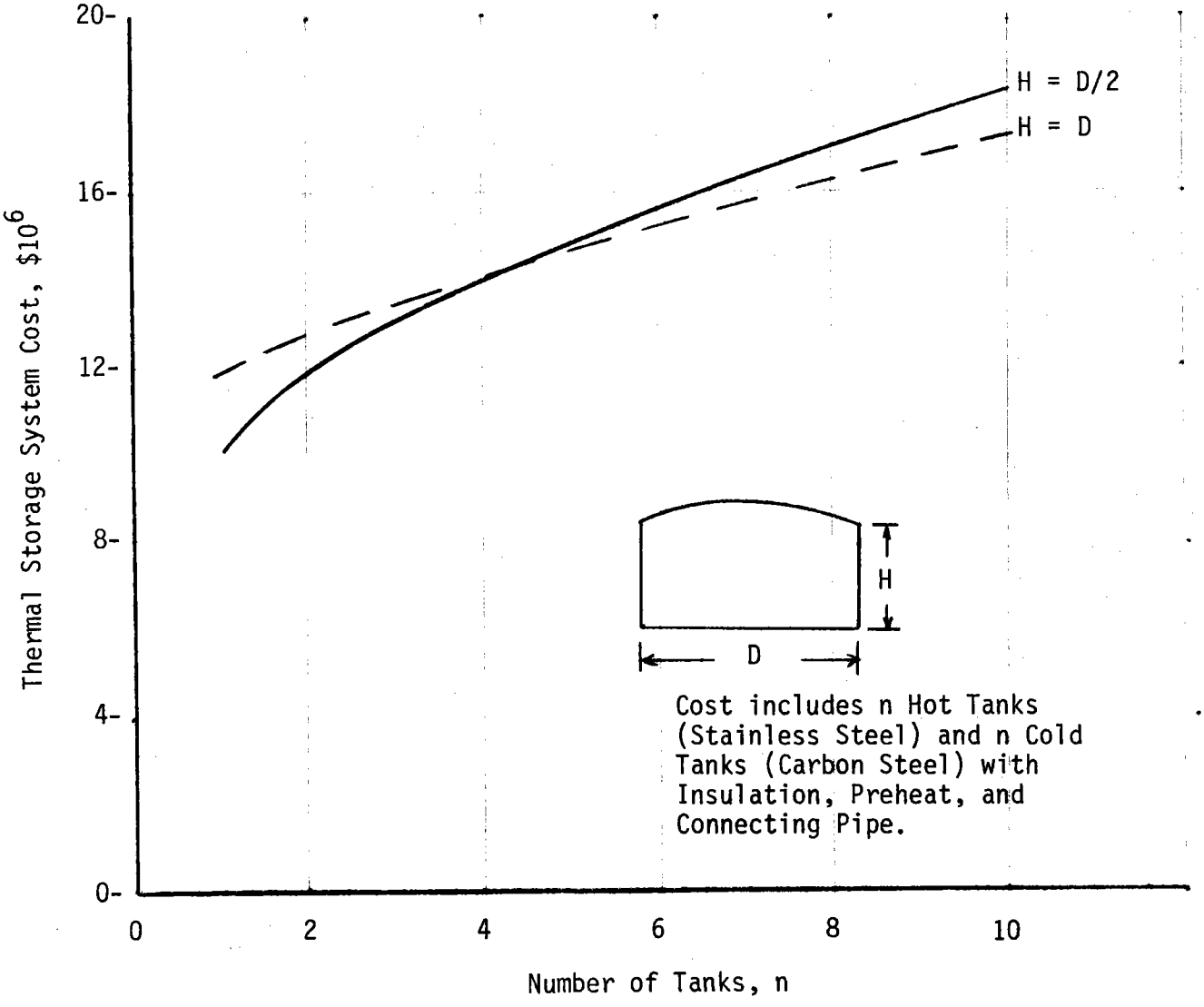

Figure 6-2. Thermal Storage System Costs

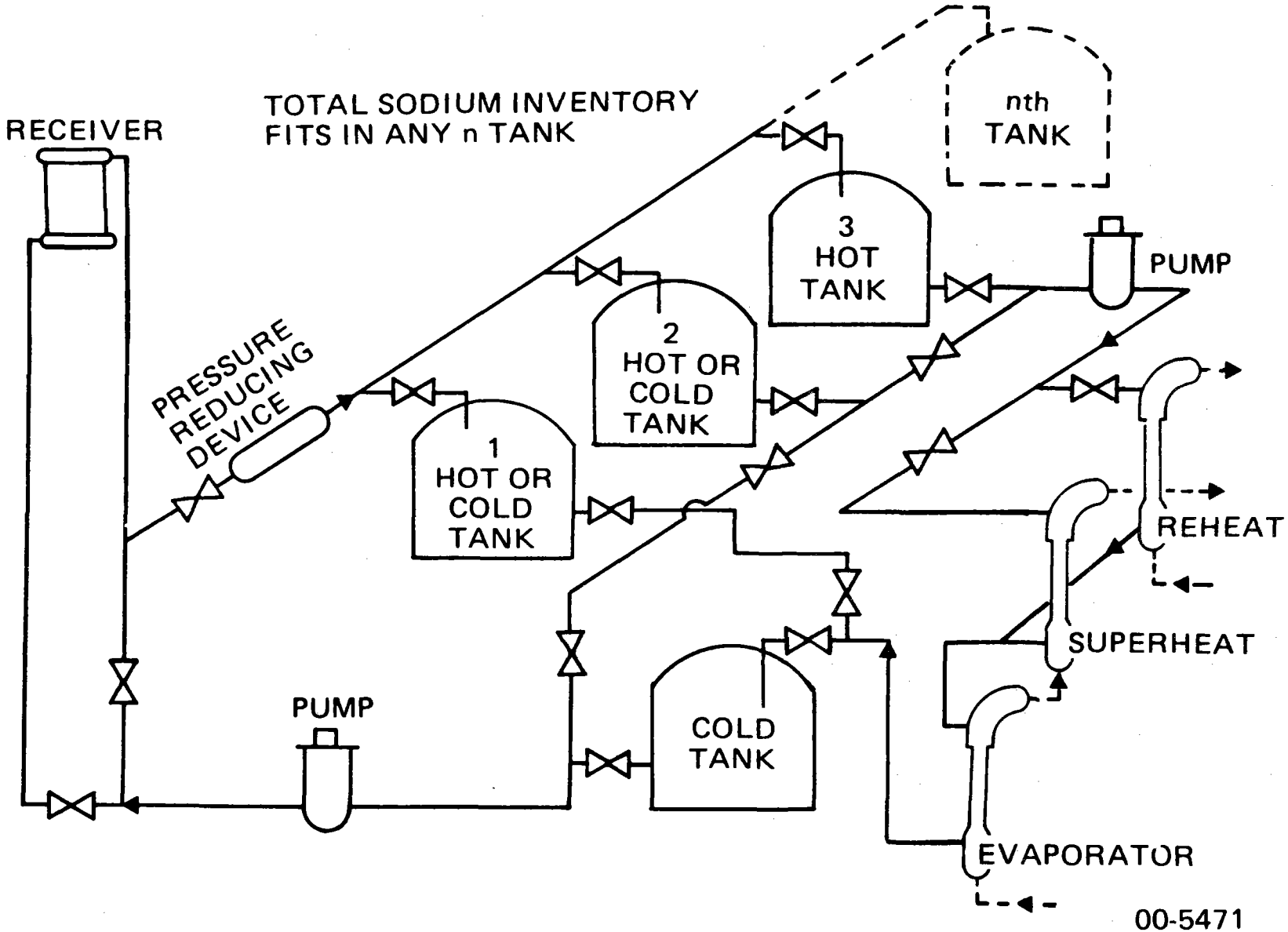

FIGURE 6-3 CONFIGURATION WITH MULTIPLE DUAL USE TANKS

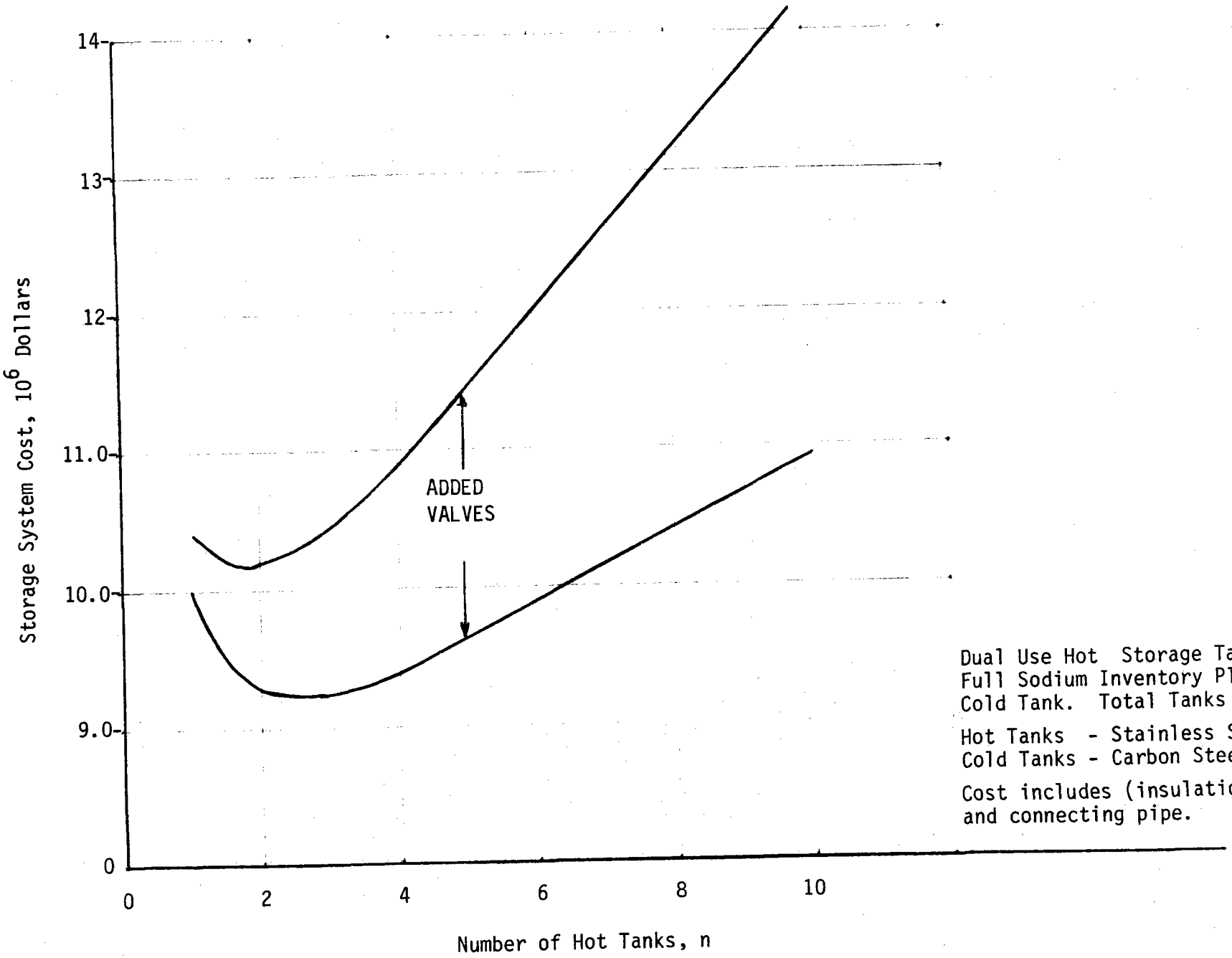

Figure 6-4. Multiple Tank, Dual Use Storage System

As a result of these studies, the baseline thermal storage system was established with one hot storage tank and one cold storage tank.

In order to minimize the storage costs, the tanks must not be subjected to tower static pressure. For the initial baseline configuration of Figure 5-2, the tower static pressure was isolated from the storage tanks by the intermediate heat exchanger (IHX), allowing the tanks to operate at tank static head only. The revised baseline configuration uses a pressure reducing device (PRD) to dissipate the tower static pressure. This device is discussed in detail in a subsequent paragraph. The use of a PRD permits the IHX and the IHX supply pump to be removed from the flow circuit with a substantial system simplification and savings in cost. A cost penalty is incurred in the operation of the receiver pump since the head requirements on this pump are approximately doubled to overcome the line losses as well as the tower static head in the riser. The added parasitic power requirements are about 1 MWe when credit is taken for the pumping power saved by removal of the IHX pump. While the pressure is dissipated by the PRD, the energy is not lost but is converted to heat energy in the liquid sodium.

6.3 Thermal Storage Subsystem Design Description

6.3.1 Thermal Storage Subsystem Design Summary

The Thermal Storage Subsystem contains the hot and cold storage liquid sodium tanks, a pump, a pressure reducing device, and interconnecting pipe. Liquid sodium from the Receiver Subsystem is stored in the hot storage tank at energy rates up to 475 MWt, which corresponds to a flow rate of 4.47×10^6 Kg/H (9.83×10^6 lb/hr). Sodium is drawn from the hot storage tank at energy rates of up to 275 MWt (2.68×10^6 Kg/H (5.90×10^6 lb/hr)) to generate steam for the Electric Power Generating Subsystem. Sodium from the steam generator units flows to the cold storage tank. During the day, hot sodium is accumulated by the hot tank in a sufficient quantity to store up to six hours of operation at 100% rated power. With this storage arrangement, plant operation is always from storage. The steam conditions provided are the same regardless of whether the receiver loop is operating or not.

The storage tanks are 38.14 m (125 ft) in diameter with a height of 17.2 m (56 ft) for the hot storage tank and 15.6 m (51 ft) for the cold. The hot tank operating at 593°C (1100°F) is made of stainless steel; the cold tank at 288°C (550°F) is made of carbon steel. The tanks operate at static head pressures only in order to minimize cost. This requires a pressure reducing device to dissipate the tower static head.

The pressure reducing device (PRD) for the baseline configuration consists of a series of orifice plates with control valves for off-design flowrates. Should the current tests of a pressure reducing drag valve in sodium confirm expected operation, a 61 cm (24-in.) valve of this type would be an excellent replacement for the PRD. A steam generator pump in this system moves the hot sodium through the steam generator units to the cold storage tank. The receiver pump identified in the Receiver Subsystem description charges the hot storage tank. The steam generator pump is similar to the CRBRP pump but with both reduced head and flow requirements. The developed head for this pump is 61 m (200 ft) at 0.95 m^3/S (15,000 gpm).

The thermal storage system characteristics are presented in Table 6-1.

Storage Tanks

The storage tanks are low pressure tanks with a height of about 1/2 the diameter. The hot tank is constructed of stainless steel with the cold tank from carbon steel. Because of the sodium density change with temperature, the cold tank is about 9% smaller than the hot tank. Each tank is sized 2% larger than the bulk sodium volume to allow for residual heat and ullage space.

TABLE 6-1

THERMAL STORAGE SUBSYSTEM SUMMARY DATA

General

Thermal Storage Capacity, MWt	1610
Maximum Charging Rate, MWt	475
Maximum Extraction Rate, MWt	286
Time at Maximum Extraction Rate, hr	6
Weight of Sodium in Subsystem, Kg (lb)	15.3×10^6 (33.6×10^6)

Low Temperature Sodium Tank

Type	Cylindrical, Low Pressure
Diameter, m (ft)	38.1 (125)
Height, m (ft)	15.5 (51)
Wall Thickness	
Top, cm (in.)	0.64 (0.25)
Bottom, cm (in.)	5.1 (2.0)
Volume, m^3 (gal)	56,700 (4.6×10^6)
Tank Material	Carbon steel
Insulation, roof and walls	Calcium silicate with aluminum weather protection
Thickness, cm (in.)	30.5 (12)
Base insulation, m (ft)	1 (3) perlitic concrete
Electric preheat temperature maintenance, kw	274
Number of Low Temp. Tanks	1
Low Sodium Temperature, ^oC (^oF)	288 (550)
Ullage Maintenance Unit	
Ullage Pressure, mn/m^2 (psi)	0.0069 (1)
Pressurization Media	Argon

TABLE 6-1 (continued)

High Temp. Sodium Tank

Type	Cylindrical, Low Pressure
Diameter, m (ft)	38.1 (125)
Height, m (ft)	17.1 (56)
Wall Thickness	
Top, cm (in.)	0.64 (0.25)
Bottom, cm (in.)	5.1 (2.0)
Volume, m^3 (gal)	18925 (5.0×10^6)
Tank Material	SS
Insulation, roof and walls	Calcium silicate with aluminum weather protection
Thickness, cm (in.)	30.5 (12)
Base insulation, m (ft)	1 (3) perlitic concrete
Electric preheat-temperature maintenance, kw	540
Number of High Temperature Tanks	1
High Sodium Temperature, ^oC (^oF)	593 (1100^oF)
Ullage Maintenance Unit	Argon

STEAM GENERATOR PUMP

Physical Description

Quantity	1
Height, w/motor, m (ft)	10.6 (35)
Tank size, m (ft)	1.8 x 6.1 (6 x 20)
Inlet Nozzle, m (in.)	0.61 (24)
Outlet Nozzle, m (in.)	0.46 (18)
Dry Weight w/motor, kg (lb)	98,200 (216,000)

TABLE 6-1 (continued)

Motor

Size, MW (hp)	0.75 (1000)
Dimensions w/coupling, m (ft)	1.5 x 3.7 (5 x 12)
Voltage	4160
Cooling	TBD

Pump Operating Conditions

Developed Head, m (ft)	61 (200)
Flow Rate, kg/hr (lb/hr)	2.68×10^6 (5.9×10^6)
Speed, rpm	1100
Temperature, ^oC (^oF)	593 (1100)
Sodium Volume, m^3 (gal)	5.7 (1500)
NPSH, m (ft)	10.6 (35)
Discharge Head, m (ft)	71.6 (235)
Speed Control, %	20-100
Pump Power (= 70%), MW (hp)	0.67 (906)

Design Conditions

Developed Head, m (ft)	61 (200)
Flow Rate, m^3/sec (gpm)	0.95 (15,000)
Speed, rpm	1100
Temperature, ^oC (^oF)	427 (800)
NPSH (Min. Required), m (ft)	7.6 (25)
Code	Section VIII, Div. 1

The tanks operate with a cover gas pressure of not more than 0.0069 MN/m^2 (1 psi) in order to exclude air from contact with the sodium surface. Since tank costs increase rapidly with increasing pressure, tank pressure is maintained as low as practical. Wall thickness is based on hydraulic static head with each course of metal becoming thicker toward the base of the tank. The base course is about 5.1 cm (2.0 in) thick. The top course, roof, and floor of the tanks are the minimum thickness of 0.6 cm (0.25 in). Roof construction would be standard design with interior column supported trusses.

The tank walls and top are insulated with 30.5 cm (12 in.) of calcium silicate. Electric preheat is installed on the tank walls.

The base is insulated with perlitic concrete or a layer of blocks of calcium silicate inset into the thick concrete base pad. Electric preheat is also installed in the base.

Steam Generator Pump

The steam generator pump characteristics are listed in Table 6-1. The performance requirements are to supply about 1.45 m^3/sec (23,000 gpm) of liquid sodium to the steam generator units with discharge into the cold storage tank. The developed head requirements are estimated to be 61 m (200 ft). The pump will have a 5 to 1 speed control range.

The physical and operational characteristics for the pump given in Table 6-1 are based on the characteristics of the sodium pump being developed for the Clinch River Breeder Reactor (CRBR). The CRBR pump has greater head and flow performance than necessary for this application; hence the parameters of Table 6-1 represent a scale-down in performance characteristics.

Pressure Reducing Device (PRD)

The PRD is required to dissipate about 213.4 m (700 ft) of static head at a flow rate of 1.58 m^3/sec (25,000 gpm). Figure 6-5 shows a schematic drawing of a PRD used at the Sodium Pump Test Facility of the Liquid Metal Engineering Center. The unit consists of a series of orifice plates and is designed for a pressure drop of 0.345 MN/m^2 (50 psi) at 1.262 m^3/sec (20,000 gpm). While the subject application has a higher pressure drop requirement, a preliminary computer analysis indicates the condition to be feasible.

A PRD operates well at the design flow conditions. The pressure loss characteristics are proportional to the flow rate (W) squared:

$$P = KW^2$$

Hence, if the flowrate is reduced by 1/2, the pressure loss in the device is reduced to 1/4 the full flow value. Since the tower static head is constant regardless of flow rate, at less than design flow conditions a variable throttling element such as one or more butterfly valves is required in series with the PRD to accomplish the static pressure reduction. Figure 6-6 shows a cutaway sketch of a drag valve which appears to be a well suited alternative to the PRD for the subject application. Valves of this type have been highly successful for many years in water/steam and petrochemical systems. One drag valve can throttle large pressure losses quietly over a wide range of flow conditions and also be designed for tight shutoff. A 15.2 cm (6-in.) valve of this type is to be tested in sodium at the Liquid Metal Engineering Center in the next several months. This testing is a prelude to procurement of a 0.61 m (24-in.) drag valve for use in a liquid sodium pump test facility with testing capability to 5.05 m^3/sec (80,000 gpm).

If the in-sodium test data confirms the performance of these valves as expected, drag valves would be the first choice solution for a pressure reducing station in the revised baseline configuration.

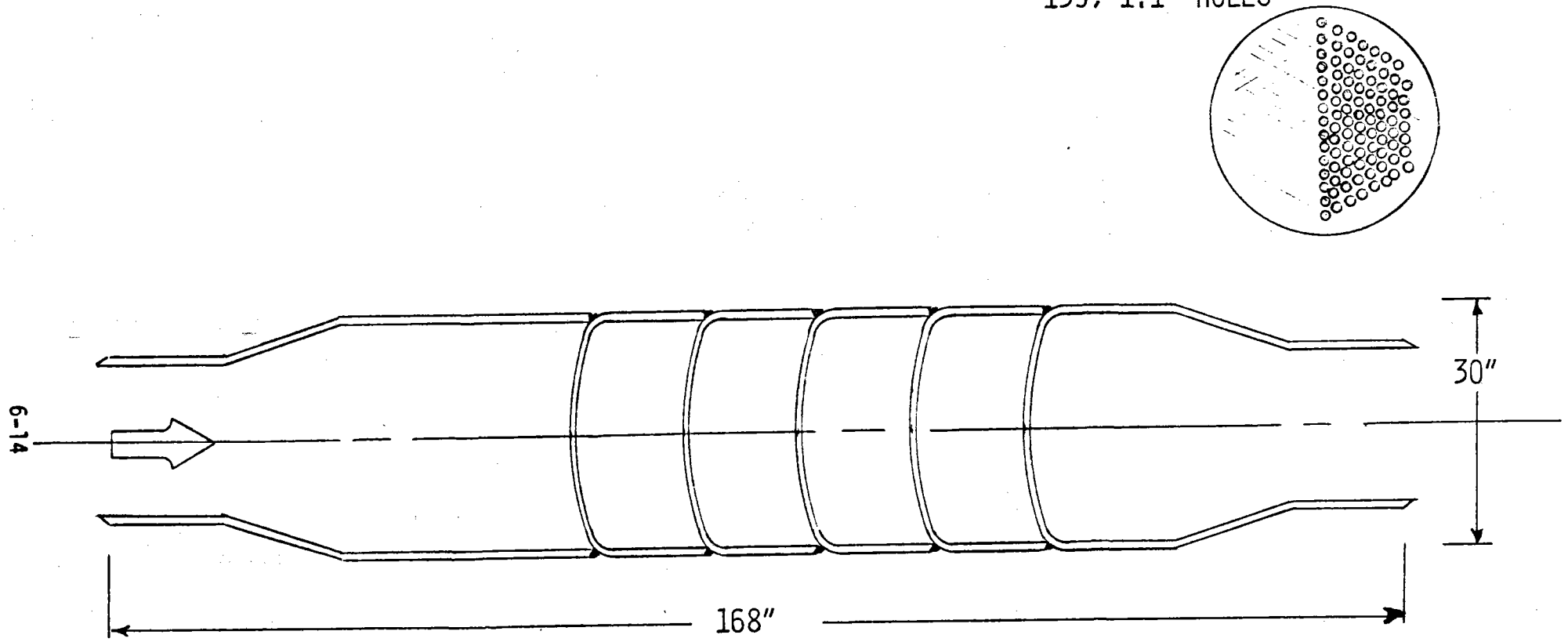

Figure 6-5 PRESSURE REDUCING DEVICE

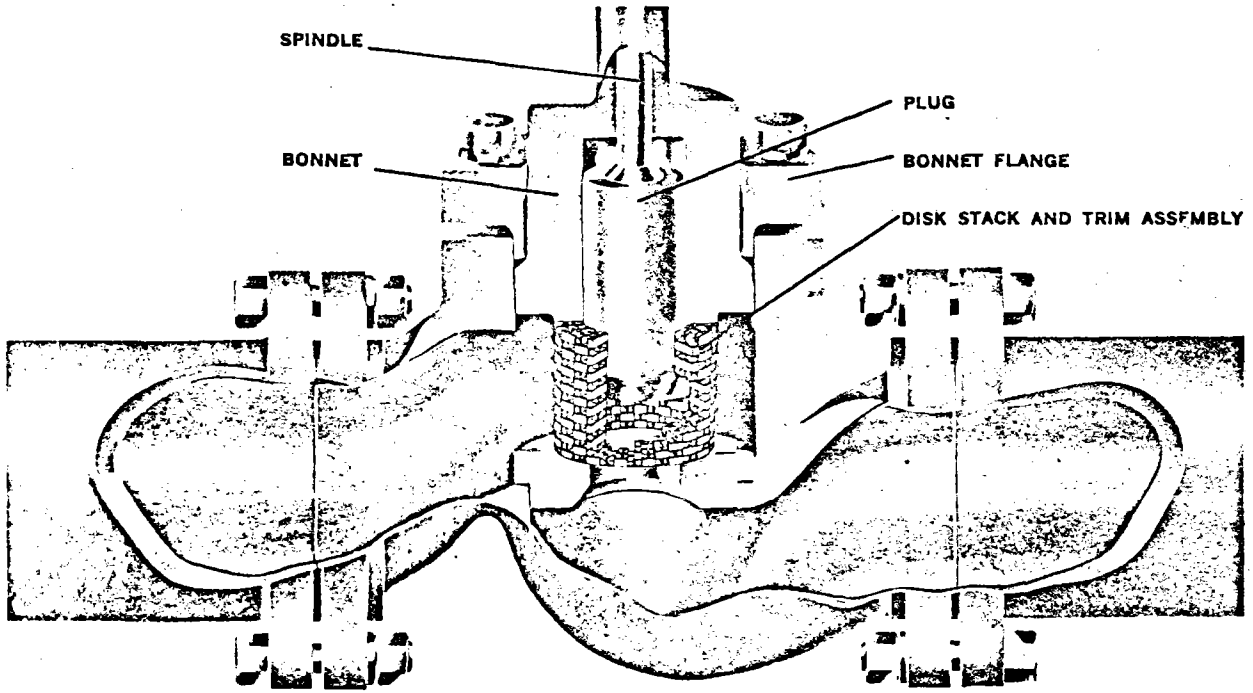

Figure 6-6 PRESSURE REDUCING DRAG VALVE

7.0 SYSTEM COST/ECONOMICS

The first generation Central Receiver Solar Plant has been designed around a superheated steam/water cycle in order to minimize technical, cost and schedule risks. The potential for higher efficiency and lower cost has led to the consideration of a second generation system based on a liquid metal cycle. The primary objectives of this study were to define the conceptual design of a 100 MWe Sodium Cooled Central Receiver Electric Power Plant and to determine its technical and economic feasibility. This section addresses the latter consideration. Following a brief review of the economic drivers associated with a liquid sodium concept, this section presents an indication of how these drivers are expected to affect costs relative to the costs projected for the water/steam receiver concept and describes the methods involved in determining the relationship.

7.1 Economic Drivers

The main advantages in a liquid sodium cooled system over the more conventional water/steam system involve improved turbine cycle, thermal storage, and receiver efficiencies which are reflected directly in a reduction in the number of heliostats required in the field and in increased annual electrical output for a given number of heliostats. The higher turbine cycle efficiency results from the availability of high temperature sodium (which serves as both the receiver coolant and the storage fluid) at the turbine building which lends itself easily to a turbine reheat cycle. Thermal storage efficiency is increased by elimination of the thermal storage heaters and maintenance of higher storage temperatures while receiver efficiency is increased mainly because of the superior heat transfer characteristics of sodium. These characteristics allow a high heat flux environment to exist on the receiver absorbing surfaces which translates into a high concentration ratio design. This, in turn, reduces receiver surface area by one-third and thereby reduces receiver heat losses. Heat losses are further reduced by the thin-walled tubes, allowed by the reduced vapor pressure of sodium, which minimize the thermal resistance and the resulting temperature gradient across the tube wall.

Output is affected because of the constant steam conditions available at all operating times. This makes daytime and nighttime gross electrical

output identical, contrasting with water/steam systems where nighttime outputs are typically 70-80 percent of the daytime levels due to reductions in steam temperatures and pressures that occur for energy routed through thermal storage. In addition, the relative advantage of the liquid sodium system over the water/steam system, in terms of annual electrical energy production, is enhanced when sites are selected with higher frequencies of cloudiness. This is a direct result of the energy degrading process which occurs for all energy routed into and out of the thermal storage media for the water/steam system during the intermittent cloud operation and which is reflected in a loss of efficiency and electrical output. By comparison, no such energy exchange process occurs in the sodium system. Although this factor may be of minimal importance for early solar plants which are sited at the best solar locations in the country, its importance will increase as more and more non-optimum sites are selected, such as the Midwest, South central, and Gulf coast portions of the country.

7.2 Relative Costs

The cost impact of these drivers along with the impact of certain cost penalties associated with a sodium system are reflected in Table 7-1. The first commercial costs are shown as projected in Volume VII, Book 2, of the May 1977 Central Receiver Solar Thermal Power System Preliminary Design Report. The costs indicated for receiver and thermal storage reflect a transfer of water/steam system heat exchanger costs out of the thermal storage cost element and into the receiver cost element which is where the costs of the steam generators are carried for the liquid sodium system. This provides a more meaningful cost comparison. The equivalent cost ratio of .87 to 1 indicates the overall sodium system advantage after differences in annual output are considered, but excluding further advantages of sodium where the number of partly cloudy days becomes significant.

Liquid sodium system costs used for comparison were derived by perturbating the water/steam baseline costs presented in the cost volume (referenced in the previous paragraph) to account for specific technical/hardware differences implied by the conceptual design for the sodium system. Further detail on the derivation of the costs is provided below.

TABLE 7-1

100 MWe LIQUID METAL COOLED SOLAR RECEIVER COSTS
RELATIVE TO WATER/STEAM SYSTEM BASELINE COSTS

CBS NUMBER(S)	COST ELEMENT	*1ST COMM WATER/STEAM ($M)	LIQUID METAL ($M)
4000-4100	LAND, LAND RIGHTS AND YARD WORK	1.53	1.45
4103-4143	BUILDINGS	4.81	4.81
4190	SOLAR PLANT EQUIPMENT	157.23	153.7
4190.1	COLLECTOR EQUIPMENT	107.62	94.58
4190.2	RECEIVER AND TOWER SYSTEM	33.34	33.08
4190.21	RECEIVER UNIT	(17.48)	(11.5)
4190.22/.33	STEAM GENERATOR/HEAT EXCHANGERS	(4.19)	(6.63)
4190.23-.24	RISER-DOWNCOMER AND HORIZONTAL PIPING	(2.19)	(6.11)
4190.25-.26	TOWER, PLATFORM, FOUNDATION & SITE PREP	(9.48)	(8.84)
4190.3	THERMAL STORAGE EQUIPMENT	11.37	14.99
4190.4	THERMAL STORAGE MEDIA	4.90	11.05
4300	TURBINE PLANT EQUIPMENT	22.84	17.48
4401	ELECTRIC PLANT EQUIPMENT	3.27	3.27
4402	PLANT MASTER CONTROL EQUIPMENT	1.78	1.78
4500, 8000 & 8100	MISCELLANEOUS PLANT EQUIPMENT, DISTRIBUTABLES, AND INDIRECT	28.83	28.77
		$220.12	$211.26
	TOTAL CAPITAL COST RATIO (211 ÷ 220)		.96
	ANNUAL KWH RATIO		1.11
	EQUIVALENT CAPITAL COST RATIO		.87

*Eventual Nth Commercial Cost Expected $1410.00/KW

7.2.1 Land and Land Rights and Yardwork

The costs for Land and Land Rights and Yardwork are based on differences in land area due to the lower number of heliostats required for the Liquid Metal system. Yardwork costs occurring outside the central building, tower, and thermal storage complex were adjusted in direct proportion to this difference. Yardwork cost within the complex has not been adjusted.

7.2.2 Buildings

It is assumed that the same buildings will be required for the Liquid Metal system as for the water/steam Central Receiver System. Thus, no adjustment in cost has been indicated.

7.2.3 Collector Equipment

Twenty-eight hundred and thirty-four fewer heliostats are required for the Liquid Sodium System due to the higher overall system efficiency. Assuming that the same heliostat may be used for the sodium system as designed for the water/steam system, the cost adjustment is a matter of extending the first unit cost, from the water/steam baseline, for the number of units (20,580) required for the liquid sodium system using cost reduction curve logic. The cost reduction curve logic makes the average heliostat cost for the sodium system slightly higher than the average cost for the water/steam system. The impact on the relative cost ratio is lost in the rounding.

7.2.4 Receiver and Tower Subsystem

The Receiver and Tower Subsystem is comprised of the receiver unit, steam generators, piping,and the tower and foundation. Although the overall cost indicates very little change, a wide range of impact is indicated for each of the subelements. A different accounting, where the steam generator/heat exchangers are carried under the Thermal Storage Subsystem would cause the total amount to change from $33.34 million to $29.15 million for the water/steam system, corresponding to $26.45 million for the liquid metal system, so that, in this sense, significant savings have been achieved in the Receiver and Tower Subsystem.

7.2.4.1 Receiver Unit

Receiver unit costs cover all elements above the top of the tower and include the contained sodium. Although similar to the water/steam receiver, a lower cost tube material is employed and the exposed surface is only 915 m^2 compared to 1,373 m^2 for the water/steam system. The sodium receiver unit costs were checked parametrically against water/steam receiver unit costs by labor and material at the major assembly level with the major drivers being exposed surface area, relative material cost, package size, and estimated support structure weight.

The same workmanship standards and construction technique are assumed for both systems, i.e., longitudinal welding of panel tubes to each other. The water/steam receiver unit is classified as a pressure boiler, and its construction is regulated by Section 1 of the ASME Code which does not permit brazing. If the sodium receiver unit utilized brazing in its construction, as permitted by Section 8 of the Code, the cost advantage of the sodium receiver may be greater, especially under an Nth plant high production scenario.

7.2.4.2 Steam Generators/Heat Exchangers

Steam generator costs for the liquid sodium system have been estimated and compared with water/steam system heat exchangers to show an increase from $4.19 million to $6.63 million. This increase may appear inconsistent with the heat exchange surface areas of the two systems where water/steam system area, including thermal storage heaters, is 12 times that for the sodium system. However, several other cost driving factors must be considered. First, the sodium system must be constructed of stainless steel rather than carbon steel, which has a major impact on cost. In addition, construction to contain sodium is more costly, and, although an attempt was made to eliminate the influence of construction requirements applicable to the Nuclear Power Industry, some of the influence is probably inherent in the estimate. Finally, the heat exchanger design required for sodium is basically more costly to construct and is relatively new. In sum, the cost may be somewhat conservative relative to that projected for the water/steam system.

7.2.4.3 Riser-Downcomer and Horizontal Piping

The riser-downcomer and horizontal piping costs have been estimated to be $6.11 million for the liquid metal system and $2.19 million for the water/steam system. Three factors account for this difference: (1) all piping must be stainless steel, (2) there is more horizontal piping, and (3) costs are included covering the contained sodium, the sodium purification system, and other special equipment required for sodium.

7.2.4.4 Tower, Platform, Foundation and Site Preparation

The costs for the tower, etc., are based on the costs developed for the water/steam system. These costs were adjusted relative to the square of the tower height and the diameter of the foundation.

7.2.5 Thermal Storage Equipment and Material

Thermal storage equipment costs have been estimated at 1.3 times the cost of the water/steam system. Although there is less total tank volume involved in the sodium system, the tanks must be constructed of stainless steel in a manner to handle sodium which requires that all welds are full penetration butt type and are 100 percent radiographed. The thermal storage material cost used for comparison is based on the current price per pound for sodium in tank cars, the weight of sodium required, and an estimated cost for pumping the sodium into the subsystem.

7.2.6 Turbine Plant Equipment

Turbine plant equipment costs for the sodium system are projected at $17.48 million as compared with $22.84 million for the water/steam system. This difference is accounted for in the cost of the turbine-generator, one-half of the cost of such equipment for the water steam system, because the turbine needs to operate at only one set of steam conditions. The cost employed is based on the actual cost of a 120 MWe installation completed in 1975 and adjusted for inflation. Other turbine plant equipment costs were assumed essentially the same as for the water/steam system.

7.2.7 Balance of Plant Costs

Balance of Plant includes costs for Electric Plant Equipment, Plant Master Control, Miscellaneous Plant Equipment, Distributables, and Indirects. Except for minor overhead adjustments in the Distributables, these costs have not been altered.